LAWRENCE
LIVERMORE
NATIONAL
LABORATORY

LLNL-TR-651842

THERMODYNAMIC DATABASE DEVELOPMENT: AL-AM-GA-PU-U

A. Perron, P. E. A. Turchi, A. Landa, P. Soderlind

March 17, 2014

Disclaimer

This work performed under the auspices of the U.S. Department of Energy by Lawrence Livermore National Laboratory under Contract DE-AC52-07NA27344.

Thermodynamic database development: Al-Am-Ga-Pu-U

Part I:

Re-assessment of the Pu-U system by integrating *ab initio* data to CALPHAD: Application to the ternary Ga-Pu-U alloy system

A. Perron[a], P. E. A. Turchi[a], A. Landa[a], P. Söderlind[a]

[a]*Physical and Life Sciences, Lawrence Livermore National Laboratory, Livermore, CA 94551, USA*

Objective

The goal of this study is about the thermodynamic re-assessment of the Plutonium-Uranium (Pu-U) system as a first step leading to the development of a plutonium-based thermodynamic database (*i.e.*, Pu with Al, Am, Ga, Mo, U…) with resulting phase diagrams and associated thermodynamic data. Indeed, phase stability trends and phase diagrams of multi-component nuclear materials are crucial for predicting properties and performance under normal, hypothetical or even accidental conditions. This work is based on a coupling between *ab initio* energetics, phenomenological thermodynamics models - based on the CALPHAD (CALculation of PHAse Diagrams) approach - and the use of the Thermo-Calc software, together with experimental data (whenever available). The present report summarizes results obtained (quarter period: 10/07/2013-01/07/2014) under the auspices of an agreement between CEA/DAM and NNSA/DP on cooperation in fundamental science supporting stockpile stewardship (P182).

Scientific production

Oral presentation: A. Perron, P. E. A. Turchi, A. Landa, P. Söderlind, "Thermodynamic assessment of Pu-based alloys: The case of Pu-U and Pu-U-Ga", LLNL-PRES-649582, TMS 2014 – 143nd Annual Meeting & Exhibition, San Diego – CA, USA (February 16-20, 2014).

Publication: A. Perron, P. E. A. Turchi, A. Landa, P. Söderlind, M. Kurata, "Revisited assessment of the Pu-U system and application to the ternary Pu-U-Ga system", *To be submitted to Journal of Nuclear Materials / Journal of Alloys and Compounds* (2014).

Highlights

The thermodynamic properties of the three binaries Pu-U, Pu-Ga, and U-Ga alloy systems have been studied, and isothermal sections of the Pu-U-Ga phase diagram have been proposed (see Fig. below). Extensive literature search on phase stability properties of Pu-U has been completed and, by recasting the *ab initio* energetics in the CALPHAD framework, the Pu-U phase diagram has been successfully re-assessed. The Pu-Ga and U-Ga thermodynamic properties and phase diagrams have been reviewed. Finally, the thermodynamic data for the three binaries have been put together to study the thermodynamic properties and the phase diagram of the ternary Pu-U-Ga alloy system. Property diagrams have been proposed to validate the thermodynamic predictions and to study the poorly known η and ζ intermediate phases.

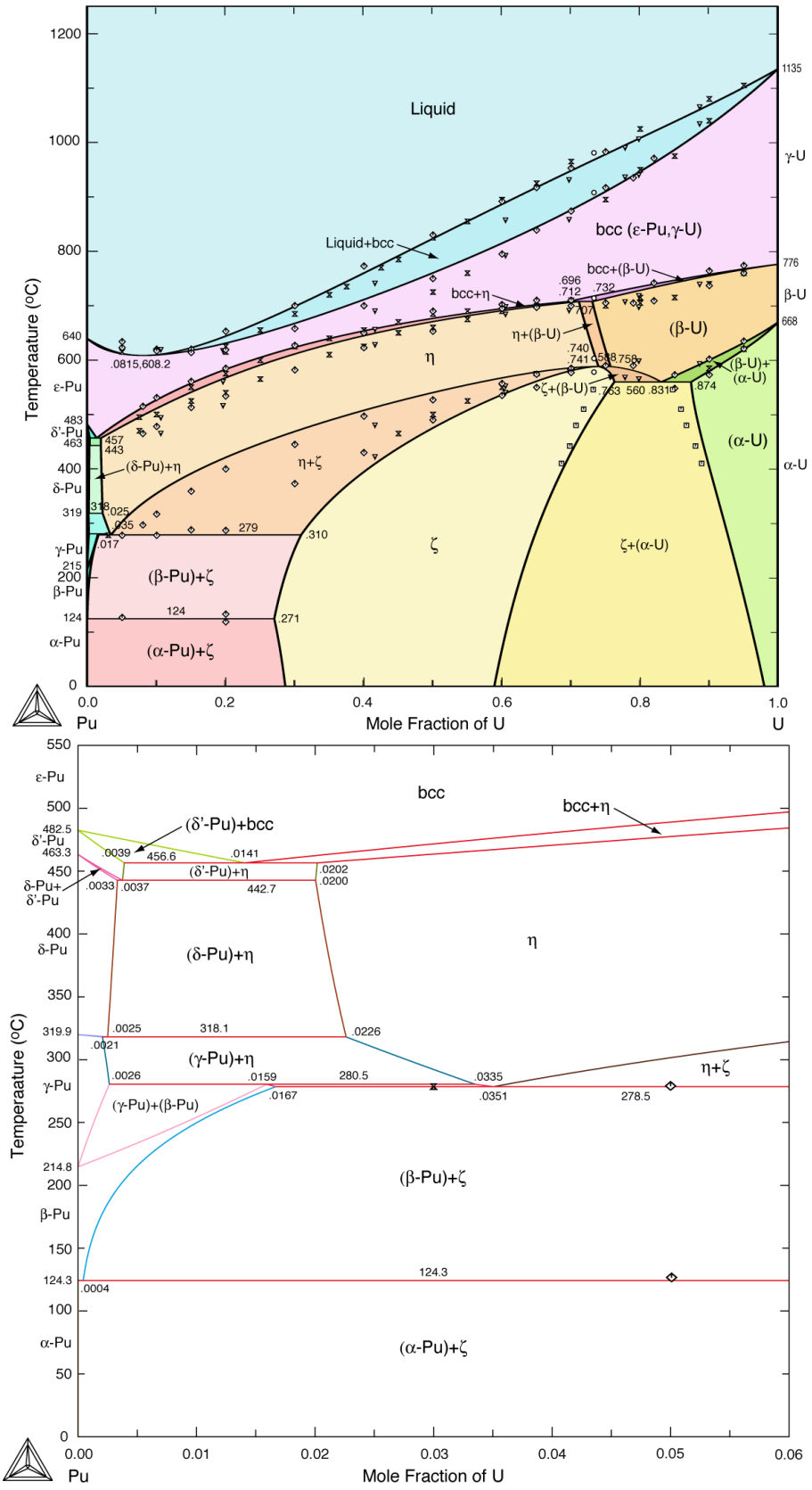

Re-assessed Pu-U phase diagram compared with experimental data (symbols).

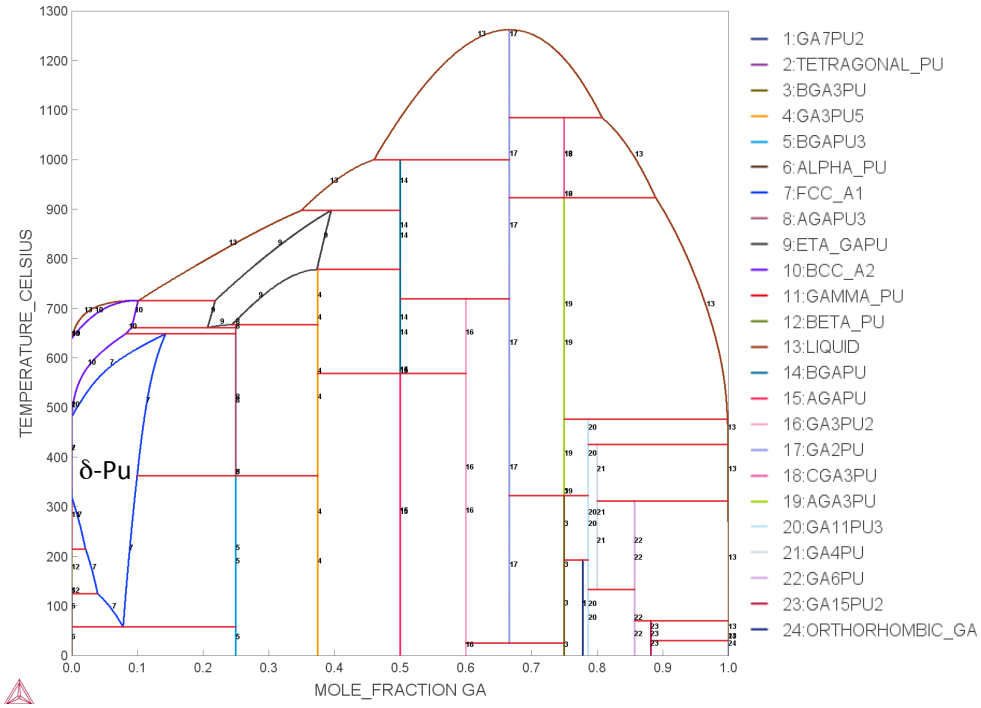

Pu-Ga phase diagram calculated from a previous assessment and integrated to our thermodynamic database.

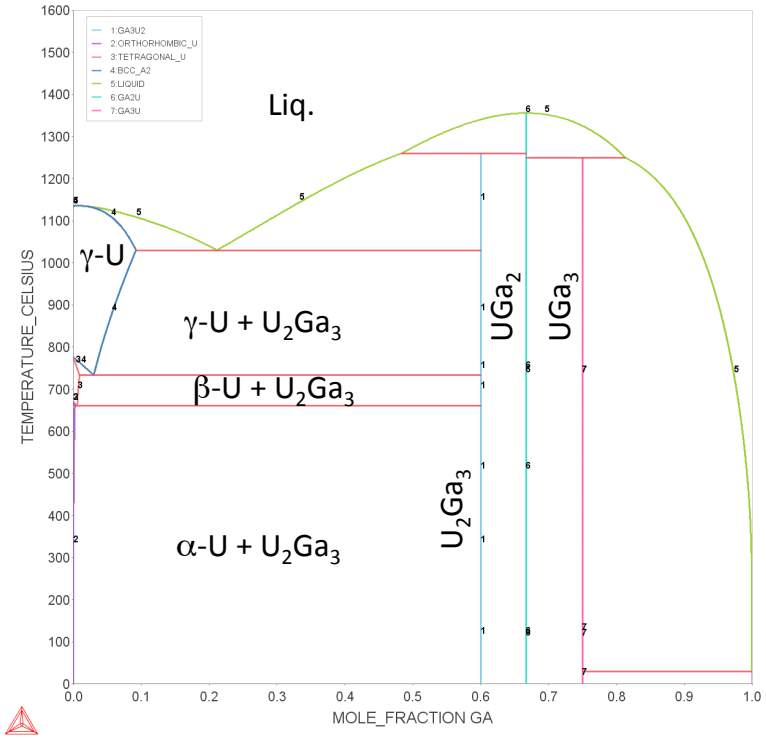

U-Ga phase diagram calculated from a previous assessment and integrated to our thermodynamic database.

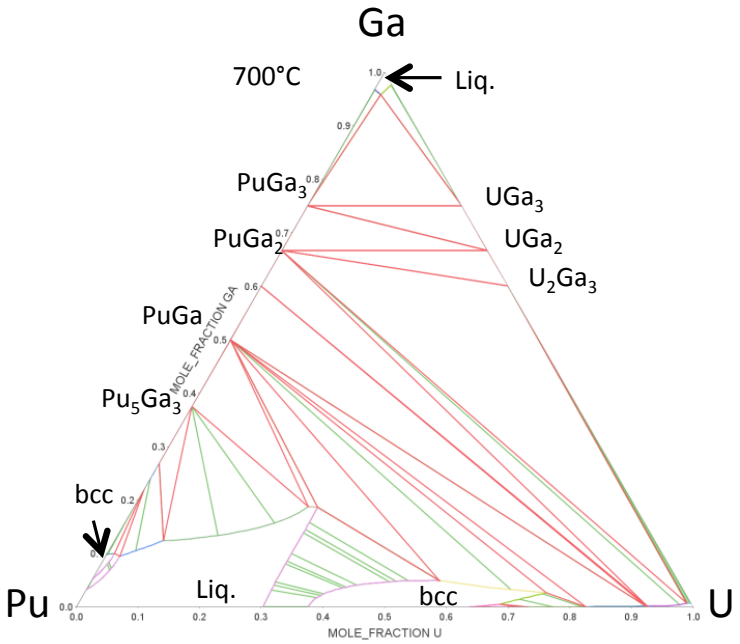

Predicted isothermal sections of the Pu-U-Ga phase diagram at 700°C.

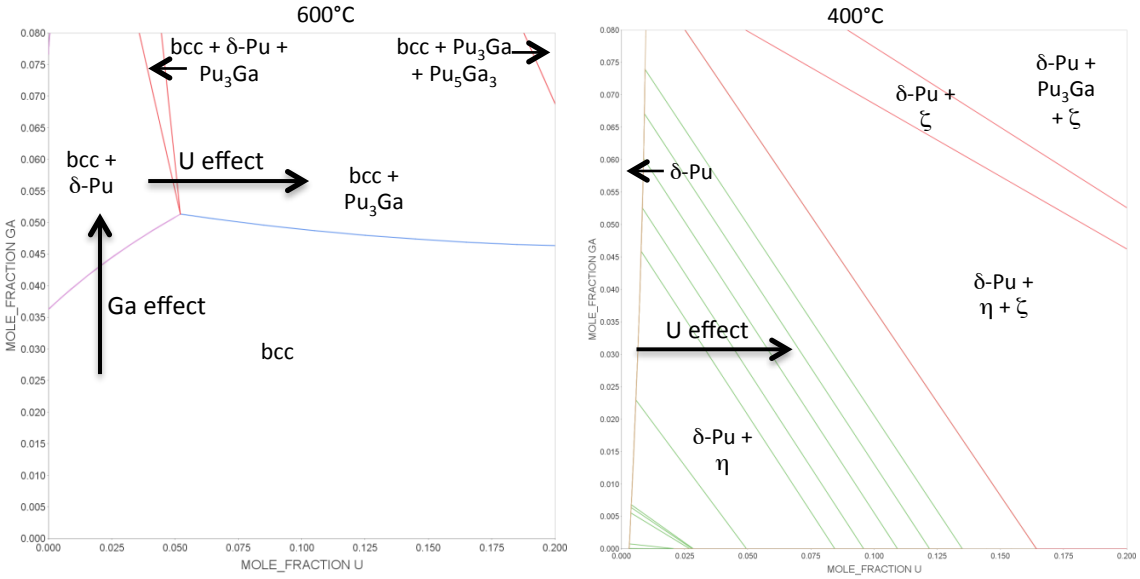

Detailed representations around the Pu-rich corner of the Pu-U-Ga alloy phase diagram at 600°C and 400°C showing the Ga and U effects on δ-phase stability.

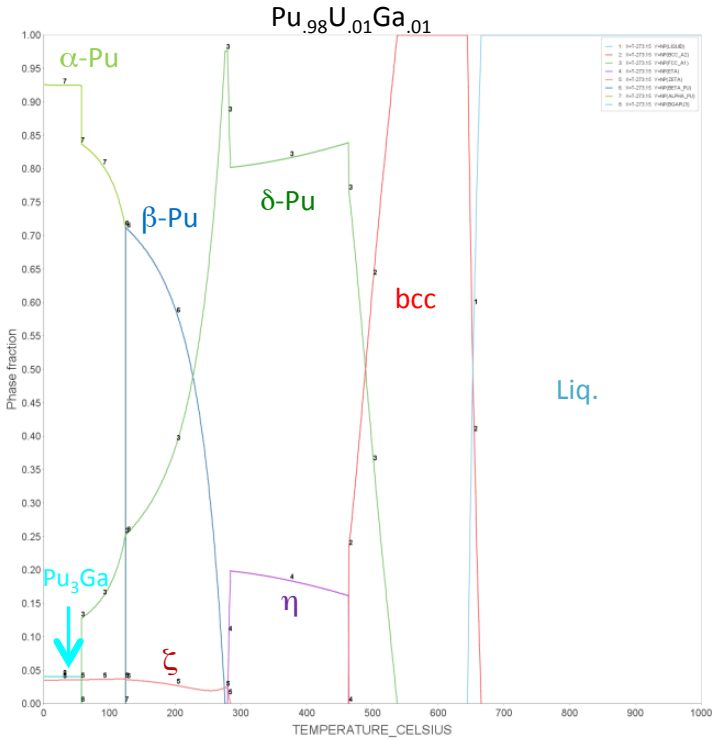

Calculated property diagram for the $Pu_{.98}U_{.01}Ga_{.01}$ ternary system.

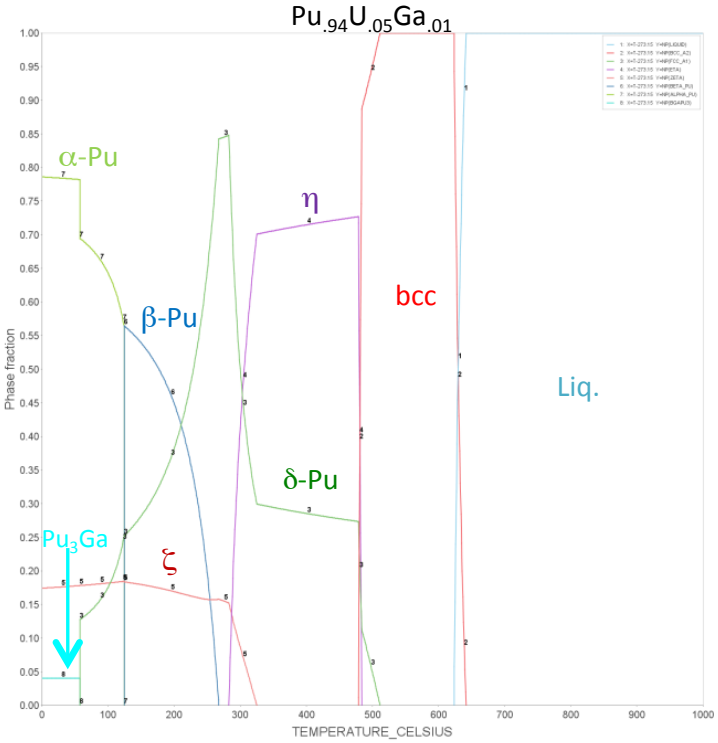

Calculated property diagram for the $Pu_{.94}U_{.05}Ga_{.01}$ ternary system.

Contents

I Introduction

The goal of this project is the development of a plutonium-based thermodynamic database (*i.e.*, Pu with Al, Am, Ga, Mo, U…) with resulting phase diagrams. As a first step towards assembling this database, the Pu-U-Ga ternary system is studied. However, the computation of any ternary, quaternary or higher-order system implies the critical evaluation and analysis of all underlying sub-systems. Thus, the thermodynamic assessment of the Pu-U, Pu-Ga, and U-Ga binaries is necessary to estimate the thermodynamic properties of the Pu-U-Ga ternary phase diagram.

The 3 binaries are investigated by employing the Thermo-Calc* commercial software using the CALPHAD (CALculation of PHAse Diagrams) approach [I.1-4]. The aim of the CALPHAD method is the Gibbs energy modeling (Appendix A). This involves selection of appropriate thermodynamic models for the Gibbs energy functions of phases, and maximum likelihood estimation of the model parameters using critically selected thermochemical and constitutional data as input. Once such functions have been assessed to reproduce phase diagrams and thermodynamic properties, they are compiled in a thermodynamic database. In practice, CALPHAD is an iterative method that adjusts the parameters describing the Gibbs energies of various phases in a system in order to construct a phase diagram that best fits the available experimental and calculated thermodynamic and phase diagram data for the system. One can see here the importance that can have the input from *ab initio* calculations (heat of formation) when experimental data are sparse or missing. Then, solution models are used to estimate the thermodynamic properties of the Pu-U-Ga system from the properties of the binary phases.

Section II is dedicated to a detailed study of the Pu-U system with the resulting re-assessment of the thermodynamic database and phase diagram (including *ab initio* input energetics). The Pu-Ga and U-Ga systems are described in Sections III and IV. Finally, the predicted isothermal sections of the Pu-U-Ga ternary phase diagram are presented and discussed in Section V. Note that the .POP file (that contains the experimental and calculated initial data for the Pu-U system) and the Pu-U-Ga thermodynamic database are reported in Appendix B and C, respectively.

* Thermo-Calc software is a product of Thermo-Calc AB.

II The Pu-U system

II.1 State of the art

Phase equilibria were firstly investigated experimentally by Ellinger *et al*. [II.1], Waldron [II.2], Bochvar *et al.* [II.3] and Elliot *et al.* [II.4]. Ellinger *et al.* published in 1959 the first reliable experimental work on the Pu-U phase diagram – resulting from thermal, dilatometric, metallographic and X-ray diffraction data [II.1]. A complete description of the Pu-U phase diagram was attempted with an emphasis on the Pu-rich part (see Fig. II.1). Authors also characterized two new intermediate phases having wide homogeneity ranges, namely eta (η) and zeta (ζ). However, the domain limits, the crystal structures, and the precipitation mechanisms related to these phases were, and are still, uncertain (see the dashed lines in Fig. II.1). The U-rich part of the phase diagram was not studied in such details. As a consequence, all two-phase domains associated with α- and β-U phases have to be considered with caution.

Later on, the Pu-U phase diagram was constructed by Peterson and Foltyn [II.5] based mainly on the work of Ellinger *et al.* [II.1] with input from the work of Calais *et al*. [II.6] for the U-rich region (see Fig. II.2.a). Note that the phase boundaries were hand drawn by means of overlapping the associated measured data points. Similar phase boundaries to [II.1] were also obtained from thermal analysis in [II.7, II.8]. In parallel, several thermodynamic assessments of the Pu-U phase diagrams have been proposed [II.9-22].

Among them, the works performed by Leibowitz *et al*. can be firstly underlined [II.17-19]. The assessed Pu-U phase diagram presented in Fig. II.2.b is in a quite good agreement with previous experimental results. The greatest difficulty was to assess the η and ζ phases, and authors mentioned internal inconsistencies in the η + ζ portion of the phase diagram (no reasonable way to extrapolate the two-phase η + ζ field to the Pu edge). The resulting U-rich region of the phase diagram presents reactions with intermediate phases that differ from experiments. However, authors pointed out the lack of experimental data in these regions.

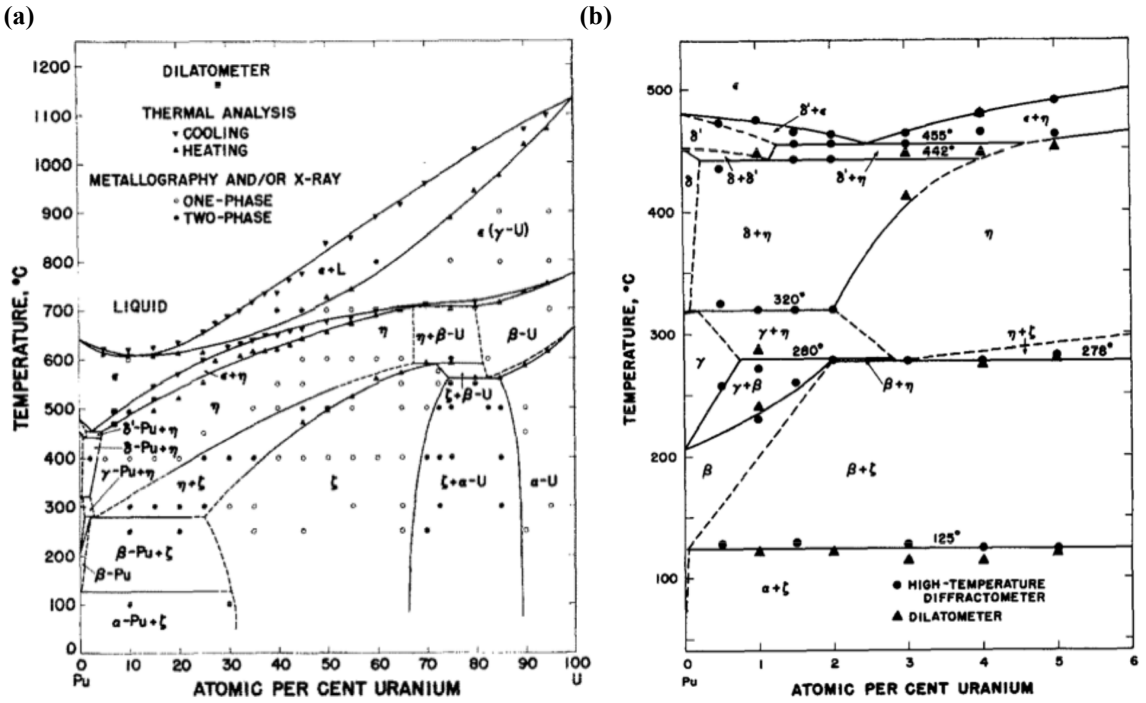

Figure II.1. (a) Experimental Pu-U phase diagram with (b) a magnification of the Pu-rich region, according to the results of Ellinger *et al*. [II.1].

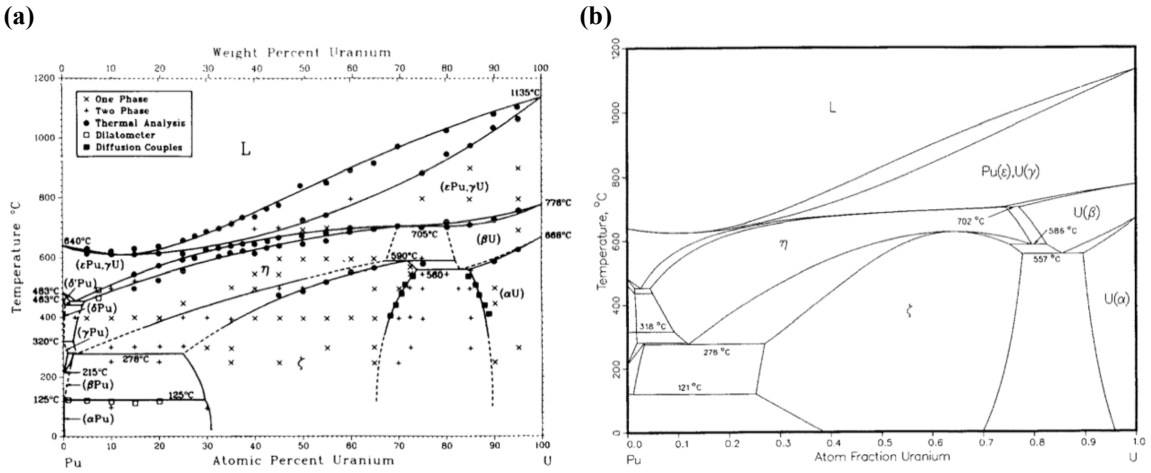

Figure II.2. (a) Phase diagram of the Pu-U system reported by Peterson and Foltyn [II.5] and (b) assessed by Leibowitz *et al.* [II.18].

Then, Kurata has reported the most complete assessment in 1999 [II.20]. This assessment, carried out using the Parrot module of the Thermo-Calc code, is reported in Fig. II.3.a. The solid lines [II.20] are, in general, in better agreement with the experimental data (symbols) than the previous calculations of Leibowitz *et al*. (dotted

lines) [II.18]. However, author mentioned that the liquidus is slightly lower than most of the experimental data and that the calculated phase boundaries between bcc (ε-Pu,γ-U) and η phases are shifted to a slightly higher temperature than the experimental ones. Finally, the largest difference between experimental data and these results is observed in the phase boundary between the η and β-U phases. The calculated η / β-U phase boundary is shifted closer to the Pu terminal than the experimental boundary.

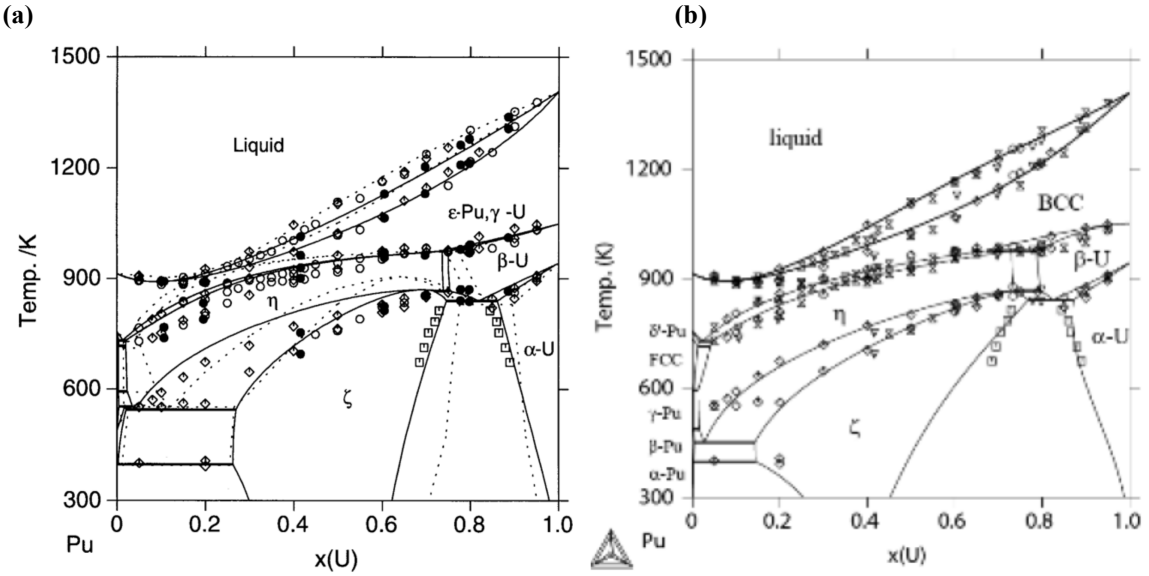

Figure II.3. (a) Phase diagram of the Pu-U system assessed by Kurata in 1999 [II.20] in comparison with Leibowitz *et al.* [II.18] and (b) re-assessed by Kurata in 2010 [II.21].

In 2010, Kurata revisited the Pu-U phase diagram to make consistent the phase boundaries in the Pu-U-Zr system and those in the Pu-U binary system [II.21]. In fact, the previous assessed liquidus for the ternary system was slightly too low. Thus, a re-assessment was performed by changing the weight of the liquidus data to improve the fit to the experimental data. The resulting phase diagram is shown in Fig. II.3.b. In spite of the fact that the upper part of the Pu-U system seems in a better agreement with experimental data, the calculated eutectoid temperature among the ζ, η and β-Pu phases is far from the experimental one. In general, this new assessment leads to changes in the stability regions of the ζ and η phases of Pu-U. This assessment, in addition to many phase diagrams of actinides alloys, was reported by Kurata in a book chapter dedicated to nuclear materials [II.22].

Recently, Turchi and Landa [II.23] underlined a big difference between 1999 and 2010 Kurata's assessments for the bcc heat of formation of Pu-U alloy at T = 0 K [II.20-21]. As observed in Fig. II.4, the last one is strongly positive – hence indicating a tendency to phase separation (*i.e.*, existence of a miscibility gap at low temperature) – whereas the first one is negative – revealing a tendency to phase formation. The energetic values obtained at T = 0 K from *ab initio* calculations for the bcc phase are in good agreement with the 1999 assessment [II.20], contrary to those most recently re-assessed [II.21]. Thus, ***it is interesting to re-assess the Pu-U phase diagram starting with energetics values obtained at T = 0 K from ab initio calculations for the bcc phase of this alloy***. In fact, these values correspond to the Redlich-Kister T-independent terms that enter the expression for the excess Gibbs energy of the bcc phase, hence constraining the Parrot fitting procedure with less parameters (only the T-dependent terms for the bcc phase, see Appendix A).

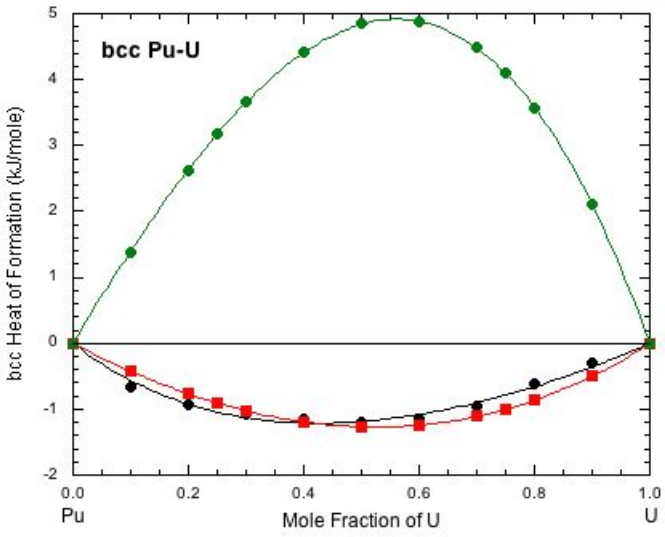

Figure II.4. Heat of formation of the bcc phase for the Pu-U alloy at T = 0 K. The positive green line corresponds to the 2010 Kurata's assessment [II.21] whereas the red and black negative lines correspond to 1999 Kurata's assessment [II.20] and to the *ab initio* results [II.23], respectively.

As the present re-assessment of the Pu-U system is mainly based on the experimental results of Ellinger *et al.*, and of the data provided by Masaki Kurata (to be discussed with respect to previous thermodynamic assessments), a detailed description of the experimental results presented in Ref. [II.1] and of past thermodynamic assessments reported in Refs [II.17-22] is discussed below. Readers interested in a general understanding of the present work can skip the next subsection, but are encouraged to read it for a better understanding of the Pu-U system.

II.2 Articles of interest

1959: F. H. Ellinger, R. O. Elliot and E. M. Cramer [II.1]

Owing to the complete mutual solid solubility of epsilon plutonium (ε-Pu) and gamma uranium (γ-U), authors mentioned that all Pu-U alloys solidify as a body-centered cubic solution (bcc). ε-Pu is the only plutonium allotrope in which uranium is appreciably soluble, whereas alpha uranium (α-U) dissolves a maximum of 15 at.% plutonium, and beta uranium (β-U) dissolves about 20 at.% plutonium. Finally, two intermediate phases, designed eta (η) and zeta (ζ), were highlighted over a wide homogeneity range with the restriction that η is stable at elevated temperature only. The reported phase diagram is presented in Fig. II.1, and peculiar points are discussed below.

Liquidus and solidus: Based on thermal-analysis data supplemented by observations of incipient melting, the region between ε-Pu and γ-U at high temperature was defined as a ***continuous*** liquid-plus-solid region revealing a ***minimum*** at about ***12 at.% U and 610°C***. Note that the liquidus is defined over most compositions by the thermal arrests obtained on cooling, and that the course of the solidus is not as well defined by thermal data except at its Pu-rich and U-rich ends. However, authors judged the solidus to be continuous throughout the intermediate composition range because of the following observations: (i) the presence of liquid in a 45 at.% U alloy and its absence in a 50 at.% U alloy, both quenched from 700°C, placed a solidus point between these compositions at 700°C; (ii) the smooth sequence of thermal arrests that marked the upper boundary of the ε (bcc) + η field does not indicate the presence of a horizontal as would be expected if the solidus intersected this field.

Intermediate phases: The ***η phase*** is formed by a peritectoid reaction between the bcc phase (ε-Pu,γ-U) and the β-U phase at approximately 70 at.% U and 705°C:

$$(\varepsilon - \mathrm{Pu}, \gamma - \mathrm{U}) + \beta - \mathrm{U} \rightarrow \eta$$

Its homogeneity range extends across the diagram to 2 at.% U at 320°C (see Fig. II.1.b), and it decomposes eutectoidally into β-Pu and ζ at about 3 at.% U and 278°C:

$$\eta \rightarrow \beta - \mathrm{Pu} + \zeta$$

The η / (η + bcc) boundary was defined by the combined data from thermal analysis, dilatometric and high-temperature X-ray diffraction studies. The η / (η + ζ) boundary was located chiefly by metallographic examination of heat-treated and quenched alloys. Authors underline that X-ray powder pattern of η is complex; however, this phase was indexed on the basis of a ***tetragonal*** unit cell with a = 10.57 Å and c = 10.76 Å for the 25 at.% U quenched from 500°C. This unit cell contains 52 atoms as calculated from 17.3 g/cm^3, the density of η deduced from dilatometric data. Note that this solution of the powder pattern is considered ***highly uncertain***.

The ***ζ phase*** forms by a peritectoid reaction between the η and β-U phases at approximately 72 at.% U and 590°C:

$$\beta - U + \eta \rightarrow \zeta$$

With decreasing temperature, the ζ field widens rapidly toward Pu-rich compositions, reaching a maximum width at 75 at.% Pu and 278°C. Below 278°C, the ζ field narrows down to about 69 at.% Pu, as determined by microscopic examination of a series of α-Pu + ζ alloys treated at ***100°C for 3 years***. As for the microstructure of the ζ phase, authors revealed that microcracks are characteristic of ζ in alloys containing about 40 at.% U and greater. By increasing U content, the course of the ζ / (ζ + α-U) was located by means of heat treating/quenching experiments made chiefly with X-ray specimens. Microstructural evidence was difficult to obtain in this composition range because of rapid intergranular oxidation, however, it was successfully shown that a 65 at.% U alloy soaked at 250°C for 890 h consisted entirely of ζ phase. The X-ray powder pattern of ζ was indexed on the basis of a primitive cubic unit cell. The lattice constant was found to decrease from a = 10.692 Å at 35 at.% U to a = 10.651 Å at 70 at.% U. The number of atoms in this unit cell approximates 58, as calculated from the observed density of 18.5 to 18.8 g/cm^3. High-temperature X-ray work revealed, however, that ζ expands anisotropically with a symmetry tentatively identified as tetragonal. Hence, the crystal structure of ***ζ may be tetragonal with an axial ratio of unity at room temperature***.

Plutonium-rich phases: The phase diagram of alloys containing up to 5 at.% U was constructed chiefly from high-temperature diffractometer data (Fig. II.1.b). The solubility of U in the Pu allotropes is quite limited, apart from that in ε-Pu (bcc). The latter forms a continuous solid solution with γ-U. The ***β-Pu + η*** field is the only one for which ***no direct experimental evidence*** was obtained. The following peritectoid reaction (280°C):

$$\gamma - \mathrm{Pu} + \eta \rightarrow \beta - \mathrm{Pu}$$

falls very nearly at the same temperature as the $\eta \rightarrow \beta - \mathrm{Pu} + \zeta$ (278°C) eutectoid invariant. It was concluded, however, that the β-Pu peritectoid invariant was at a higher temperature because, on heating at less than 0.5°C/min, the β-Pu → η transition of alloys containing 3 or more at.% U was sharp and rapid, and there was no evidence obtained for the formation of γ-Pu. Hence, the existence of a very narrow β-Pu + η field is indicated. Also, the γ-Pu + η region could not extend beyond 3 at.% U.

Uranium-rich phases: Thermal analysis revealed that the α-U → β-U transformation is lowered to 560°C by the solution of plutonium, at which temperature α-U dissolves about 15 at.% Pu. Below 560°C the solubility decreases somewhat, reaching about 11 at.% Pu at 250°C. β-U will dissolve a somewhat greater proportion of Pu than α-U, the maximum being about 20 at.% Pu at 705°C. Below 705°C the solubility decreases to about 18 at.% Pu at 560°C where β-U decomposes eutectoidally into α-U and ζ:

$$\beta - \mathrm{U} \rightarrow \alpha - \mathrm{U} + \zeta$$

The solution of Pu in γ-U lowers the β-U → γ-U transformation to 705°C, that corresponds to the temperature of the following peritectoid reaction:

$$\gamma - \mathrm{U} + \beta - \mathrm{U} \rightarrow \eta$$

As already described, γ-U and ε-Pu form a continuous series of solid solution (bcc). Finally, it is interesting to remember that, ***whereas a 85 at.% U alloy quenched from the β-U field is retained as β-U at room temperature*** (initially, β-U has to contain at least 10 at.% Pu in solution), ***the same composition quenched from the γ-U field will transform to α-U***.

1988-1997: L. Leibowitz, E. Veleckis, R. A. Blomquist and A. D. Pelton [II.17-19]

First, Leibowitz *et al*. employed a dual approach that involves thermodynamic calculation and experimental determination to study the solidus and the liquidus of the U-Pu-Zr system [II.17]. As mentioned by these authors, the computation of an unknown ternary phase diagram implies the critical evaluation and analysis of all relevant phase diagrams and thermodynamic data for the three binary sub-systems with the objective of obtaining mathematical expressions for the thermodynamic properties of all binary phases as functions of composition and temperature. Following this, interpolation techniques based upon solution models are used to estimate the thermodynamic properties of the ternary phases from the properties of the binary phases. Thus, the Pu-U system at high-temperature has been investigated. Note that all calculations were performed with programs of the FACT (Facility for the Analysis of Chemical Thermodynamics) computer system. The liquidus and solidus for Pu-U reported in Fig. II.5 have been measured by Ellinger *et al.* [II.1] and by Mound Laboratory [II.7]. The ***liquidus*** curves of these two studies ***agree*** to within better than ***15°C***, but the ***solidus*** curves ***diverge*** by up to ***40°C***. Ellinger *et al.* reported the minimum to be at 610°C and 12 at.% U on the basis of their solidus point. Leibowitz *et al*. report from Ref. [II.1] that Ellinger *et al*. had difficulties in obtaining reproducible solidus measurements. However their liquidus measurements place the minimum closer to 620°C, which is the minimum temperature reported by Mound Laboratory [II.7]. Finally, another author reports a minimum at 624±2°C and 9 at.% U [II.9]. The main conclusion about the assessment of the high-temperature part of the Pu-U phase diagram revealed an inconsistency between the recommended enthalpy of fusion of U [II.11] and the published Pu-U solidus [II.7, II.9]. Thus, ***these authors concluded that the Pu-U solidus may be incorrect and should be reexamined***.

A few years later, Leibowitz *et al.* published a thermodynamic assessment of the Pu-U system in the entire range of composition and temperature [II.18]. As the solubility of U in Pu phases is very low, the authors have thus treated these as Henrian solid solutions. Note that the solubility of U in α-Pu was considered to be negligible. Although the solubility of Pu in α-U and β-U ranges up to 20 at.%, the authors found that these phases could also be treated satisfactorily as Henrian solid solutions. The two bcc phases,

ε-Pu and γ-U, form a solid solution in the whole composition range. ***The intermediate η and ζ phases***, which ***present the greatest difficulties in performing the assessment***, also exist over fairly wide composition and temperature ranges. Despite the complexity of this system, the authors report that they were able to describe it by using sub-regular models.

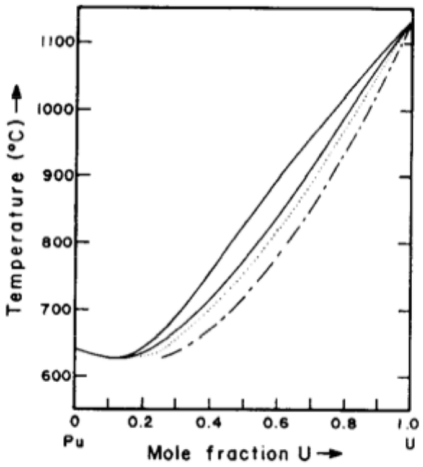

Figure II.5. Pu-U phase diagram at high temperature [II.17]. The solid, dashed, and dotted lines correspond to calculated [II.17] and experimental results [II.1, II.7], respectively.

During the assessment, Gibbs energies of hypothetical pure η-Pu, η-U, ζ-Pu and ζ-U were required. Authors expected that extrapolation of the appropriate phase boundaries to pure Pu and pure U would provide some guidance for estimating hypothetical transition temperatures. This gave some initial indications of reasonable values to use. However, as can be seen from Fig. II.2.a [II.5], there is no reasonable way to extrapolate the ***two-phase η + ζ field*** to the Pu edge. The authors took this as an indication of some ***internal inconsistency*** in that portion of the diagram. Other regions of the diagram were also used to help determine parameters for these two fields. For example, as the boundaries of the wide two-phase ζ + α-U are essentially parallel, the entropies of the ζ → α-U transitions for both pure U and pure Pu were taken to be 0.

The authors also mentioned that the region of the diagram containing the ***two invariants at 560 and 590°C*** was ***crucial*** in selecting the appropriate thermodynamic properties of the η and ζ phases. The calculated phase diagram is presented in Fig. II.2.b. By comparison with Fig. II.2.a, the solidus is higher because of the value chosen for the enthalpy of fusion of U. The bcc + η boundaries are consequently shifted at higher

temperatures as well. The minimum in the calculated solidus-liquidus appears at 626°C and about 10 at.% U.

The region shown in Fig. II.2.a between 560 and 705°C contains three invariants. The calculated invariant at 702°C agrees well with Fig. II.2.a. The calculated two-phase ***η + β-U*** field differs from that shown in Fig. II.2.a, but there are ***essentially no experimental data in that region***. At 590°C the authors could not maintain the broad ζ + α-U field and thus produce a peritectoid. They chose to maintain the ζ + α-U region because it appeared to be well supported experimentally, and to modify the transition at 590°C to produce an eutectoid reaction. The calculated eutectoid invariant at 557°C (β-U → ζ + α-U) is in good agreement with Fig. II.2.a. The authors emphasized the fact that, in general, only a small number of experimental points need to be rejected in the calculated diagram. However, based on information from diffusion studies obtained during a private communication with M. C. Petri and M. A. Dayananda, the authors indicate that the ***two-phase bcc + β-U field may be wider***.

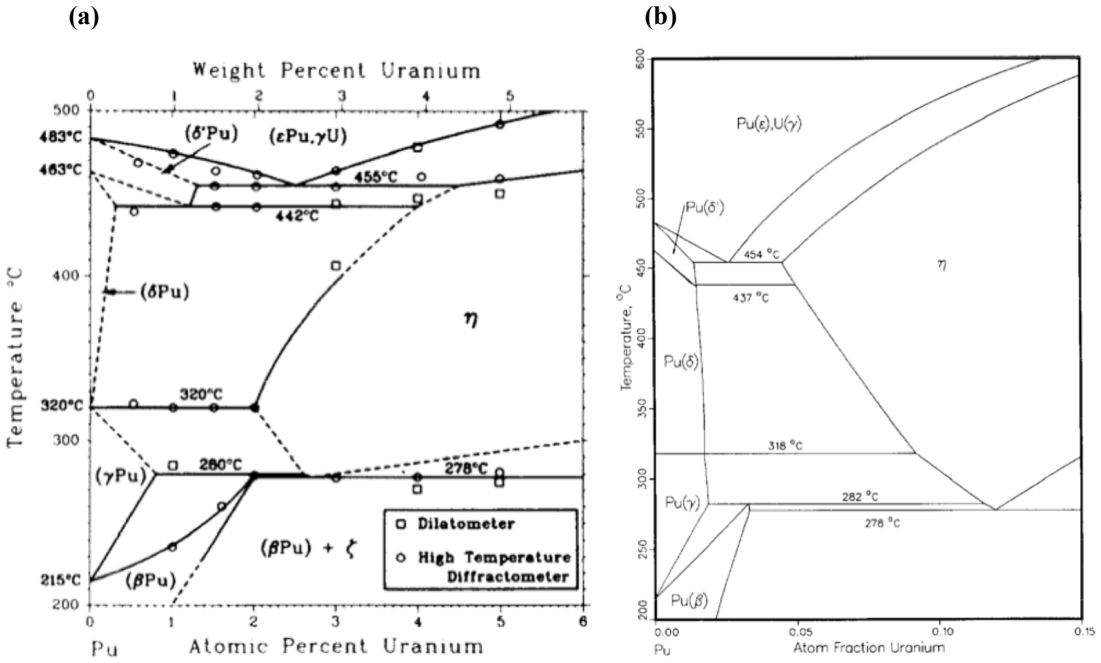

Figure II.6. Pu-rich region of the Pu-U phase diagram (a) reported by Peterson and Foltyn [II.5] and (b) calculated by Leibowitz *et al*. [II.18].

The Pu-rich regions, presented in Fig. II.6, are quite similar with a few notable exceptions. The authors report that because the enthalpy of the transition from δ-Pu to δ'-Pu is so small, the corresponding ***two-phase field must be very narrow*** (as calculated). The invariants shown in Fig. II.6.a at 455 and 442°C appear in the calculated diagram at 454 and 436°C, and at compositions reasonably close to the experimental ones. The behavior of the δ-Pu and γ-Pu phases presented another difficulty. For the authors, it appeared unlikely that the solubility of U would increase with increasing temperature in the δ-Pu phase and decrease with increasing temperature in the γ-Pu phase. In the calculated diagram, the solubility of U is essentially independent of temperature, and a very narrow transition region appears around 318°C. The invariants shown at 280 and 278°C in Fig. II.6.a are calculated at 282 and 278°C. The chemical composition of the last eutectoid (η → β-Pu + ζ) is different in the two diagrams. However, ***experimental data are limited***.

Finally, it is interesting to note that an alternative Pu-U phase diagram has been published by Pelton in 1997 [II.19]. In this last published phase diagram, the main difference with previously published work is that the bcc phase doesn't form a continuous solid solution across the whole composition range. Indeed, the η field intersects the solidus (Fig. II.7).

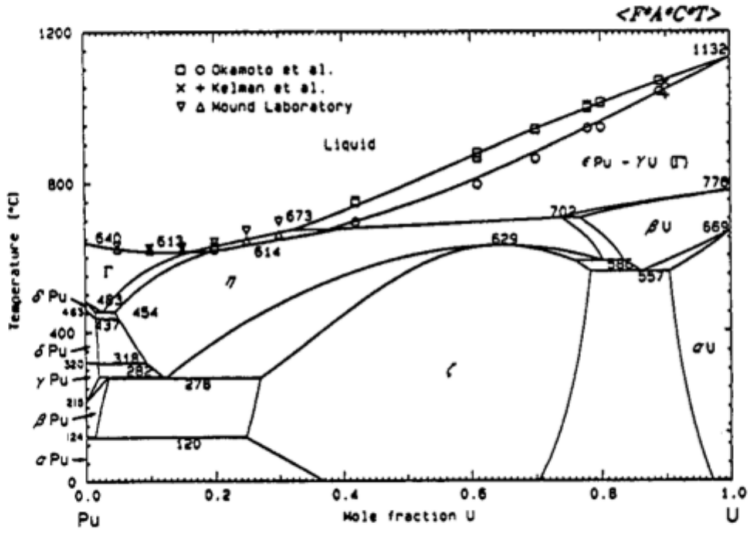

Figure II.7. Calculated optimized Pu-U phase diagram taken from Ref. [II.19].

1999-2012: M. Kurata [II.20-22]

The most complete thermodynamic assessment of the Pu-U phase diagram was reported by Kurata in 1999 [II.20]. The assessment for the Pu-U system was carried out using mainly the thermodynamic data reported in [II.24-25] and the phase diagram data reported in [II.14]. The data in [II.1, II.7] for the Pu-rich region and that in [II.6] for the U-rich region were also used to optimize the Gibbs energies for the low-temperature Pu allotropes and ζ / α-U phase boundaries, respectively. Kurata mentioned that ***the amount of relevant experimental data is limited in the narrow region of the Pu-rich region below approximately 527°C***.

The Pu-U phase diagram calculated using the optimized parameters is reported from Ref. [II.20] in Fig. II.3.a with the experimental data from Refs. [II.1, II.6-7, II.25] and the previous calculation from Ref. [II.18]. The author underlines that the results are, in general, in better agreement with the experimental data than those from the previous calculation. The liquidus is slightly lower than the previous experimental data [II.1, II.6] but agrees well with recent data [II.25]. The minimum in the calculated solidus-liquidus appears at 618°C and approximately by 9 at.% U. These values are comparable with the previously obtained values, *i.e.*, 610°C and 12 at.% U [II.1] and 620°C and 10 at.% U [II.25]. Even though the calculated phase boundaries between the bcc (ε-Pu, γ-U) and η phases are shifted to a slighter higher temperature than the experimental ones, the bcc phase forms a continuous solid solution. The largest difference between the experimental data and the results of this calculation is observed in the phase boundary between the η and β-U phases. The calculated η / β-U boundary is shifted closer to the Pu terminal phase than the experimental phase boundary. The author assumed that this might be due to the ***error in the assumption of the Gibbs energies for η and β-U***.

Later, Kurata revisited the Pu-U phase diagram [II.21] based on new experimental results on the ternary Pu-U-Zr, and made minor modifications to his earlier assessed data for the Pu-U thermodynamics that led to changes in the stability regions of the liquid, ζ and η phases of Pu-U. The resulting phase diagram is shown in Fig. II.3.b. In spite of the fact that the upper part of the Pu-U system seems in a better agreement with experimental data, the calculated eutectoid temperature among the ζ, η, and β-Pu phases is far from the experimental one.

II.3 CALPHAD assessment

Seven allotropes including the liquid phase exist for plutonium (Pu) as follows: simple monoclinic (α-Pu), body-centered monoclinic (β-Pu), face-centered orthorhombic (γ-Pu), face-centered cubic (δ-Pu), body-centered tetragonal (δ'-Pu), body-centered cubic (ε-Pu) and liquid. Four allotropes exist for uranium (U) as follows: base-centered orthorhombic (α-U), tetragonal (β-U), body-centered cubic (γ-U) and liquid. The Gibbs energies for pure stable phases (α-, β-, γ-, δ-, δ'-, ε- and liquid Pu, α-, β-, γ- and liquid U) are given by Dinsdale [II.26]. However, the Gibbs energies for metastable phases, such as the Gibbs energy of Pu for the α- and β-U phases and that of U for α-, β-, γ-, δ-, δ'-Pu phases, are not given in the SGTE database. These functions have been evaluated by Kurata [II.20-21] and are reported in Table II.1. As mentioned by Kurata, although the interaction parameters optimized for these metastable phases do not directly represent the thermodynamic character of the corresponding phases, the combination of the assumed Gibbs energies of the metastable phases and the optimized interaction parameters is considered adequate for the thermodynamic properties of the corresponding phases.

Table II.1. The Gibbs energy for the pure elements, U and Pu (in J/mole), reported from [II.20] and [II.21].

Element	Phase	Kurata 1999	Kurata 2010	Present study
U	α-Pu	-	$^{\circ}G_U^{\alpha-U} + 5000$	-
	β-Pu	$^{\circ}G_U^{\alpha-U} + 2000$	$^{\circ}G_U^{\alpha-U} + 5000$	$\mathbf{^{\circ}G_U^{\alpha-U} + 2000}$
	γ-Pu	$^{\circ}G_U^{\alpha-U} + 2000$	$^{\circ}G_U^{\alpha-U} + 5000$	$\mathbf{^{\circ}G_U^{\alpha-U} + 2000}$
	δ-Pu	$^{\circ}G_U^{\alpha-U} + 2000$	$^{\circ}G_U^{\gamma-U} + 5000$	$\mathbf{^{\circ}G_U^{\alpha-U} + 2000}$
	δ'-Pu	$^{\circ}G_U^{\alpha-U} + 2000$	$^{\circ}G_U^{\gamma-U} + 5000$	$\mathbf{^{\circ}G_U^{\alpha-U} + 2000}$
	η	$^{\circ}G_U^{\beta-U} + 229.2$	$^{\circ}G_U^{\beta-U} + 118.7$	$\mathbf{^{\circ}G_U^{\beta-U} + 229.2}$
	ζ	$^{\circ}G_U^{\gamma-U} + 332.1$	$^{\circ}G_U^{\gamma-U} + 337.8$	$\mathbf{^{\circ}G_U^{\gamma-U} + 332.1}$
Pu	α-U	$^{\circ}G_{Pu}^{\alpha-Pu} + 2026$	$^{\circ}G_{Pu}^{\beta-Pu} + 652.7$	$\mathbf{^{\circ}G_{Pu}^{\alpha-Pu} + 2026}$
	β-U	$^{\circ}G_{Pu}^{\delta-Pu} + 227.5$	$^{\circ}G_{Pu}^{\delta'-Pu} + 209.6$	$\mathbf{^{\circ}G_{Pu}^{\delta-Pu} + 227.5}$
	η	$^{\circ}G_{Pu}^{\delta-Pu} + 103.4$	$^{\circ}G_{Pu}^{\gamma-Pu} + 51.1$	$\mathbf{^{\circ}G_{Pu}^{\delta-Pu} + 103.4}$
	ζ	$^{\circ}G_{Pu}^{\varepsilon-Pu} + 500$	$^{\circ}G_{Pu}^{\beta-Pu} + 500$	$\mathbf{^{\circ}G_{Pu}^{\varepsilon-Pu} + 500}$

In the present study, the values determined by Kurata in 1999 are taken with more confidence (Table II.1). Moreover, the Gibbs energy function of U for α-Pu was not taken into account, because the solubility of U in the α-Pu phase is negligible. In addition to these end-members, the heat of formation of bcc Pu-U alloy resulting from *ab initio* calculations at T = 0 K can be used to constrain the Parrot fitting procedure. In fact, these values correspond to the Redlich-Kister T-independent terms that enter the expression for the excess Gibbs energy of the bcc phase (Appendix A). By fitting the *ab initio* data shown in Fig. II.4 with a Redlich-Kister polynomial, two sets of interaction parameters are obtained for the bcc phase:

$$^{0}L_{Pu,U} = -4808 + b_0*T \qquad \text{or } ^{0}L_{Pu,U} = -4745 + b_0*T$$
$$^{1}L_{Pu,U} = -1389 + b_1*T \qquad \text{or } ^{1}L_{Pu,U} = -1389 + b_1*T$$
$$\text{or } ^{2}L_{Pu,U} = -443 + b_2*T$$

Table II.2. Interaction parameters for solution phases (J/mole).

Phase	Interaction parameter	Kurata 1999	Kurata 2010	Present study
Liquid	^{0}L	4751.6 – 12.0 T	32231 - 31.5 T	**13839 – 19.6 T**
	^{1}L	-2284.3	-8980.2	**-7093**
bcc (ε-Pu, γ-U)	^{0}L	**-5062.3**	**19374** - 17.3 T	**-4808 +0.2 T**
	^{1}L	506.8	-4939.5	**-1389**
α-Pu	^{0}L	-	5000	**-**
β-Pu	^{0}L	-2550	5000	**-4343**
γ-Pu	^{0}L	3620	4342.7	**4090**
δ-Pu	^{0}L	3620	723.8	**3136**
δ'-Pu	^{0}L	3000	495.4	**2411**
α-U	^{0}L	-9581.4	6176.5	**-12689 + 3.9 T**
	^{1}L			**9712 - 11.8 T**
β-U	^{0}L	-4870.7	5287.3	**-12577 + 8.9 T**
η	^{0}L	-5772.4 + .19 T	4049.1 – 1.5 T	**-12970 + 8.3 T**
	^{1}L		-617.4 – 3.4 T	**2690 – 3.5 T**
ζ	^{0}L	-64447.6 + 68 T	-6336.9 + 10.4 T	**-87904 + 99.2 T**
	^{1}L	-4517.9 + 21.6 T	-19997 + 24.6 T	**-23547 + 54.6 T**
	^{2}L	7968.5 + 4.8 T	12364 – 7.8 T	**33907 – 19.9 T**

The subregular-solution model (defined by two Redlich-Kister coefficients) was preferred because one should try to avoid using many coefficients in a Redlich-Kister series. In particular, one may have serious problems when extrapolating a binary system, with many Redlich-Kister coefficients, to a ternary or higher order system because the phase may then appear in quite different region of the composition space, where higher-ordre binary Redlich-Kister coefficients may not give a reasonable description. As a general rule, there should be a special reason for using more than the first three Redlich-Kister terms. The Redlich-Kister T-independent terms for the bcc phase are reported in Table II.2.

The present re-assessment of the Pu-U system is based on the experimental work of Ellinger *et al*. [II.1], and of the data compiled and provided by Masaki Kurata (see modified .POP file in Appendix B). The interaction parameters determined using the Parrot module of the Thermo-Calc software are reported in Table II.2 in comparison with the ones previously calculated by Kurata [II.20-21]. The resulting Pu-U phase diagrams are displayed in Fig. II.8-10. In addition, the characteristics (chemical composition and temperature) of the 10 invariant reactions are summarized in Table II.3.

As a first observation, ***the new Pu-U phase diagram that was assessed with starting T = 0 K energetics from ab initio data for the bcc phase (Redlich-Kister T-independent terms) is in agreement with experimental data***. The comparison between the measured values and the calculated values resulting from the assessment are shown in Fig. II.11. The perfect match between measured and calculated values is symbolized by the solid lines. As observed in Fig. II.11.a, the temperature of the invariant reactions (triangles) is in a very good agreement and all other data (composition of phases and phase fractions, activities…) are also in a good agreement (Fig. II.11.b). It is an important result because this assessment proves that, starting from *ab initio* data, the number of unknown parameters can be reduced, and still lead to ***thermodynamic data that are valid not only from a phase diagram point of view (invariants) but also from an energetic point of view (ab initio)***. In fact, a binary system can be assessed from phase diagram information only, but without energetics there is no reasonable way to extrapolate it to multi-component systems. A detailed comparison between the various assessments is presented in the next section.

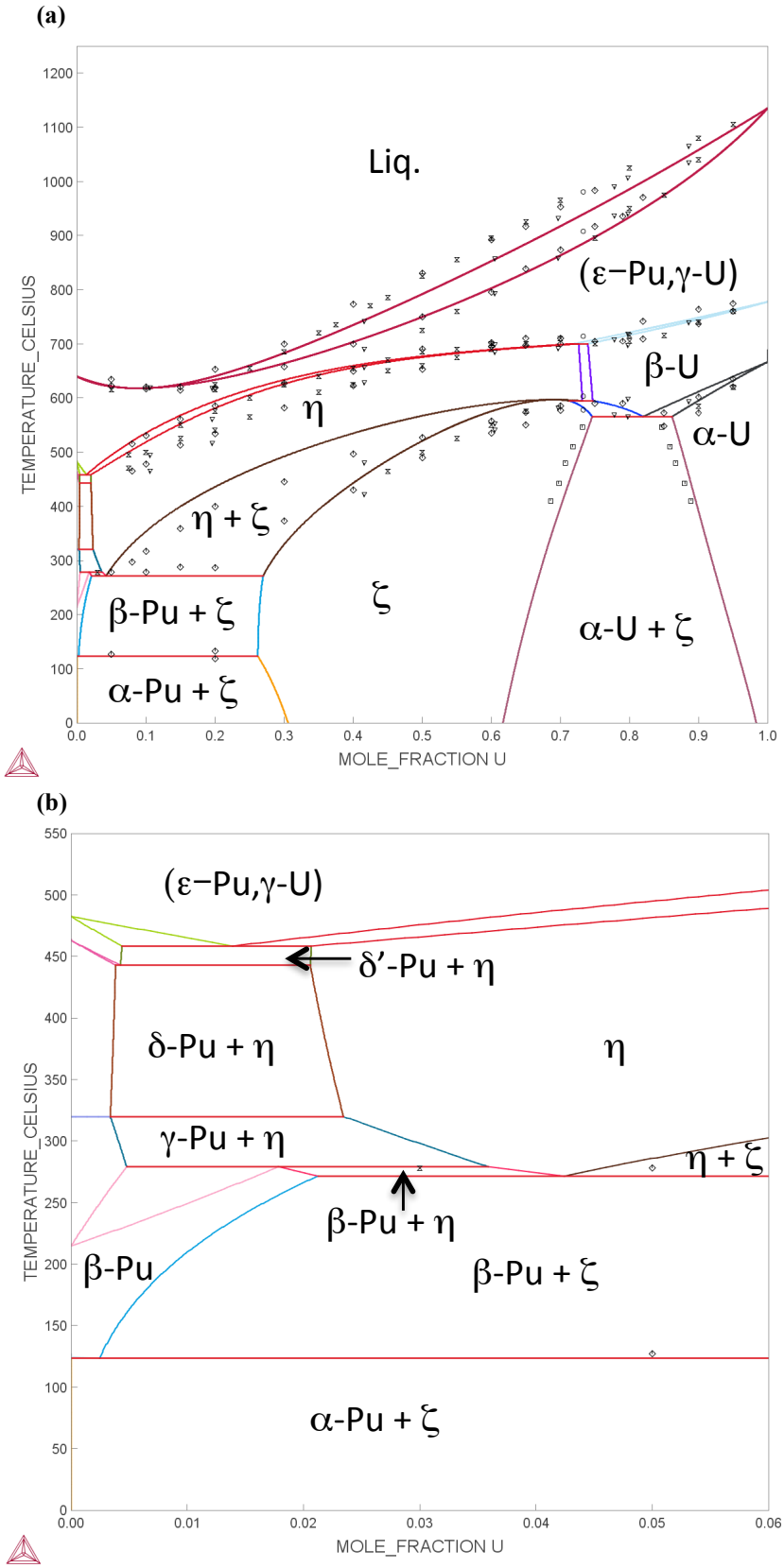

Figure II.8. (a) Calculated Pu-U phase diagram with (b) an emphasis on the Pu-rich region with data taken from [II.20] (1999).

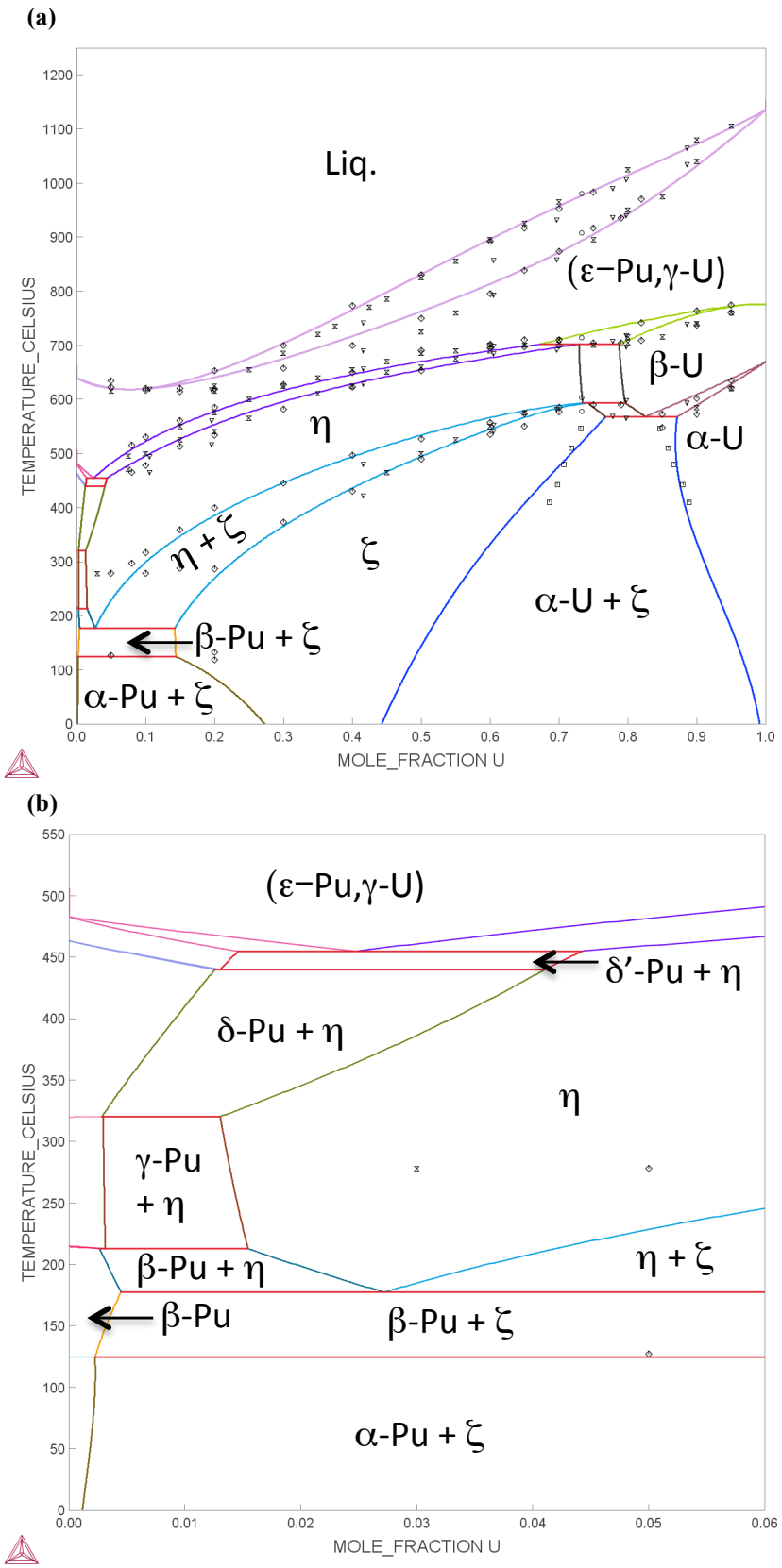

Figure II.9. (a) Calculated Pu-U phase diagram with (b) an emphasis on the Pu-rich region with data taken from [II.21] (2010).

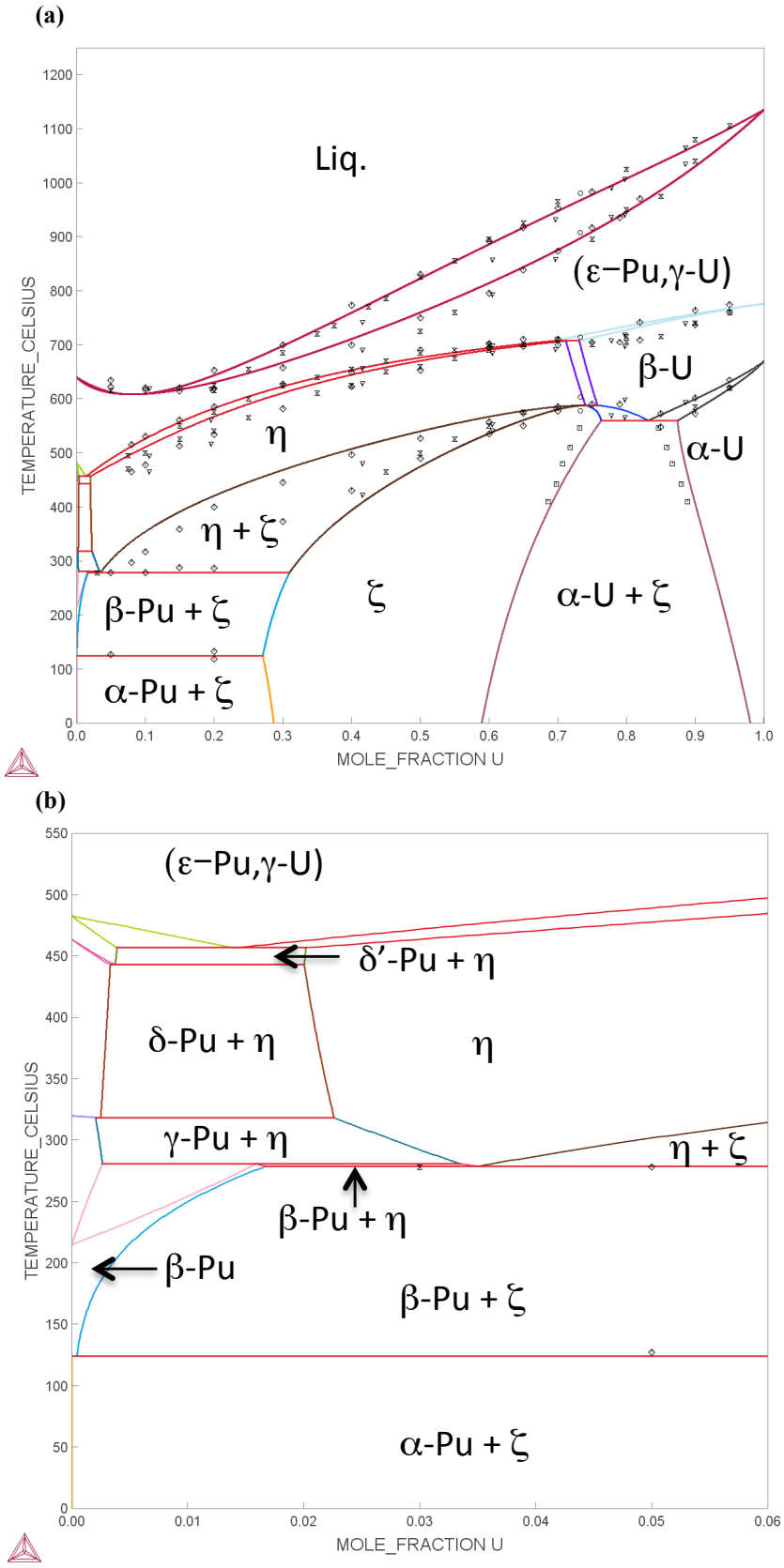

Figure II.10. (a) Re-assessed Pu-U phase diagram with (b) an emphasis on the Pu-rich region.

Table II.3. Invariant reactions (numbered from 1 to 10) for the Pu-U system.

Reaction type	Reaction	U (at.%)			T (°C/K)	Reference
1 Congruent	Liquid ↔ bcc	12	12		610 / 883	[II.1]
					626 / 899	[II.7]
		8.9	8.9		618 / 891	[II.20]
		7.7	7.7		619 / 892	[II.21]
		8.1	8.1		608 / 881	Present work
2 Peritectoid	$bcc + \beta - U \leftrightarrow \eta$	≈70	≈80	≈70.5	705 / 978	[II.1]
					702 / 975	[II.7]
		72	74	72.6	700 / 973	[II.20]
		67.3	78.7	72.9	702 / 975	[II.21]
		69.6	73.2	71.2	707 / 980	Present work
3 Peritectoid	$\beta - U + \eta \leftrightarrow \zeta$	≈82	≈67.5	≈72	590 / 863	[II.1]
					586 / 859	[II.7]
		74.7	73.2	71.4	595 / 868	[II.20]
		79.6	73.5	74.3	593 / 866	[II.21]
		75.8	74.0	74.1	588 / 861	Present work
4 Eutectoid	$\beta - U \leftrightarrow \alpha - U + \zeta$	≈82	≈85	≈74	560 / 833	[II.1]
					557 / 830	[II.7]
		82	86.2	74.6	566 / 839	[II.20]
		82.5	87.2	76.8	568 / 841	[II.21]
		83.1	87.4	76.3	560 / 833	Present work
5 Eutectoid	$bcc \leftrightarrow \delta' - Pu + \eta$	≈2.5	≈1.3	≈4.5	455 / 728	[II.1]
					454 / 727	[II.7]
		1.4	0.4	2.1	459 / 732	[II.20]
		2.5	1.5	4.4	455 / 728	[II.21]
		1.4	0.4	2.0	457 / 730	Present work
6 Eutectoid	$\delta' - Pu \leftrightarrow \delta - Pu + \eta$	≈1.2	≈0.3	≈4	442 / 715	[II.1]
					437 / 710	[II.7]
		0.43	0.38	2.1	443 / 716	[II.20]
		1.31	1.26	4.1	440 / 713	[II.21]
		0.37	0.33	2.0	443 / 716	Present work
7 Peritectoid	$\delta - Pu + \eta \leftrightarrow \gamma - Pu$	≈0.2	≈2	≈0.3	320 / 593	[II.1]
					318 / 591	[II.7]
		0.34	2.3	0.34	320 / 593	[II.20]
		0.28	1.3	0.29	320 / 593	[II.21]
		0.25	2.3	0.21	318 / 591	Present work
8 Peritectoid	$\gamma - Pu + \eta \leftrightarrow \beta - Pu$	≈0.8	≈2.9	≈2	280 / 553	[II.1]
					282 / 555	[II.7]
		0.48	3.6	1.8	279 / 552	[II.20]
		0.31	1.5	0.27	213 / 486	[II.21]
		0.26	3.3	1.6	281 / 554	Present work
9 Eutectoid	$\eta \leftrightarrow \beta - Pu + \zeta$	≈3	≈2	≈26	278 / 551	[II.1]
					278 / 551	[II.7]
		4.2	2.1	27	272 / 545	[II.20]
		2.7	0.45	14.3	177 / 450	[II.21]
		3.5	1.7	31	279 / 552	Present work
10 Eutectoid	$\beta - Pu \leftrightarrow \alpha - Pu + \zeta$	≈0.1	≈0	≈30	125 / 398	[II.1]
					121 / 394	[II.7]
		0.25	0	26	124 / 397	[II.20]
		0.23	0.23	14.4	124 / 397	[II.21]
		0.04	0	27.1	124 / 397	Present work

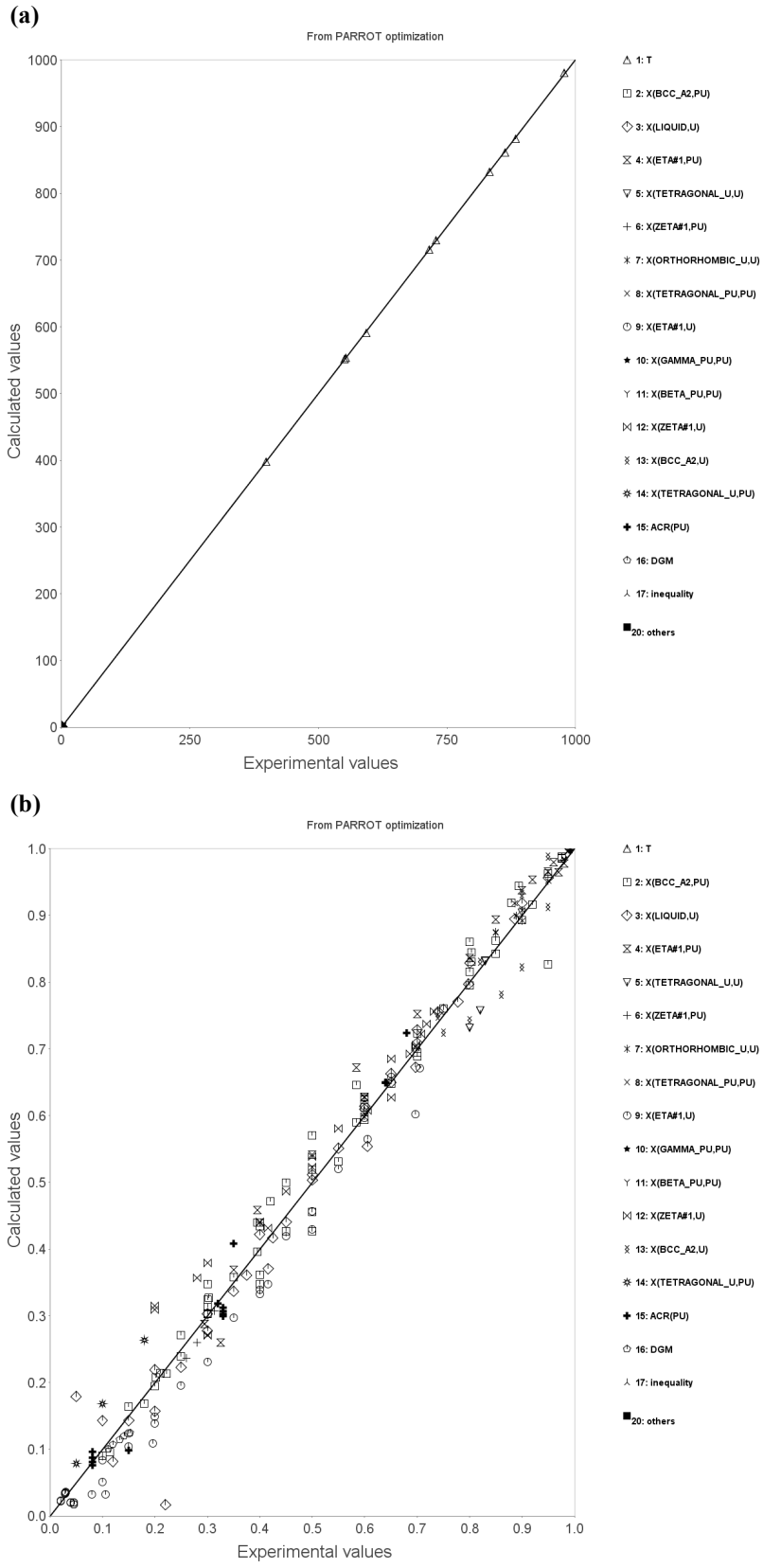

Figure II.11. Calculated vs experimental values after the present assessment for (a) the temperature of the 10 invariant reactions (K) and (b) all other data (composition of phases and phase fractions, activities…).

II.4 Discussion

II.4.1 Invariant reactions

➢ ***Invariant 1: Liquid and bcc phase.***

The liquidus and solidus curves presented in Fig. II.10.a, resulting from the present assessment, are in good agreement with experiments. By comparing with the results of Kurata (Fig. II.8-9.a), the curves are comparable to those from the 2010 assessment. In fact, the 1999 assessed liquidus was slightly lower than most of the experimental data. Thus, the liquid phase boundary of our Pu-U phase diagram should be consistent with the phase boundaries in the Pu-U-Zr system (as the 2010 assessment).

As observed experimentally [II.1], a continuous liquid-plus-solid region forms at high temperatures between ε-Pu and γ-U, and reveals a minimum at about 8 at.% U and 608°C (Table II.3). This value is in quite good agreement with the experimental ones defined by Ellinger *et al*. (12 at.% U and 610°C) [II.1], Rosen *et al.* (9 at.% U and 624±2°C) and Okamoto *et al*. (11 at.% U and 619°C) [II.14], and to the previous calculated ones by Leibowitz *et al*. (10 at.% U and 626°C) [II.18], Kurata in 1999 (~9 at.% U and 618°C) [II.20] and in 2010 (~8 at.% U and 619°C) [II.21]. As the congruent reaction in the Pu-U system seems to be not well characterized, the weight in the present assessment was mainly put on the experimental data defining the solidus and liquidus curves, and not on the congruent reaction itself during the assessment.

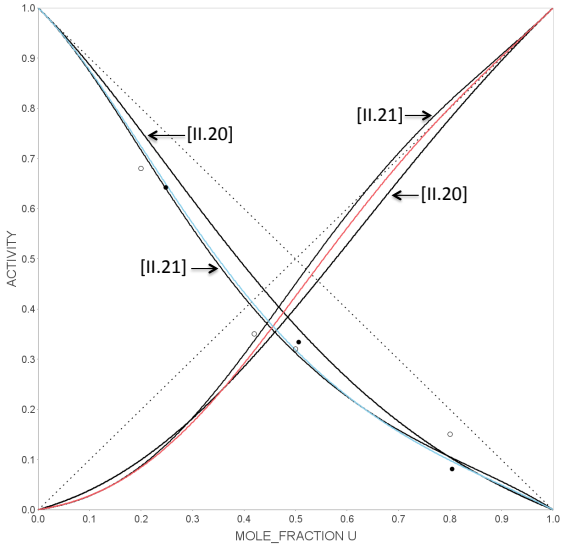

Figure II.12. Calculated Pu and U activities at 1200°C in the Pu-U system: present assessment (colored lines) and previous assessments from Kurata (black lines, [II.20-21]). The dotted lines represent the ideality of the liquid alloys assumed by Leibowitz *et al.* [II.18]. The experimental data (symbols, Pu-activity) are taken from [II.22]. Reference state: Pu and U in the liquid state at 1200°C.

The resulting liquidus and solidus lines are in a very good agreement with experiments, except for the Pu-rich region where experimental data are sparse. This can also explain the slight difference between our minimum and the previous ones.

The activity calculations of Pu and U in the liquid phase at 1200°C are presented in Fig. II.12, and compared with previous simulations and experiments. The Pu-activity curve is similar to the one determined by Kurata in 2010 and agrees with experiment. The U-activity curve has the same shape than the one of the 2010 assessment but is mainly shifted in between the 1999 and 2010 assessments data.

Starting from the energetic values obtained at T = 0 K from *ab initio* calculations for the bcc phase (which are in good agreement with the 1999 assessment [II.20], contrary to those most recently re-assessed [II.21]), ***the high temperature region of the Pu-U phase diagram has been successfully re-assessed.***

- ***Invariants 2-4: intermediate phases in U-rich region***

As reported in Table II.3, invariant temperatures are generally closer to those performed by Ellinger *et al*. than by other authors. The η phase that is formed by a peritectoid reaction (invariant 2) agrees well with experiment for the bcc and η phase compositions. However, the β-U assessed domain is wider than experimentally observed in Ref. [II.1]. β-U phase reaches ~27 at.% Pu from our calculation and only 20 at.% Pu experimentally. This result is similar to the 1999 Kurata's assessment. This author mentioned that the largest difference between experimental data and his work is observed in the phase boundary between the η and β-U phases (The calculated η / β-U phase boundary is shifted closer to the Pu-rich region than the experimental boundary). Leibowitz *et al*. also indicated their two-phase η + β-U field differs from the experiments but that there are essentially no experimental data in that area [II.18]. In addition, the bcc + β-U is not clearly defined yet. The present width of this domain is in between the 1999 and 2010 Kurata's assessments. In parallel, and based on information from diffusion studies obtained during a private communication with M. C. Petri and M. A. Dayananda, Leibowitz *et al*. indicate that the two-phase bcc + β-U field may be wider. As a consequence, ***more experimental data are needed to characterize the η + β-U and bcc + β-U phase domains of stability***.

By lowering the temperature, the ζ phase is formed by a peritectoid reaction from the η + β-U phases (invariant 3). This reaction is quite well described by the present assessment and the 2010 Kurata's assessment and not by the 1999 and Leibowitz ones (Fig. II.8.a and Fig. II.2.b). The calculated eutectoid at 560°C (β-U → ζ + α-U) is in good agreement with published data (invariant 4). Finally, the ζ + α-U domain that extends down to room temperature seems more coherent than the 2010 Kurata's assessment (even if more experimental data would be needed).

- ***Invariants 5-10: Pu-rich region***

The two eutectoid reactions at high temperature (5: bcc → δ'-Pu + η and 6: δ'-Pu → δ-Pu + η) are in quite good agreement with experiment. The chemical composition of the phases is better described by the 2010 Kurata's assessment (Table II.3). However, the experimental composition of the η phase is not clearly determined (see dashed lines in Fig. II.1.b). The resulting bcc + η region of the present assessment is better reproduced compared with the 1999 Kurata's assessment (too high) but is not as good as the 2010 one. As for the δ + δ' region, the calculated two-phase field is always very narrow compared with experiment. This results is supported by the small enthalpy of transition from δ- to δ'-Pu [II.19].

By decreasing temperature, two peritectoid (7,8) and one eutectoid (9) reactions involving the η phase occur (Table II.3). Reactions 7 and 8 are not described in details experimentally (Fig. II.1.b). Indeed Ellinger *et al*. underlined that the β-Pu + η field is the only one for which no direct experimental evidence was obtained. But, the present assessment is in agreement with these reactions. The eutectoid (9: η → β-Pu + ζ) is well described by the present and 1999 Kurata's assessment. It is interesting to note that reactions 8 and 9, involving the η phase, are out of the range of the 2010 Kurata's assessment (Table II.3). ***According to currently available experimental data, it seems difficult to assess properly the η phase in both the high and low temperature regions of the Pu-U phase diagram***. Thus, Kurata mentioned in 2010 that thermodynamic data for the η phase are required for further improvement of the database [II.21].

Finally, the last eutectoid is well reproduced in the present work and in agreement with the 1999 Kurata's assessment but not the 2010 one (ζ phase composition). This

confirms the validity of the 2010 Kurata's assessment at high temperatures, and of the 1999 one at low temperatures with ***the present assessment combining both advantages***.

II.4.2 Metastable behavior

- ***One-phase metastable regions***

Metastable phase diagrams are plotted by considering only one phase at a time: namely the liquid, bcc, η, and ζ phases (Fig. II.13-15). The liquid phase displays a miscibility gap at low temperature that extends to pretty high temperature for the 2010 Kurata's assessment compared with the other two assessment results. It is difficult to interpret the pure liquid behavior at low temperature, however results are consistent among the databases.

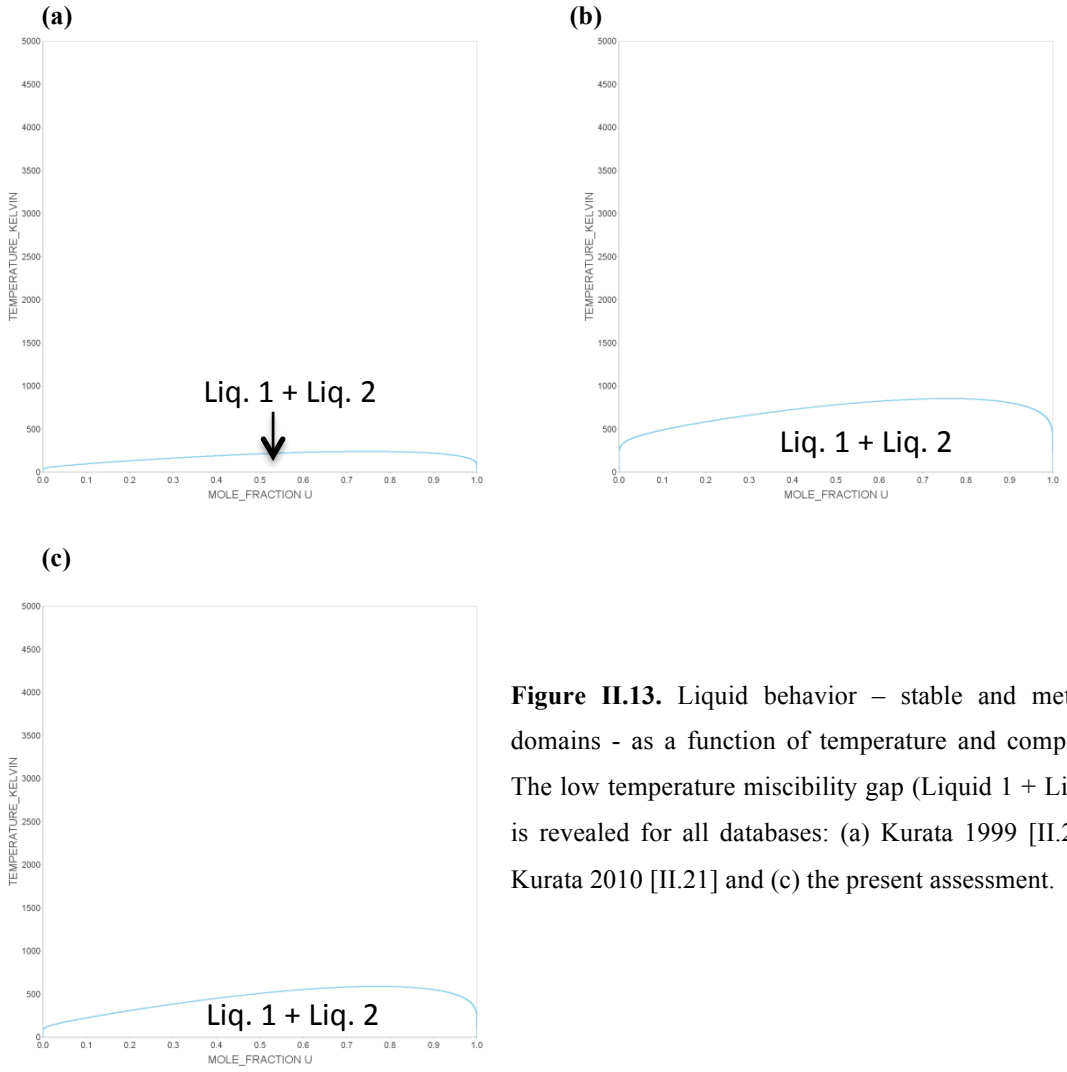

Figure II.13. Liquid behavior – stable and metastable domains - as a function of temperature and composition. The low temperature miscibility gap (Liquid 1 + Liquid 2) is revealed for all databases: (a) Kurata 1999 [II.20], (b) Kurata 2010 [II.21] and (c) the present assessment.

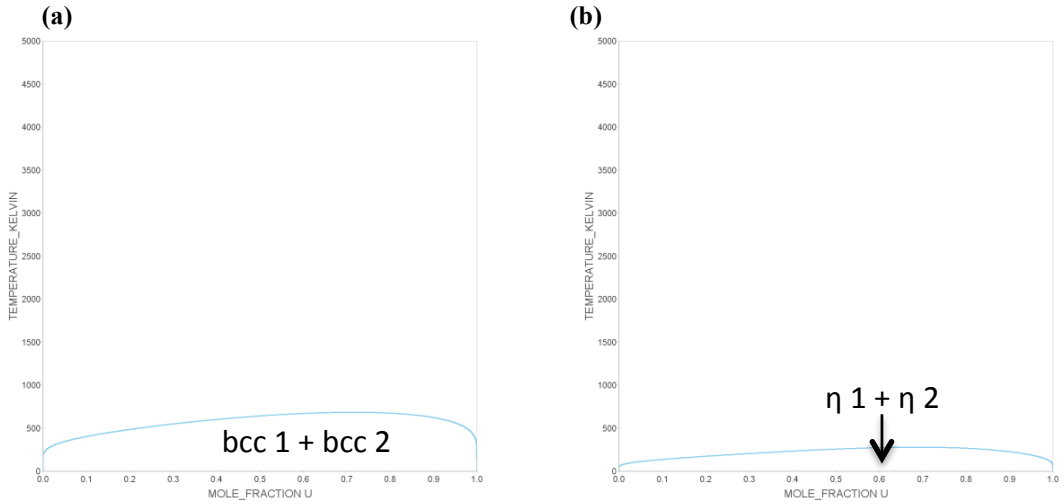

Figure II.14. (a) bcc and (b) η phase miscibility gaps at low temperature, from Kurata 2010 [II.21].

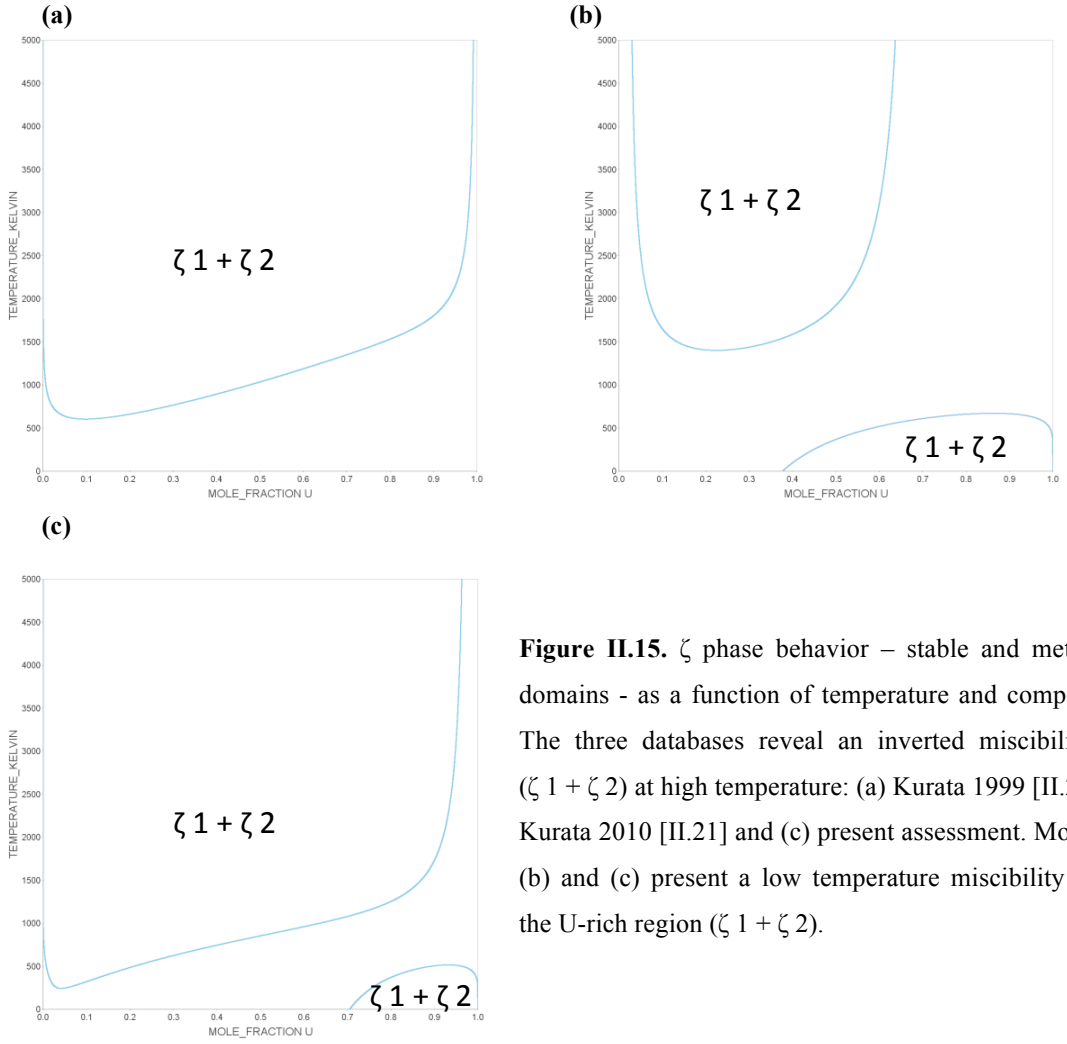

Figure II.15. ζ phase behavior – stable and metastable domains - as a function of temperature and composition. The three databases reveal an inverted miscibility gap (ζ 1 + ζ 2) at high temperature: (a) Kurata 1999 [II.20], (b) Kurata 2010 [II.21] and (c) present assessment. Moreover, (b) and (c) present a low temperature miscibility gap in the U-rich region (ζ 1 + ζ 2).

The liquid miscibility gaps are the result of the interaction parameters presented in Table II.2. Indeed, the first positive value of the Redlich-Kister parameter (0^{th} order) induces a phase separation tendency. As the negative T-term is very low at low temperature, a miscibility gap is generated. Thus, the more the first value is positive the more the miscibility gap extends at high temperature (if the T-terms are similar). As observed in Fig. II.13, the most important miscibility gap is associated to the greatest T-independent ^{0}L value in Table II.2 (in bold blue). At higher temperatures, the T-term becomes predominant and stabilizes the liquid solution. The important point is that ***any inverted miscibility gap in the liquid phase is revealed at elevated temperatures***, a gap which in reality does not exist and which can be produced during assessment.

The bcc phase doesn't reveal a miscibility gap for the 1999 Kurata's and the present assessments. This result is consistent with Fig. II.4 where both heats of formation at 0 K are negative. The corresponding *ab initio* values and Kurata's parameters are reported in Table II.2. On the contrary, the huge positive heat of formation at 0 K (Fig. II.4, ~5000 J/mole) and the corresponding interaction parameters (Table II.2) of the 2010 Kurata's assessment for the bcc phase produces a miscibility gap (Fig. II.14.a). The 2010 Kurata's assessment presents also a low-temperature miscibility gap for the η phase (Fig. II. 14.b).

Finally, the ζ phase behavior is reported in Fig. II.15. All thermodynamic data reveal an inverted miscibility gap over a wide composition range. In addition, a low-temperature miscibility gap is observed in the two most recent assessments. ***This complex behavior of the metastable ζ phase is difficult to explain but sheds light on questions about this phase***. Indeed, many parameters are required (Table II.2) to fit properly the experimental data. The ζ phase is stable over wide ranges of composition and temperature (Fig. II.1). However, many options for the assumed region of stability are hypothetical (dashed lines) and even the crystallographic structure is uncertain. In fact, Ellinger *et al*. [II.1] reported that the crystal structure of ζ might be tetragonal with an axial ratio of unity at room temperature. ***Further experiments and crystallographic studies will be necessary to characterize the ζ phase and to understand its relationship with α-, β-Pu, and α-U.***

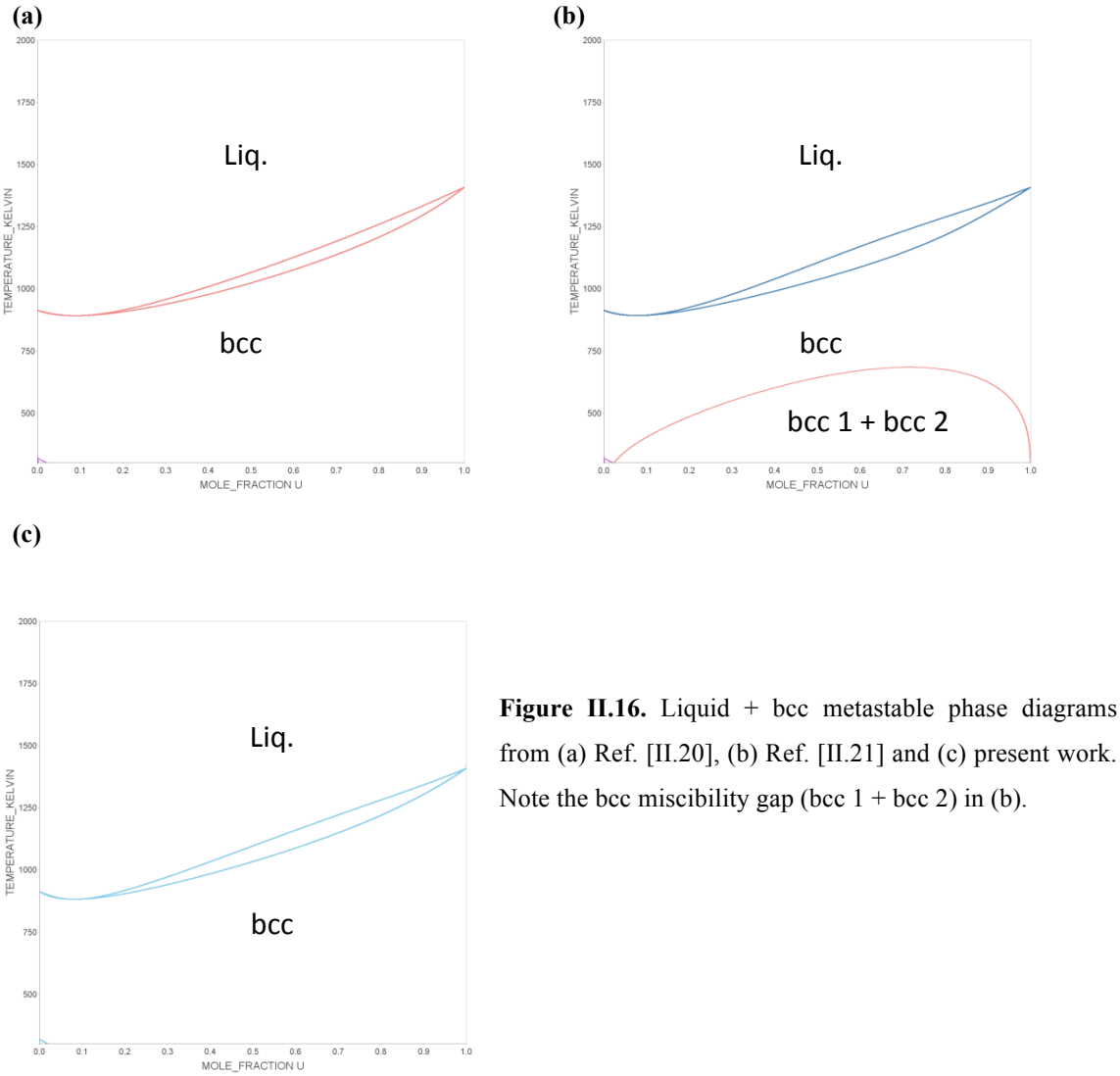

Figure II.16. Liquid + bcc metastable phase diagrams from (a) Ref. [II.20], (b) Ref. [II.21] and (c) present work. Note the bcc miscibility gap (bcc 1 + bcc 2) in (b).

➢ ***Two-phase metastable regions***

As for the one-phase metastable phase diagrams, metastable phase diagrams considering only two phases can be plotted. The high-temperature phases (Liquid and bcc) are shown on Fig. II.16. As expected, the 2010 Kurata's assessment reveals a bcc miscibility gap at low temperature. Surprisingly enough, all assessments indicate that liquid re-appears at very low temperature and U-composition. This result doesn't come from the interaction parameters but from an ***internal inconsistency in the pure SGTE database between Liquid-Pu and ε-Pu (bcc)*** [II.26] ***already underlined*** in Ref. [II.27].

The same result is found for the Liquid + η metastable phase diagrams (Fig. II.17). A small η miscibility gap appears at very low temperature for the 2010 Kurata's assessment (Fig. II.14.b). However, the proper closer of the two-phase domains towards the pure elements and the non re-appearance of the η phase at high temperature are positive features.

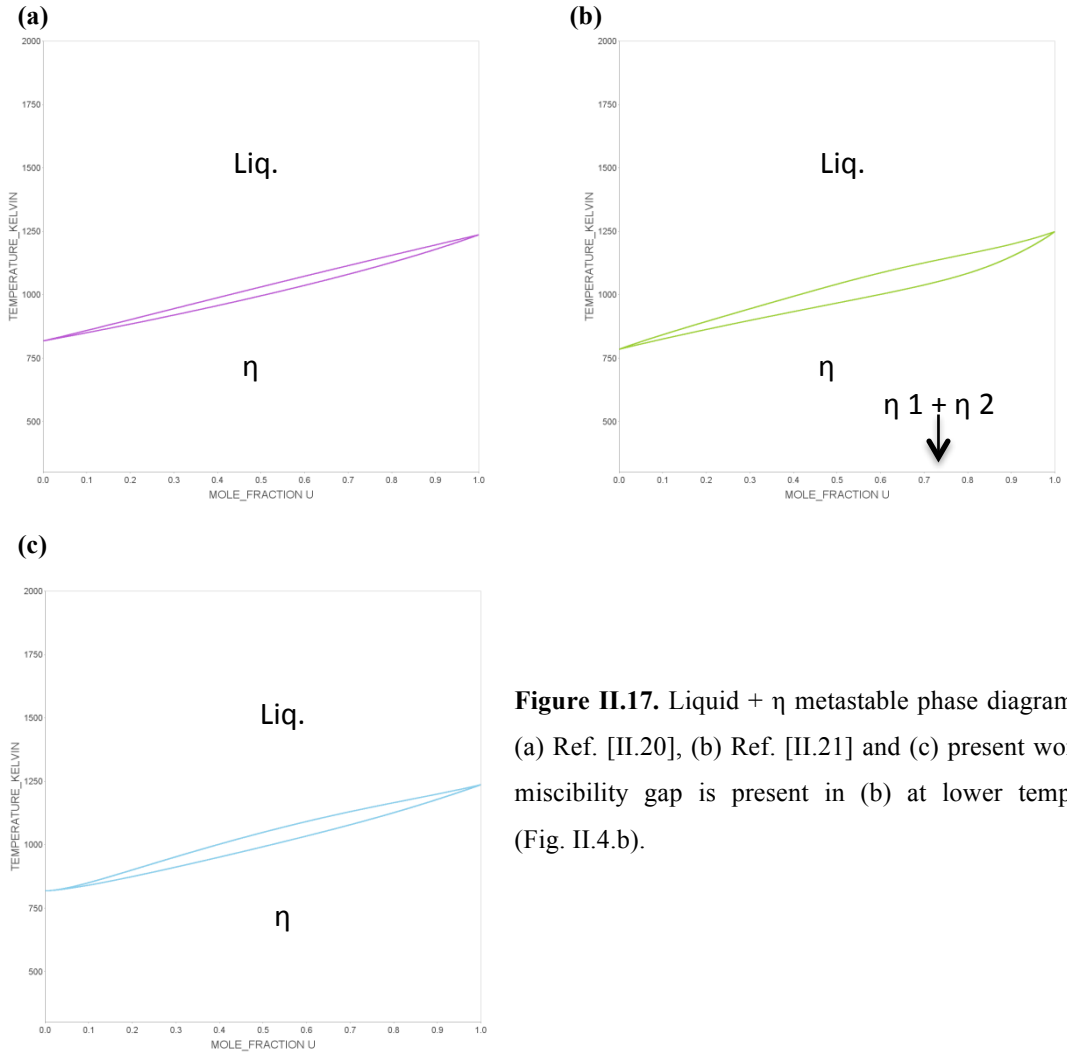

Figure II.17. Liquid + η metastable phase diagrams from (a) Ref. [II.20], (b) Ref. [II.21] and (c) present work. A η miscibility gap is present in (b) at lower temperature (Fig. II.4.b).

Finally, the Liquid + ζ metastable phase diagrams are presented on Fig. II.18. The simplest behavior is obtained for the 2010 Kurata's assessment in which the two-phase domain close at each phase diagram boundary with a ζ miscibility gap at low temperature corresponding to the one observed in Fig. II.15.b. For the 2010 Kurata's and present assessments, the high-temperature inverted ζ miscibility gap disappears in favor of the

stable Liquid phase. The strangest case is the 1999 Kurata's assessment in the Pu-rich region. A small amount of the inverted ζ miscibility gap remains, and the Liquid + ζ phases region re-appears at low temperature. In addition to the ζ miscibility gap observed at low temperature in Fig. II.18.c, note that the Liquid + ζ region does not close in the present assessment. This may be due to +500 J/mole added to bcc-Pu to define the Gibbs energy of pure Pu in the ζ phase (Table II.1), hence perhaps the two-phase region ζ + Liquid that extends at 0 K without closing since there is no other phase to compete with ζ. It may also be due to the re-entrant liquid phase (compared with bcc, or 500 J/mole + bcc) occurring at low temperatures for pure Pu [II.26-27]. As it appears at low temperature, and as the ζ phase does not re-appear at high temperature – and without any new data, authors conclude that there is not too much to worry about concerning the self-consistency of the database.

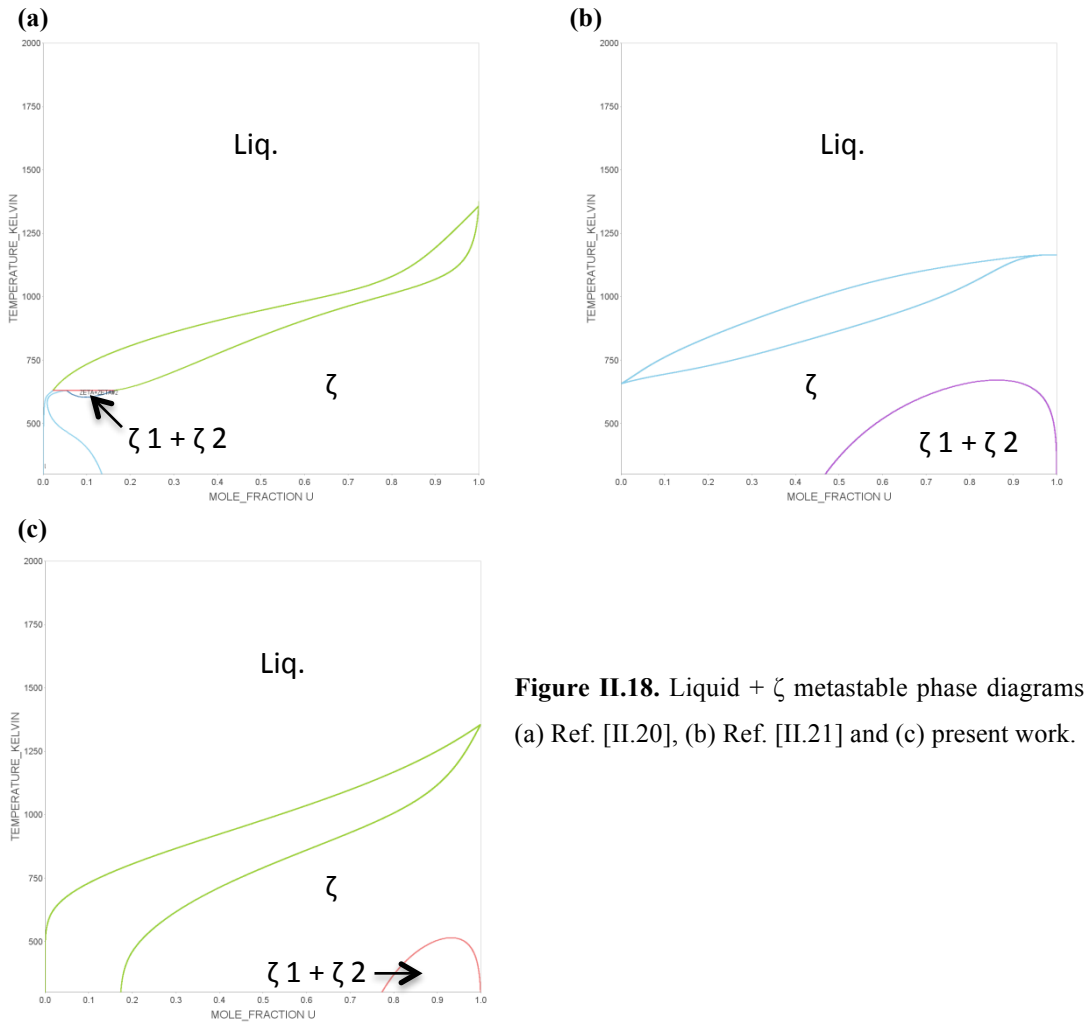

Figure II.18. Liquid + ζ metastable phase diagrams from (a) Ref. [II.20], (b) Ref. [II.21] and (c) present work.

II.5 Conclusion & Guidelines for additional experimental studies

The revisited assessment of the Pu-U system starting from *ab initio* energetics for the bcc phase is, in general, in better agreement with the experimental data than the results of the previous calculations. It combines most of the qualities of the 1999 and 2010 Kurata's assessments with new validated energetic values. However, several points still have to be clarified or checked and can be used as guiding lines for future experimental studies:

- ***Liquidus / Solidus***

The chemical composition and the temperature of the congruent reaction between the Liquid and bcc (ε-Pu, γ-U) phases are still subject of debate. As for the liquidus and solidus curves, disparity among the experimental data exists. Thus, new experimental studies only dedicated to the refinement of this part of the phase diagram (and so to the related thermodynamic database) would be useful for a validated extrapolation to higher-order systems.

- ***U-rich region***

The U-rich region is of importance regarding its application in nuclear power plants. However, the high-temperature bcc + β-U is still difficult to assess and especially the eutectoid reaction leading to the formation of the η phase. Moreover, unpublished studies assume that the two-phase bcc + β-U field may be wider. New experiments would possibly confirm the extent of the bcc + β-U domain and the η phase precipitation mechanism.

An other interesting point about the β-U phase is that since this phase contains at least 10 at.% Pu in solution, it can be retained at room temperature by water-quenching from the β-U region. This influence of Pu on β-U phase stability is annealed in the γ-U region. Indeed, whereas a 15 at.% Pu alloy quenched from the β-U region is retained as β-U at room temperature, the same composition quenched from the γ-U region will transform to α-U [II.1]. Thus, the β-U phase extend and stability should be studied.

- ***Pu-rich region***

Let us recall that the amount of relevant experimental data is limited in the narrow region of the Pu-rich region below approximately 527°C [II.20]. For instance, no direct experimental data on the availability of the β-Pu + η two-phase region exist. As a consequence, this part of the phase diagram has to be considered cautiously. Moreover, most of the invariant reactions deal with the poorly characterized η and ζ intermediate phases. Thus, a dedicated study of Pu-0-15 at.% U alloys between room temperature to the melting temperature (including the congruent reaction) would provide useful information geared toward a validation of the thermodynamic database.

- ***Intermediate phases***

The two intermediate phases, namely η and ζ, are revealed as single phases over wide ranges of composition and temperature in the Pu-U phase diagram. Moreover, if one considers the two-phase domains containing η or ζ, intermediate phases are present in about 90% of the phase diagram below ~700°C. The two unique and large enough domains to mention that do not involve the intermediate phases are the α-U and β-U phases. In spite of the fact that these intermediate phases contribute widely to the Pu-U phase diagram, they are still poorly known.

The high-temperature η phase is assumed to be tetragonal – with high uncertainty [II.1] – and reveals two-phase domains limits that are really unknown. First, the η + β-U region is clearly undefined. Then, many boundaries between η and Pu-phases are simply "artistically drawn" (Fig. II.1.b). The high-temperature bcc + η region is very difficult to model properly in agreement with the low-temperature transformations involving η phase with β-Pu phase (see 1999 and 2010 Kurata's assessments, Leibowitz assessments and the present assessment). Finally the η + ζ domain is not well characterized at both Pu-rich and U-rich sides. The phase transformations, especially at the U-rich side between intermediate phases and U-phases, are unclear.

The ζ phase, stable between ~30-70 at.% U, exhibits a complex structure [II.1]. More recently, Lawson *et al.* [II.28] characterized the ζ phase at one alloy composition ($Pu_{0.60}U_{0.40}$), and revealed that the structure is similar to α-Mn with 58 atoms in an approximately ***cubic unit cell***. However, the authors concluded that because of the large

number of short- and long-bonds, the structure is a very complicated self-intermetallic compound, and thus there is still plenty work to do. A theoretical crystallographic study is planned to understand the relationship between α-Pu, β-Pu, and α-U with the ζ phase. In addition, they obtained data on the η phase but were not able to satisfactory index the diffraction pattern, and decided to postpone the discussion – ***underlying the complexity of the η phase***. Concerning the ζ phase, new bulk properties and photo-electron spectroscopy measurements were performed in 2011 [II.29]. However, as mentioned recently in literature, ***although the Pu-U alloy system forms the basis for fast reactor metallic fuels containing plutonium and for the popular MOX fuel for most existing light-water reactors, few physical property studies have been carried out on the binary system alone***. One of the reasons commonly invoked is "the extremely poor properties of samples containing even small amount of the ζ phase" [II.30-31].

- ***Guidelines***

In order to highlight new results leading to the complete characterization and to a deeper understanding of the Pu-U phase diagram, and not only to take previous results – even the hypothetical dashed lines – as granted, new experiments are necessary. However, since sample preparation is challenging, the present CALPHAD assessment allows us to select some alloy compositions that are of the greatest interest and to design critical experiments. Indeed, the thermo-chemical results derived from the optimization process are available and can be directly compared with differential scanning calorimetry (DSC) measurements that provide a quantitative determination of the heats of transformation. In addition, *in situ* XRD experiments and dilatometric measurements can provide data on crystallographic structures (phase determination as a function of temperature and composition) and on invariant reactions (phase fractions, phase composition, temperature of transformation). These data, assembled to build a phase diagram, could be used to validate and to finally fine-tune the present assessment.

Three alloy compositions are proposed in Fig. II.19. The first one (1 at.% U) would help to understand the interaction of U with pure Pu-phases. The second one, $Pu_{0.40}U_{0.60}$, would focus on the study of the two intermediate phases (η and ζ). The last one, $Pu_{0.22}U_{0.78}$, would be necessary to shed light on the reactions between intermediate

phases and U-phases (especially the α-U and β-U phases). For instance, the property diagrams – phase fraction and chemical composition as functions of temperature – presented on Fig. II.20 can be directly compared to XRD results and dilatometry measurements. In addition, molar enthalpy and its derivative *dH/dT* presented in Fig. II.21 can be checked out and compared with DSC results.

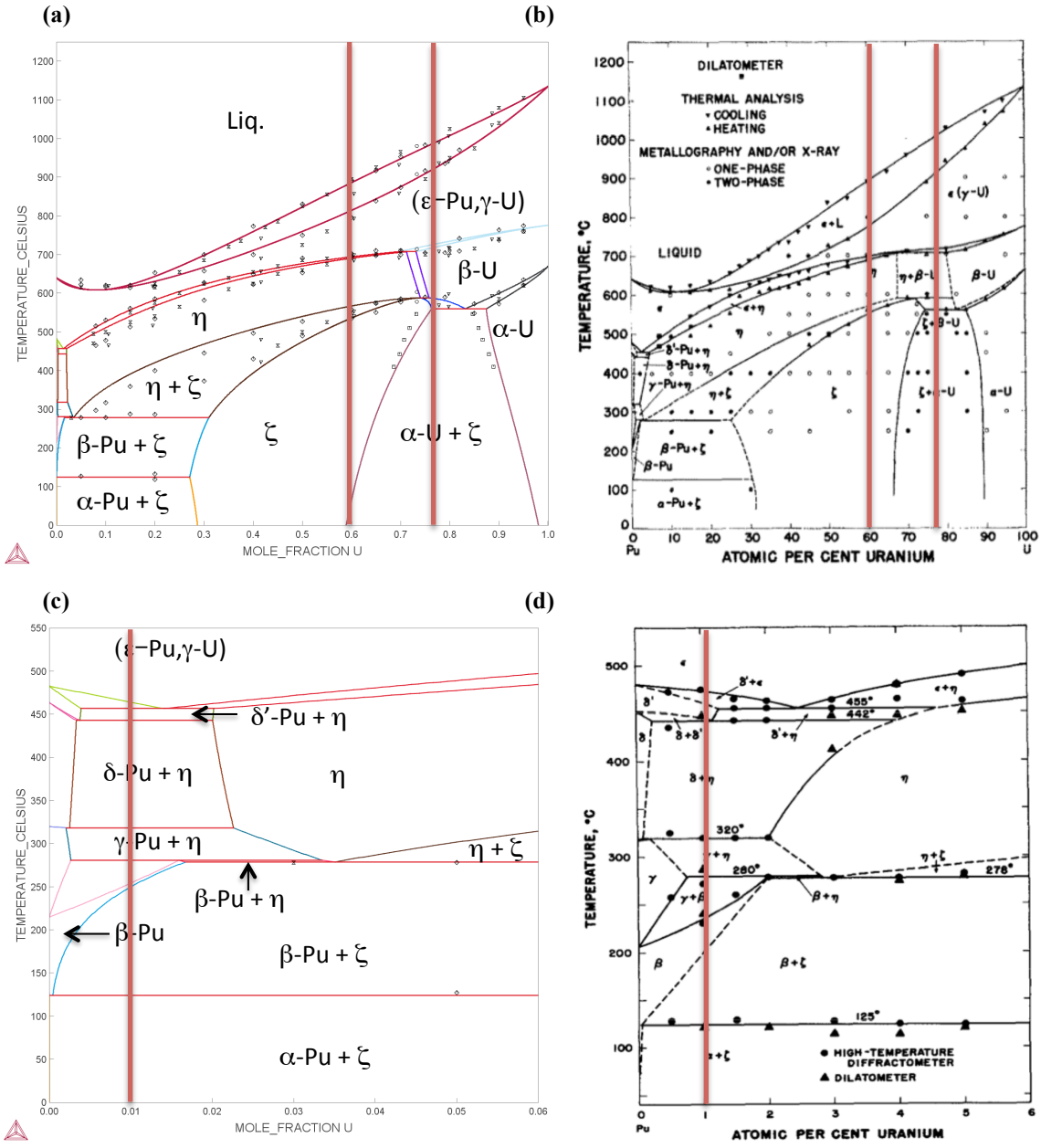

Figure II.19. Newly assessed (a,c) and experimental Pu-U phase diagram [II.1]. The vertical lines represent the three compositions of interest.

(a)

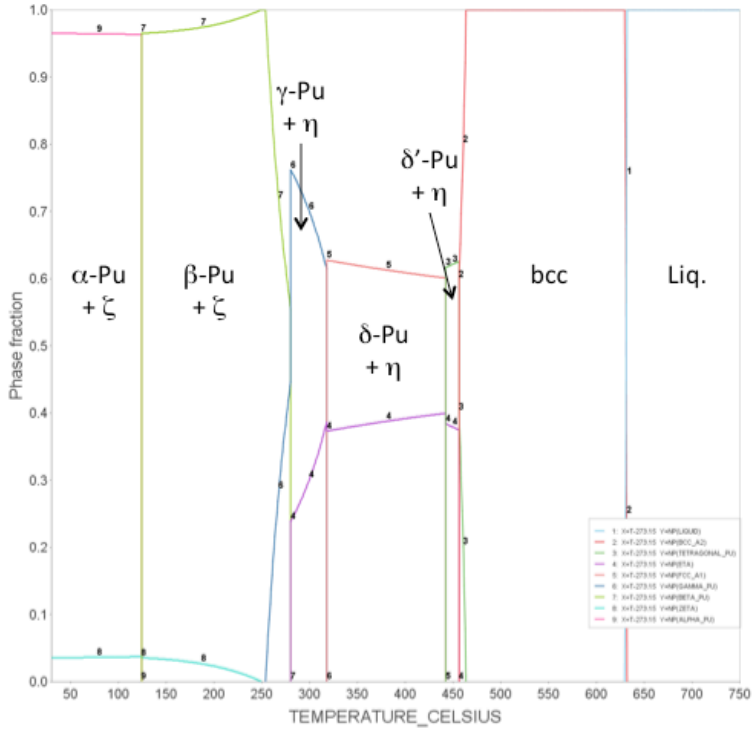

(b)

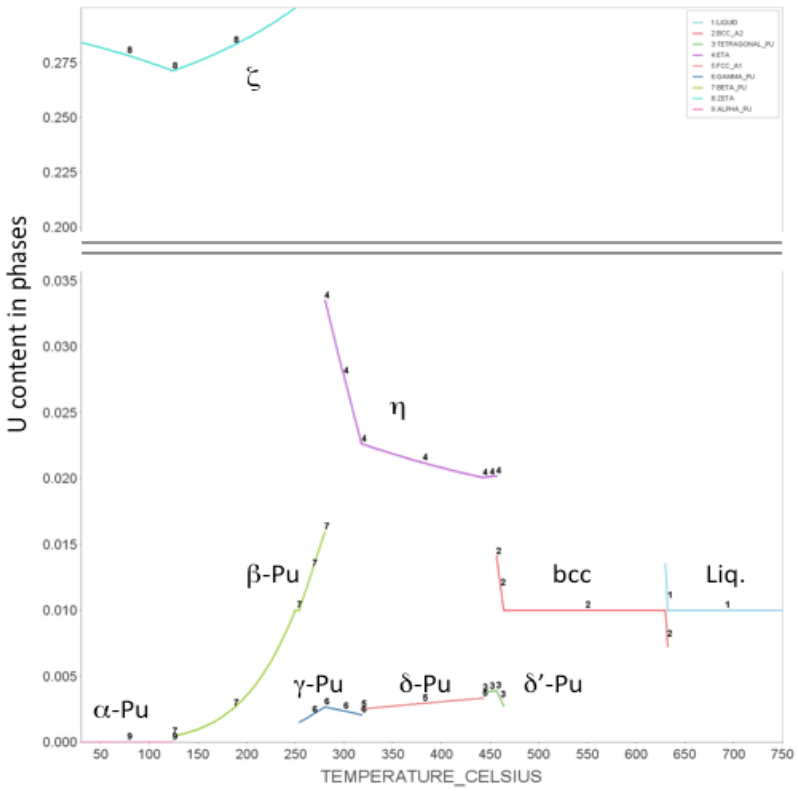

Figure II.20. Property diagrams for the $Pu_{0.99}U_{0.01}$ alloy. (a) Phase fraction versus temperature and (b) phase composition versus temperature.

(a)

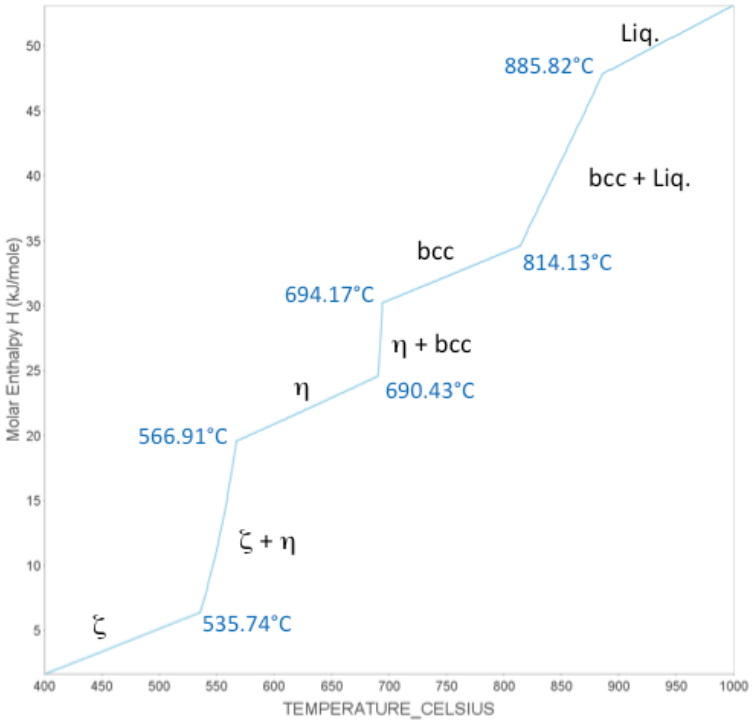

(b)

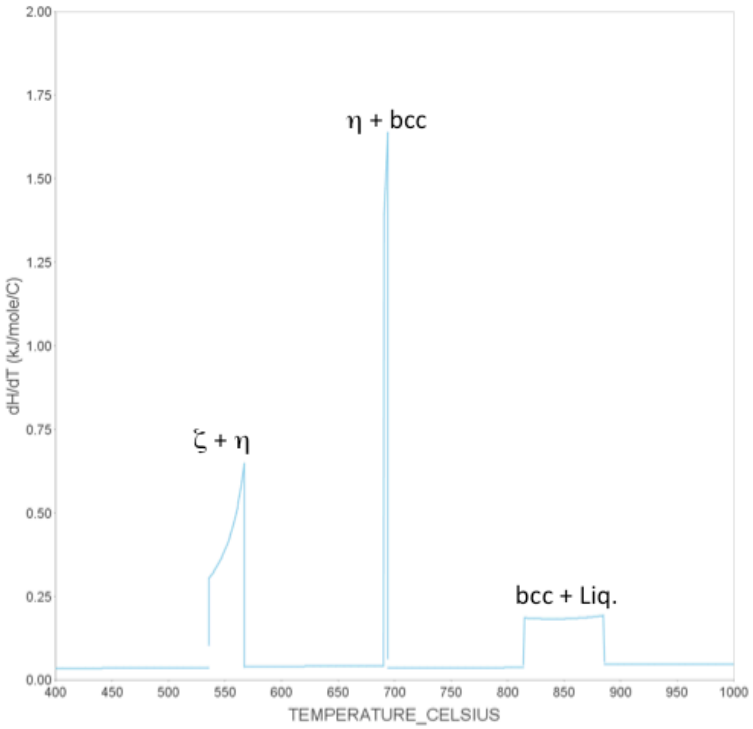

Figure II.21. Property diagrams of the $Pu_{0.40}U_{0.60}$ alloy. (a) Molar enthalpy and (b) its derivative dH/dT versus temperature.

III The Pu-Ga system

The thermodynamic assessment of the Pu-Ga system has been performed by Turchi (LLNL) *et al*. in 2004 [III.1-2]. A complete description of the literature, data and models used is given in Ref. [III.1]. Moreover, CEA – Centre de Valduc has already capitalized on this thermodynamic database by successfully studying martensitic transformation and reversion in Pu-1 at.% Ga alloy [III.3-4]. Thus, this database has proved its efficiency and has been considered unchanged in the present work (Fig. III.1).

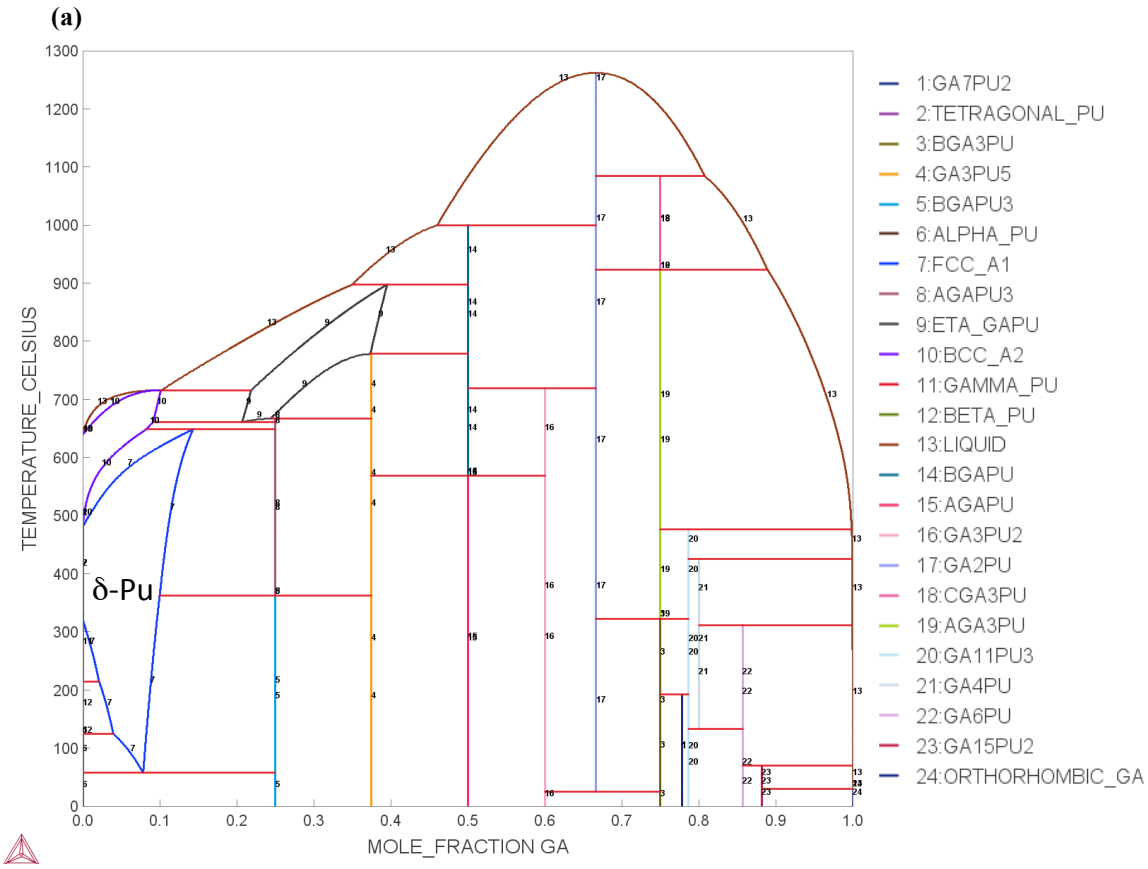

(b)

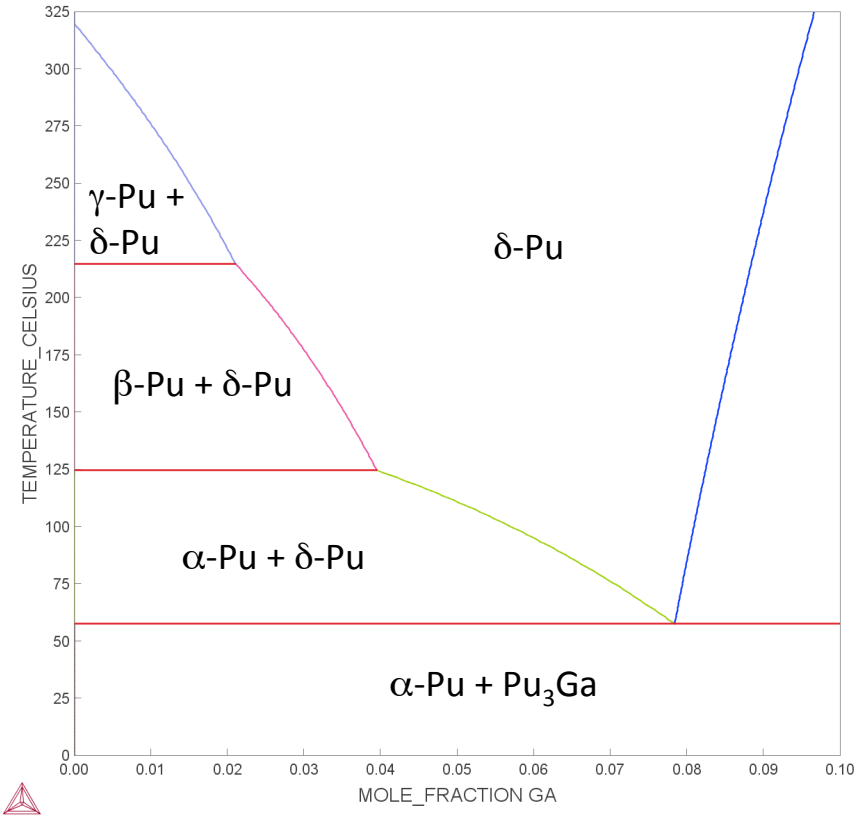

Figure III.1. (a) Calculated Pu-Ga phase diagram with (b) an emphasis on Pu-rich region, from database published in Ref. [III.1].

IV The U-Ga system

IV.1 State of the art

The thermodynamic assessment of the U-Ga system was carried out in 2008 by Wang *et al*. in the framework of the CALPHAD method with the use of experimental data including thermodynamic properties and phase equilibria [IV.1]. As reported by these authors, the experimentally determined U-Ga phase diagram consists of three intermetallic compounds (Ga_3U, Ga_2U and Ga_3U_2) and the liquid phase [IV.2]. In addition, the existence of the GaU and Ga_5U_3 compounds were also mentioned in Refs. [IV.3-4]. However, the decomposition reaction and the phase stability of these compounds are unknown (and consequently not taken into account during the assessment). Phase equilibria in the U-rich region were estimated by Gardie *et al*. from the measured activity of Ga in the liquid phase [IV.5]. Based on the experimental data reported in previous works [IV.2-4], the phase diagram of the U-Ga system was reported by Okamoto [IV.6] (see Fig. IV.1a).

Johnson and Feder [IV.7] and Lebedev *et al.* [IV.8] derived the thermodynamic properties of the UGa_3 compound based on fused salt EMF measurements. Alcock *et al*. [IV.9] measured the Ga vapor pressures and derived the Gibbs free energies of formation of the Ga_3U, Ga_2U and Ga_3U_2 compounds. The thermodynamic data of the U-Ga system reported in previous works [IV.7-9] were reviewed by Chiotti *et al*. [IV.10]. More recently, Prabhahara *et al* [IV.11] determined the enthalpies of formation of the intermetallic compounds Ga_3U and Ga_2U using high-temperature liquid Ga solution calorimetric measurements. Wang *et al*. underlined [IV.1] that disagreements exist among the thermodynamic data of the compounds determined by molten salt EMF [IV.7-8], vapor pressure measurements [IV.9], and reaction calorimetry [IV.11] methods. After considering the experimental methods and conditions, Wang *et al.* decided to use the data reported by Gardie *et al.* [IV.2] and Prabhahara *et al.* [IV.11] for the assessment of the U-Ga system (reported in Fig. IV.1b). The calculated phase diagram is in good agreement with the experimental data, except for the liquid composition in the reaction $L + Ga_2U \rightarrow Ga_3U_2$. The authors mentioned that the calculated liquid composition in this reaction is 48.3 at.% Ga, but is 44.5 at.% Ga in Buschow's report [IV.2].

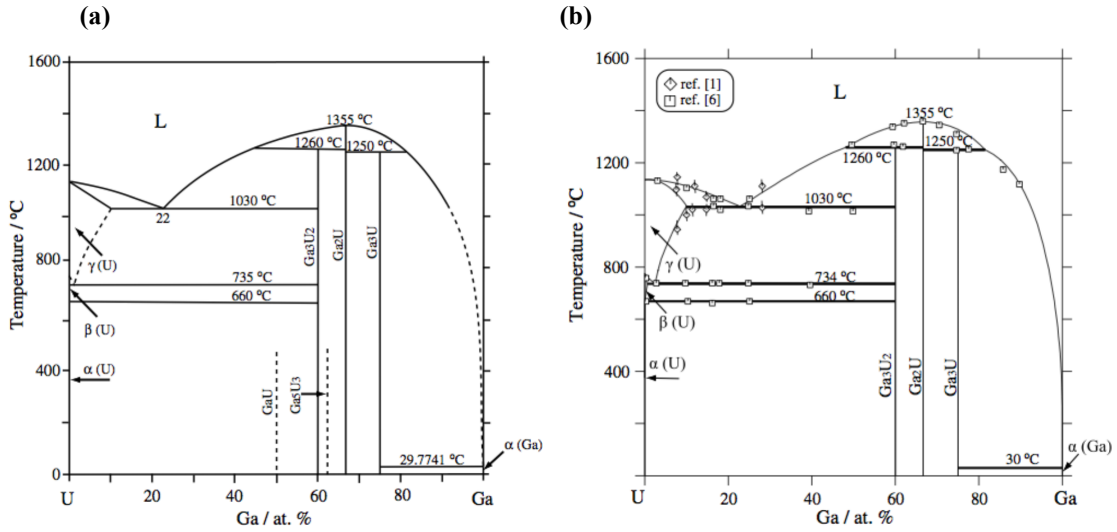

Figure IV.1. (a) Phase diagram of the U-Ga system reviewed by Okamoto [IV.6] and (b) calculated by Wang *et al*. [IV.1] and compared with experimental data from Refs. [IV.2, IV.5] (corresponding to ref. [6] and ref. [1] in the original figure, respectively).

The enthalpies and entropies of formation of the intermetallic compounds calculated by Wang *et al.* at 400°C are reported in Fig. IV.2. In addition, the calculated activities of Ga and U in the liquid phase at 1127°C and 1377°C compared with experimental data are reproduced in Fig. IV.3 from [IV.1]. Reasonable agreement is observed.

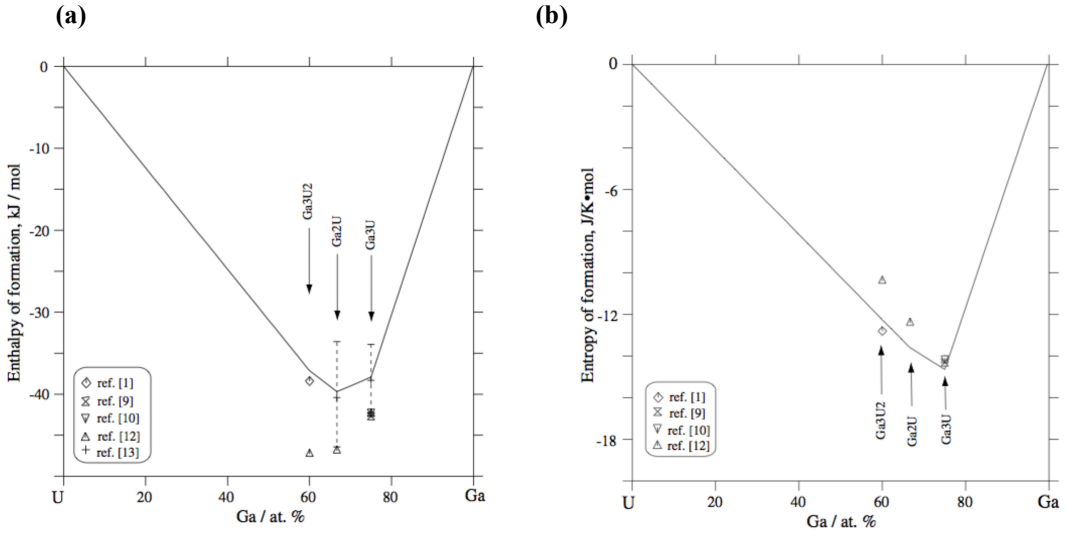

Figure IV.2. Calculated (a) Enthalpies and (b) entropies of formation of intermetallic compounds at 400°C in the U-Ga system by Wang *et al.* [IV.1]. The experimental symbols [ref.1, refs. 9-10, refs. 12-13] in the original figures correspond to Refs. [IV.5, IV.6-7, IV.9-10], respectively.

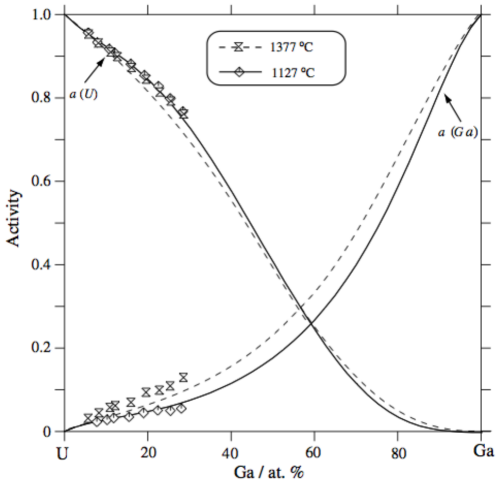

Figure IV.3. Calculated activity (reported from [IV.1]) of Ga and U in the liquid phase at 1127°C and 1377°C compared with experimental data from [IV.2]. (The reference states: liquid (Ga) phase and liquid (U) phase).

IV.2 Reproduction of the thermodynamic database

The optimized thermodynamic parameters for the U-Ga system published by Wang *et al.* [IV.1] have been integrated in our thermodynamic database (see Appendix C). The U-Ga phase diagram, presented in Fig. IV.4, is well reproduced. The invariant reactions reported in Table IV.1 are also in agreement with the assessment by Wang *et al*. and Buschow's report [IV.1-2].

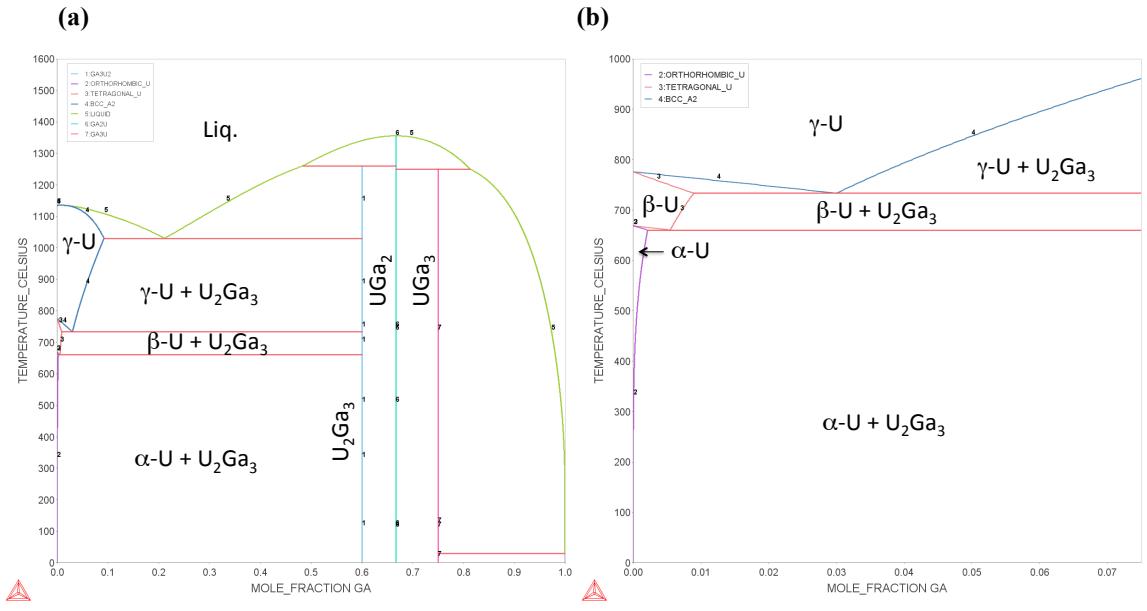

Figure IV.4. (a) U-Ga phase diagram reproduced from the assessment of Wang *et al.* [IV.1] with (b) a magnification of the U-rich region.

Table IV.1. Invariant reactions in the U-Ga system.

Reaction type	Reaction	Ga (at.%)			T (°C)	Reference
Eutectic	L → γ(U) + Ga_3U_2	22.0	9.2	60	1030	IV.2
		21.4	9.9	60	1030	IV.1
		21.1	9.2	60	1030	Present work
Peritectic	L + Ga_2U → Ga_3U_2	44.5	66.7	60	1260	IV.2
		48.3	66.7	60	1260	IV.1
		48.4	66.7	60	1260	Present work
Congruent	L → Ga_2U	66.7			1355	IV.2
		66.7			1355	IV.1
		66.7			1356	Present work
Peritectic	L + Ga_2U → Ga_3U	81.5	66.7	75	1250	IV.2
		81.5	66.7	75	1250	IV.1
		81.3	66.7	75	1250	Present work
Eutectoid	γ(U) → Ga_3U_2 + β(U)	≈ 1	60	≈ 0.1	735	IV.2
		3	60	0.1	734	IV.1
		3	60	0.9	733	Present work
Eutectoid	β(U) → Ga_3U_2 + α(U)	-	60	-	660	IV.2
		0.05	60	0.01	660	IV.1
		0.5	60	0.2	660	Present work

The only noticeable difference between the results published by Wang *et al*. and values calculated from our database (based on their interaction terms) is the Ga content in α- and β-U for the two low-temperature eutectoid reactions (Table IV.1). A magnification of this region – based on our calculations - is presented in Fig. IV.4.b. One may suspect that this difference originates from the definition of the unaries. Indeed, the thermodynamic functions published by Wang *et al*. for α-U, β-U and α-Ga are slightly different from those given by Dinsdale [IV.12] that are considered as the "standard" reference. However since the Ga content is very low in this region (below 1 at.%) and the experimental results are sparse, this difference is not critical.

Finally, the enthalpy and entropy of formation of the intermetallic compounds were calculated, and are reported in Table IV.2 (with the reference states being the liquid (Ga) and α-U phases). The results are similar to those presented in Fig. IV.2. As for the activity curves, the results presented in Fig. IV.3 and the calculated ones are identical (Fig. IV.5).

Table IV.2. Enthalpy and entropy of formation of intermetallic compounds at 400°C.

	Ga_3U_2	Ga_2U	Ga_3U
Enthalpy of formation (kJ/mole)	-37.147	-39.682	-37.894
Entropy of formation (J/K•mole)	-12.2	-13.5	-14.6

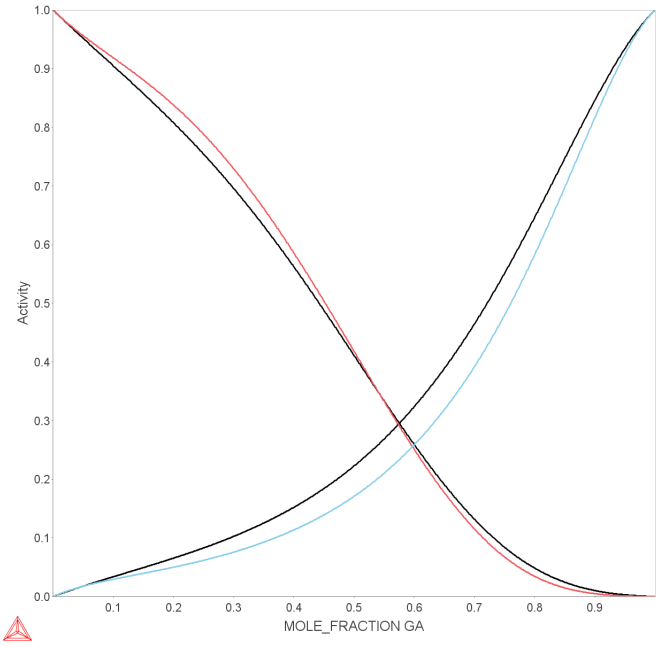

Figure IV.5. Calculated activity of Ga and U in the liquid phase at 1127°C (colored curves) and 1377°C (black curves). The reference states: liquid (Ga) phase and liquid (U) phase.

IV.3 Conclusion

Based on the assessment of Wang *et al*. [IV.1], that summarized the results of previous experimental studies [IV.2-5, IV.7-11], the U-Ga phase diagram and the associated thermodynamic properties were evaluated and successfully integrated in our thermodynamic database. From an experimental point of view, it would be interesting to characterize the U-rich part of the phase diagram in more details (see the two eutectoid reactions in Table IV.1 and Fig. IV.4.b).

V The Pu-U-Ga ternary system

The thermodynamic data of the three binaries, Pu-U, Pu-Ga and U-Ga, have been put together in a consistent way, see Fig. V.1 and Appendix C, to calculate isothermal sections of the Pu-U-Ga alloy system.

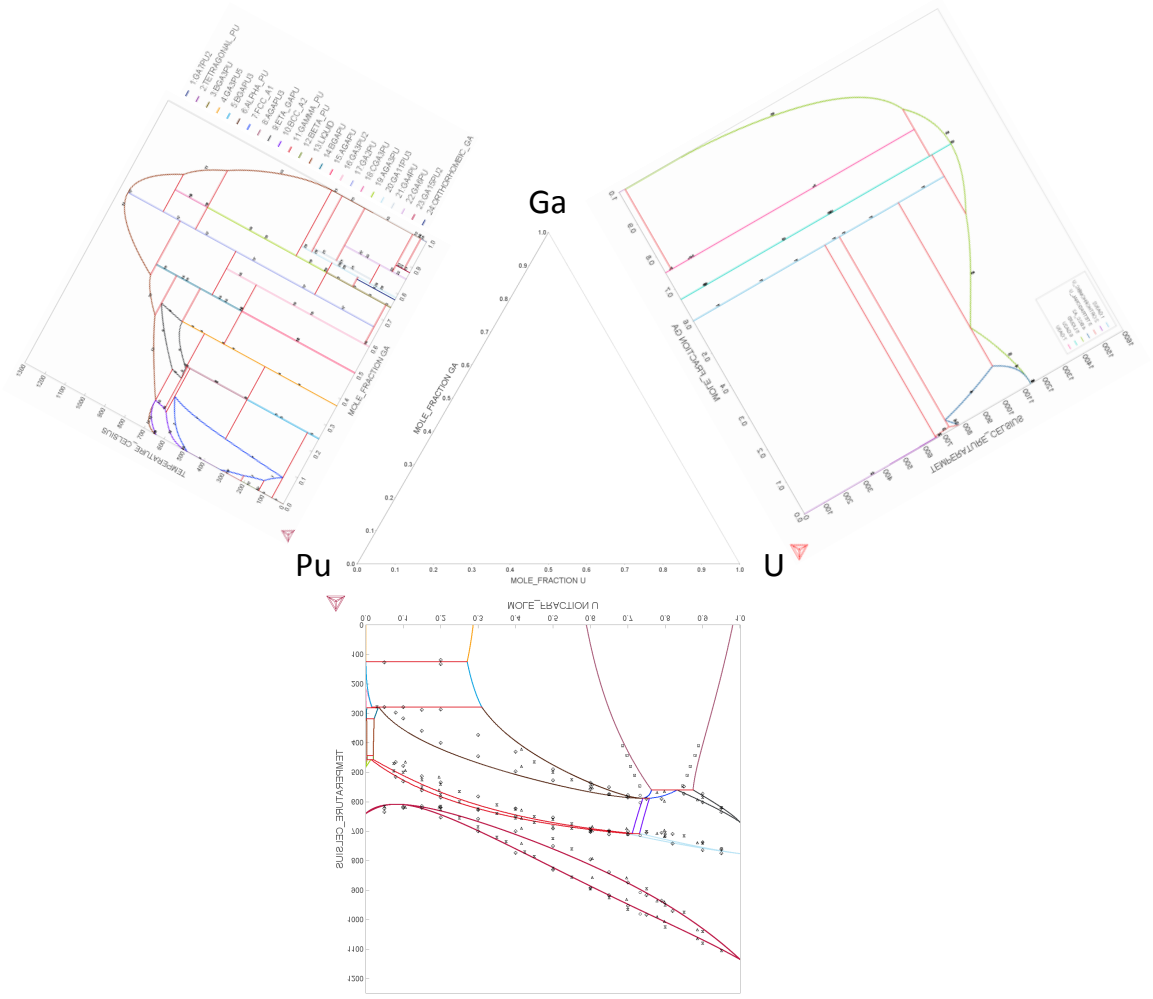

Figure V.1. Summary of the thermodynamic data in terms of binary phase diagram data for Pu-U, Pu-Ga and U-Ga, that are used to predict the phase properties in the ternary Pu-U-Ga alloy system.

Let us recall that no experimental data are available for this ternary system. As a consequence, the solubility of Ga in Pu-U intermediate phases (η and ζ), and of U in η-Pu-Ga phase is considered as inexistent. Moreover, contribution to the excess Gibbs energy from ternary interaction parameters is ignored. For instance, the interactions in the bcc phase – where the 3 elements are present – are based on the interactions from the

binaries without any ternary correction. Finally, because of the complexity of the ternary systems in general, it is anticipated that other compounds that strictly form in the ternary system may exist. This implies that the isothermal sections that are presented below should be considered as representations if not in the stable equilibrium, at least of the metastable equilibrium state. When more experimental data on new compounds in the ternary system will be available, it will be possible to introduce their thermodynamic description in the database.

Isothermal sections of the Pu-U-Ga phase diagram are shown in Fig. V.2. It should be mentioned that because of the complexity of these phase diagrams in terms of the number of phases that can form at various temperatures, only a few major phase equilibria, in some instances, have been indicated in the isothermal sections for the sake of clarity. As observed, the first compound to precipitate is UGa_2. Then, by decreasing temperature, the U_2Ga_3 and UGa_3 are precipitating. This sequence of precipitation is in agreement with the U-Ga binary system (Fig. IV.4). On the Pu-Ga rich side, $PuGa_2$ precipitates at high temperature, and is followed by $PuGa_3$, PuGa, Pu_5Ga_3 and the numerous compounds revealed in the Pu-Ga binary system (Fig. III.1). The Ga-rich corner (top of the isothermal sections presented in Fig. V.2) remains liquid until ~30°C, as expected. It is interesting to note that the liquidus surface is continuously reduced to the Pu-rich corner (except for a tiny Ga-rich corner). The bcc phase starts to extend from the U-corner to the Pu-corner from 1100°C to 800°C. Then, the α-U, β-U and η phases appear along the Pu-U axis. Finally, the Pu-rich corner at 0°C is composed of pure α-Pu phase, Pu_3Ga compound and intermediate ζ phase.

In order to understand the phase transformations involved around the Pu-rich corner, detailed representations of calculated equilibria within the following composition: Ga (0 → 8 at.%) and U (0 → 20 at .%); and as functions of temperature are presented in Fig. V.3. At 700°C, the bcc phase (mainly ε-Pu integrating a few percent of U) starts to precipitate from the Pu-Ga binary boundary. By decreasing the temperature down to 600°C, the liquid phase completely disappears. This result is in agreement with the solidus curves observed in the Pu-Ga and Pu-U binaries (cf. Fig. III.1 and Fig. II.10, respectively).

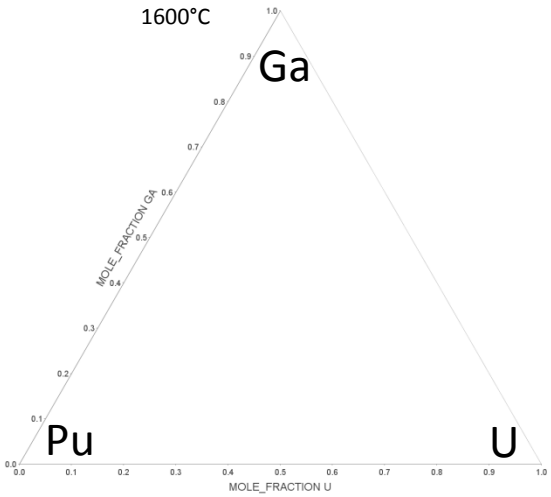
1600°C
Ga
Pu
U
MOLE_FRACTION GA
MOLE_FRACTION U

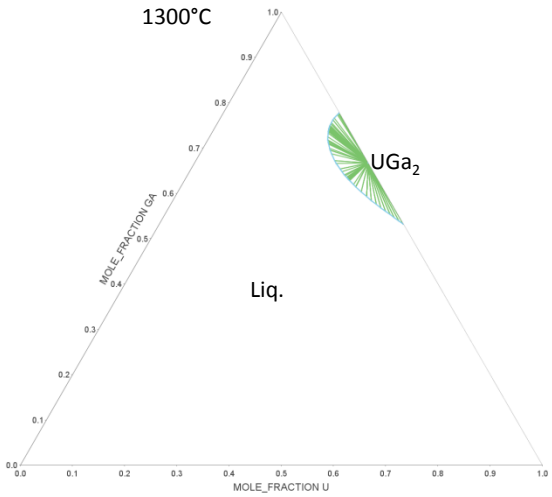
1300°C
UGa2
Liq.
MOLE_FRACTION GA
MOLE_FRACTION U

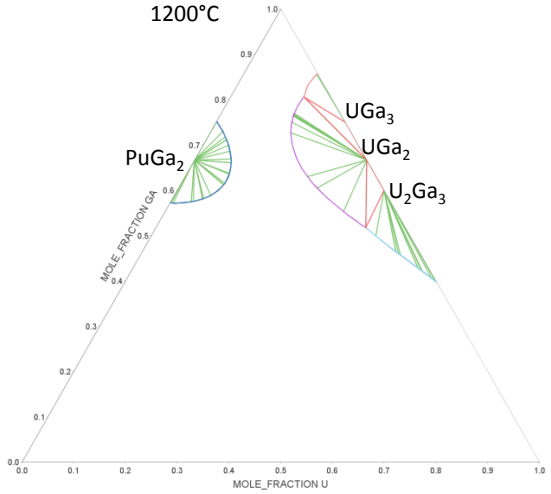
1200°C
PuGa2
UGa3
UGa2
U2Ga3
MOLE_FRACTION GA
MOLE_FRACTION U

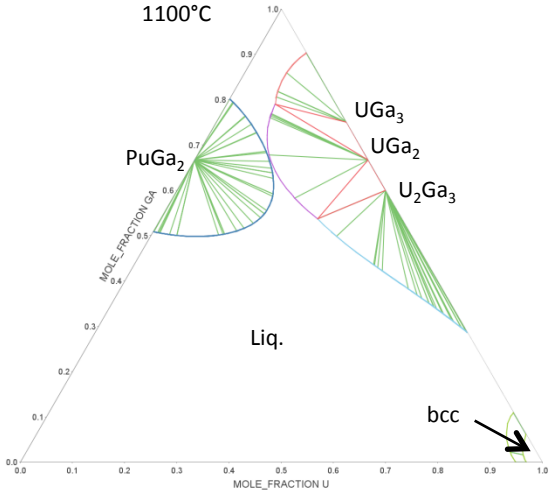
1100°C
PuGa2
UGa3
UGa2
U2Ga3
Liq.
bcc
MOLE_FRACTION GA
MOLE_FRACTION U

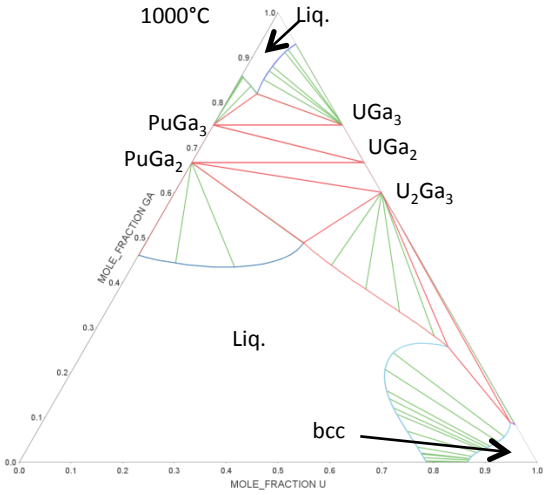
1000°C
Liq.
PuGa3
PuGa2
UGa3
UGa2
U2Ga3
Liq.
bcc
MOLE_FRACTION GA
MOLE_FRACTION U

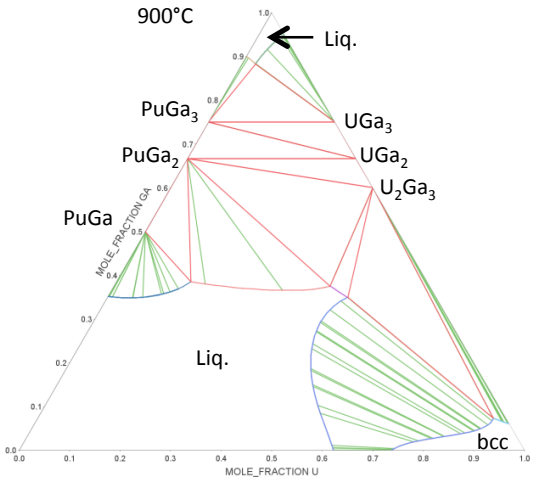
900°C
Liq.
PuGa3
PuGa2
PuGa
UGa3
UGa2
U2Ga3
Liq.
bcc
MOLE_FRACTION GA
MOLE_FRACTION U

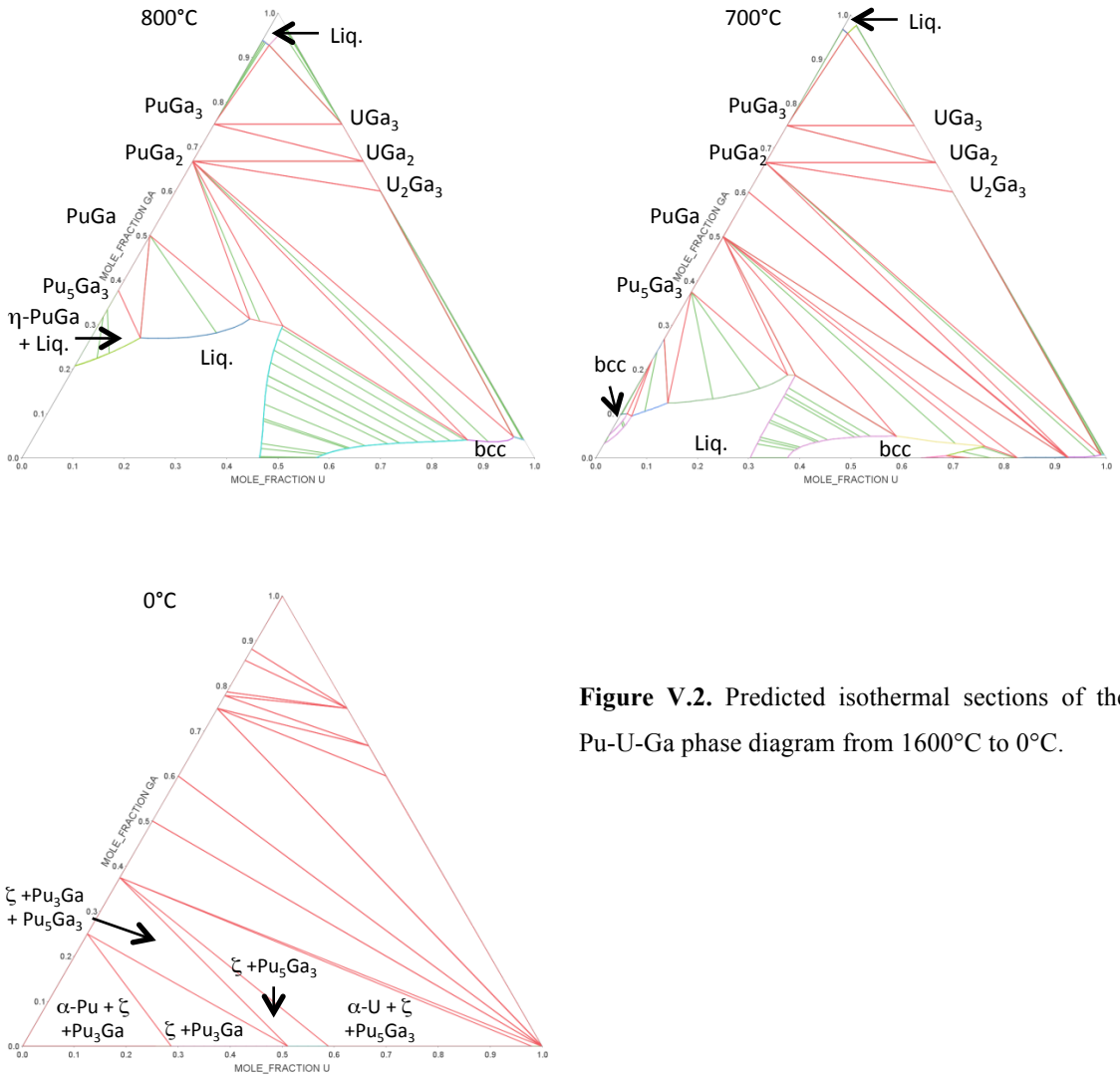

Figure V.2. Predicted isothermal sections of the Pu-U-Ga phase diagram from 1600°C to 0°C.

Instead of the liquid phase, the bcc phase is present in all phase domains at 600°C in the Pu-rich corner. Below ~3.5 at.% Ga, the single bcc phase is observed. At higher Ga content and for low U content, the δ-Pu phase is stabilized. This confirms the ***δ-stabilizing effect of Ga***. However, by adding U to the bcc + δ-Pu two-phase region, the δ-Pu phase is progressively replaced by the bcc phase, and Ga atoms precipitate via stoichiometric compounds (Pu_3Ga, Pu_5Ga_3). This result is in agreement with the admitted fact that U does not act as a "*δ-stabilizer"* element.

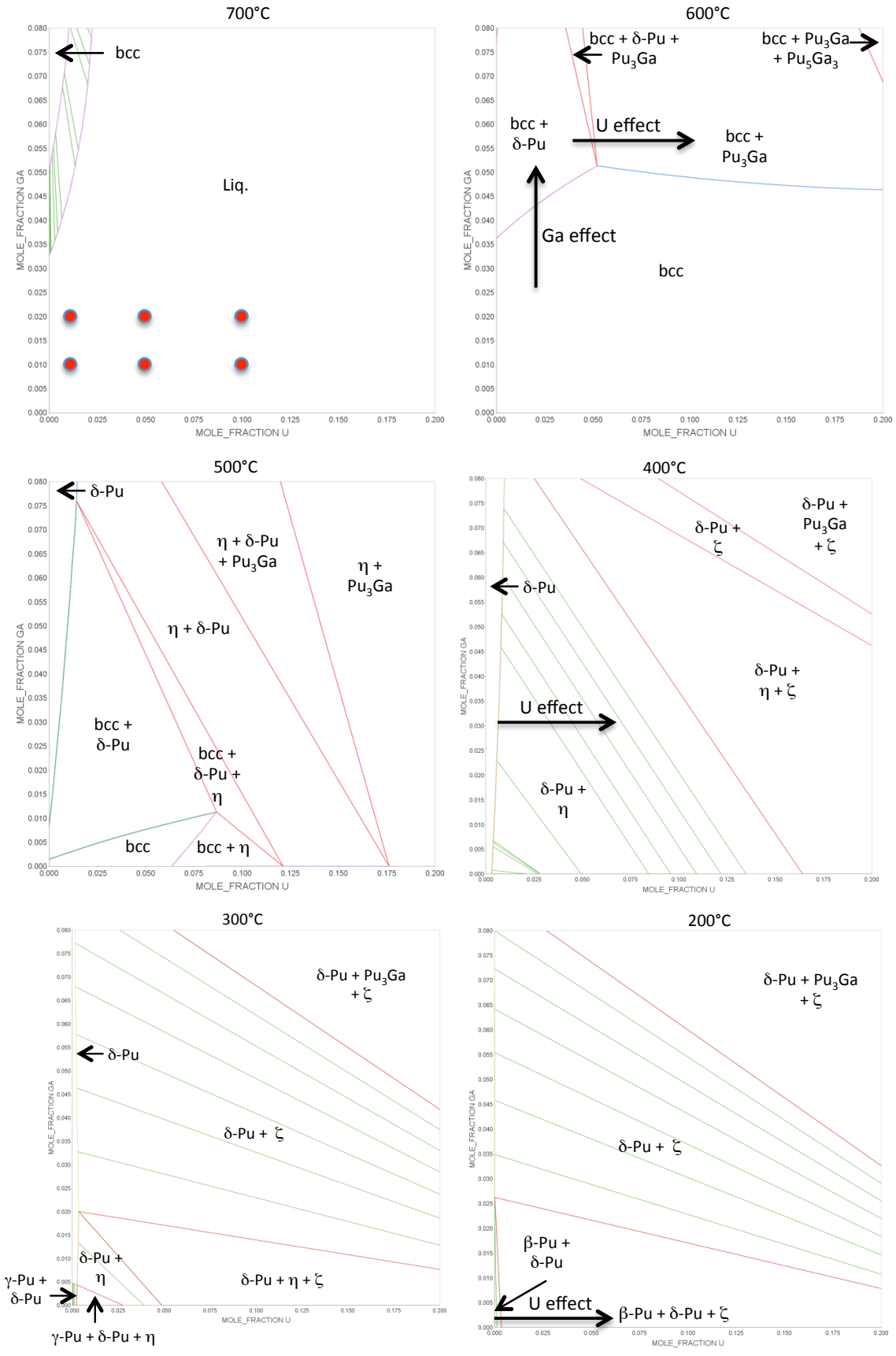
700°C
bcc
Liq.
600°C
bcc + δ-Pu + Pu3Ga
bcc + Pu3Ga + Pu5Ga3
bcc + δ-Pu
U effect
bcc + Pu3Ga
Ga effect
bcc
500°C
δ-Pu
η + δ-Pu + Pu3Ga
η + Pu3Ga
η + δ-Pu
bcc + δ-Pu
bcc + δ-Pu + η
bcc
bcc + η
400°C
δ-Pu + Pu3Ga + ζ
δ-Pu + ζ
δ-Pu
δ-Pu + η + ζ
U effect
δ-Pu + η
300°C
δ-Pu + Pu3Ga + ζ
δ-Pu
δ-Pu + ζ
δ-Pu + η
δ-Pu + η + ζ
γ-Pu + δ-Pu
γ-Pu + δ-Pu + η
200°C
δ-Pu + Pu3Ga + ζ
δ-Pu + ζ
β-Pu + δ-Pu
U effect
β-Pu + δ-Pu + ζ
MOLE_FRACTION GA
MOLE_FRACTION U

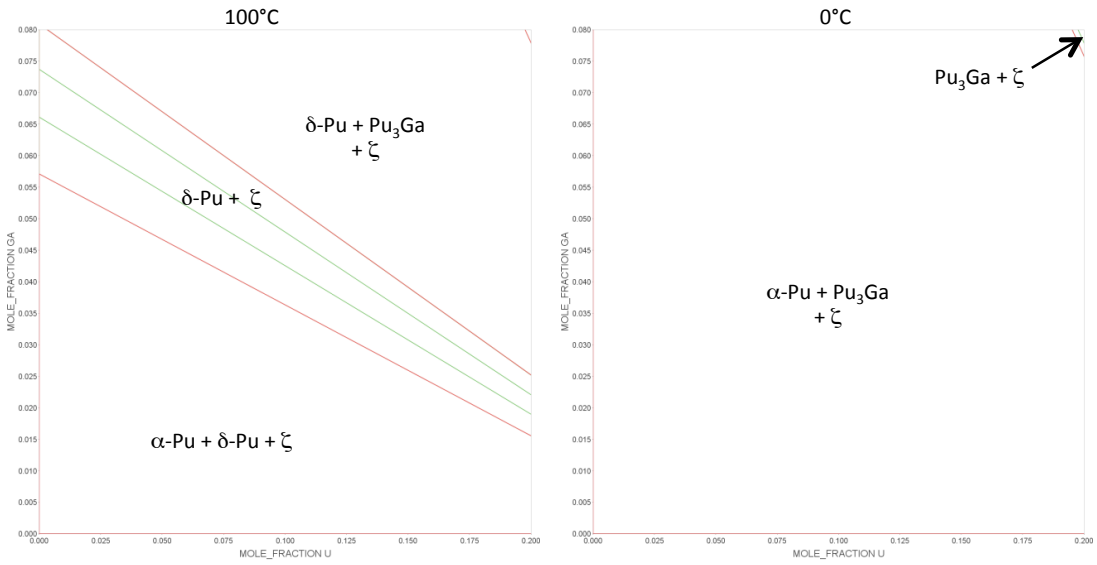

Figure V.3. Detailed representations around the Pu-rich corner of the Pu-U-Ga alloy phase diagram from 700°C to 0°C. In addition, six proposed alloy compositions are symbolized by circles at 700°C.

At 500°C, one can note the appearance of a thin single δ-phase domain that slightly increases with Ga content. Moreover the δ phase is present in most domains except for the very low Ga content where the bcc phase remains and the intermediate η phase appears. It is worth noting that the intermediate η phase becomes very important at 400°C. ***Only a small amount of U added to the Pu-Ga alloy stabilized in δ phase is enough to drag the precipitation of the η phase***. By varying chemical composition, the ζ phase can also precipitate. The precipitation of self-intermetallic compounds like the intermediate η and ζ phases is crucial. Indeed, these complex phases are not known but if we consider examples in "classical" metallurgy, the precipitation of such complex phases like the σ phase in stainless steels (austenitic, duplex…) has a detrimental effect on both mechanical (embrittlement) and corrosion behavior. Thus, ***the impact of U in Pu-Ga alloys should not be underestimated even at a small level of U composition***. At 300°C, the intermediate phases extend, and the γ-Pu phase precipitates only at very low Ga and U contents. This can be explained by the fact that intermediate phases admit no solubility in Ga in our assessment, consequently Ga atoms are always retain in Pu-phases. Thus, the δ phase is stabilized even at low temperature. By lowering again the temperature down to 200°C, ***the ζ phase precipitates in most domains, and one can see here the influence of U***.

Finally, at 100°C and 0°C, the remaining δ phase progressively transforms to pure Pu in the α-phase and Pu_3Ga compound in addition to the ζ phase that is always present. Note that due to the extremely slow kinetics, this last eutectoid decomposition (δ-Pu → α-Pu + Pu_3Ga) is never observed.

As the problematic of the Pu-Ga phase stability is of the greatest interest, we selected two initial Pu-Ga alloy compositions, namely Pu- 1 at.% Ga and Pu- 2 at.% Ga, and studied the influence of U on stability by varying composition from 1 to 5 to 10 at.% U. The alloys composition is presented at 700°C in Fig. V.3. The calculated property diagrams – phase fraction versus temperature – are given in Fig. V.4 for the corresponding alloys: $Pu_{.98}U_{.01}Ga_{.01}$, $Pu_{.94}U_{.05}Ga_{.01}$, $Pu_{.89}U_{.10}Ga_{.01}$, $Pu_{.97}U_{.01}Ga_{.02}$, $Pu_{.93}U_{.05}Ga_{.02}$, $Pu_{.88}U_{.10}Ga_{.02}$. The columns (rows) allow us to compare the influence of U (Ga) on stability for a similar Ga content (for the same U content). For all compositions, the same phases (Liquid, bcc phase, η and ζ phases, δ-Pu, β-Pu, α-Pu and Pu_3Ga) are involved, and only their phase fractions vary. The high-temperature parts of the property diagrams are similar: the liquid phase transforms to the bcc phase. Then, the bcc phase fraction decreases and is replaced by the δ phase and the η phase. Note that for both Ga content, the η-phase amount increases greatly with the U content (from ~10-20 % at 400°C for 1 at.% U to ~75-85 % for 10 at.% U). Then, by decreasing temperature, the η phase is replaced by the ζ phase, and an increase in the δ-phase is observed. It is interesting to mention that beyond the phase transformations involving Pu-phases (β-Pu, α-Pu and Pu_3Ga), the ζ phase is stable until room temperature (in agreement with the Pu-U phase diagram). The ζ phase fraction is varying from ~4 % (1 at.% U) to 35 % (10 at.% U). However it is important to recall that results are presented in molar phase fraction and not in volume phase fraction. So far only few crystallographic data exist for this phase without any in-depth characterization of its physical properties. Thus, as for the Pu-U binary system, ***characterization of the ζ phase has to be performed in the Pu-U-Ga ternary system to know if detrimental effects induced by the ζ-phase precipitation can occur during aging.***

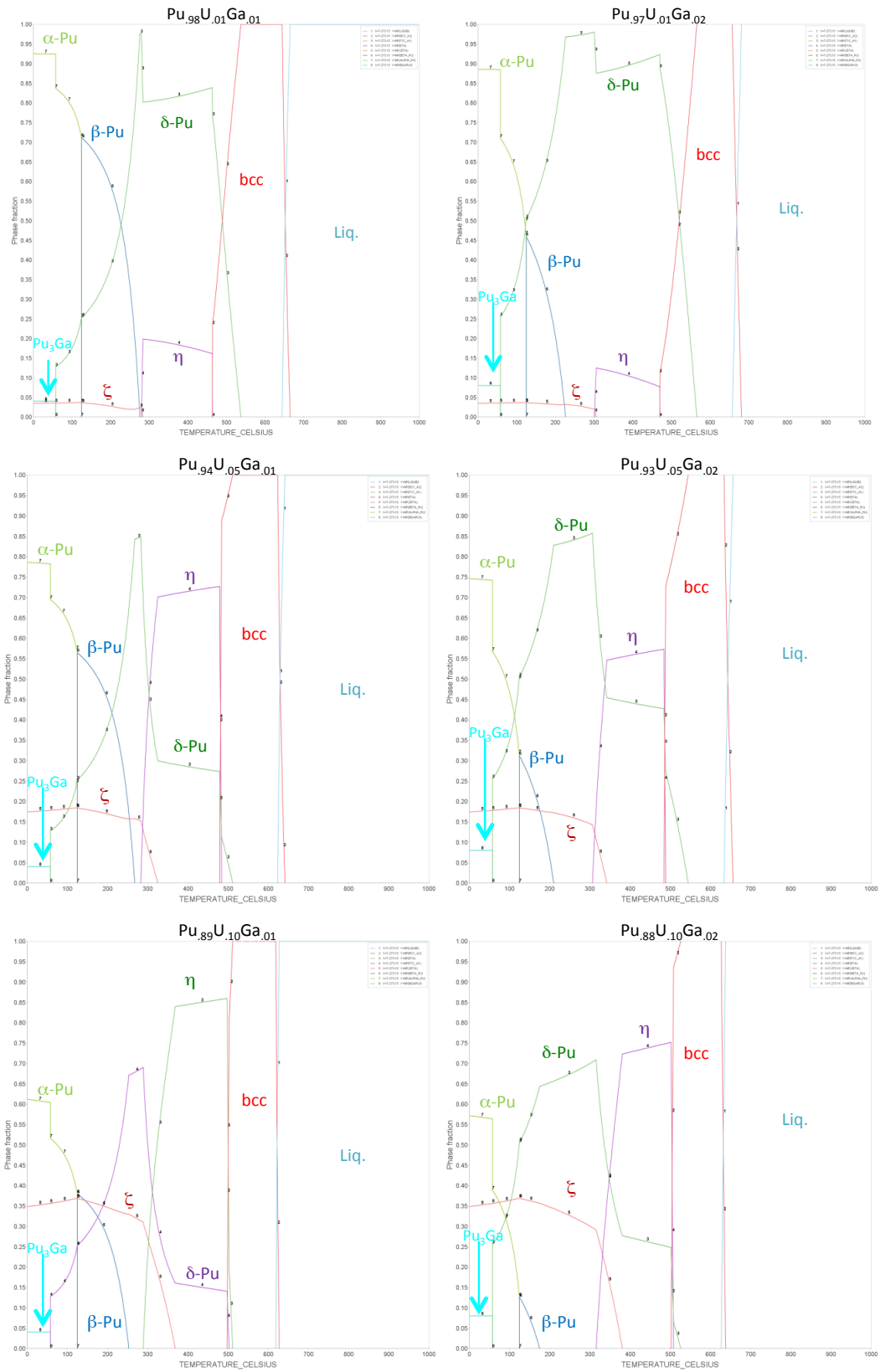

Figure V.4. Calculated property diagrams for the ternary Pu-U-Ga with the following compositions: $Pu_{.98}U_{.01}Ga_{.01}$, $Pu_{.97}U_{.01}Ga_{.02}$, $Pu_{.94}U_{.05}Ga_{.01}$, $Pu_{.93}U_{.05}Ga_{.02}$, $Pu_{.89}U_{.10}Ga_{.01}$, $Pu_{.88}U_{.10}Ga_{.02}$.

VI General Conclusion

The thermodynamic properties of the three binaries Pu-U, Pu-Ga, and U-Ga alloys systems have been studied, assembled in a new thermodynamic database, and isothermal sections of the Pu-U-Ga phase diagram have been proposed. However it is worth emphasizing that, based on what is currently known on the three binaries in terms of thermodynamics, it is difficult to fully validate our ternary predictions without any metallographic characterization, thermal analysis, XRD or dilatometry measurements. In summary, for the first quarter (10/07/2013-01/07/2014) the accomplishments are:

1. Extensive literature search on phase stability properties of Pu-U has been completed.
2. By recasting the *ab initio* energetic information in the CALPHAD framework, the Pu-U phase diagram has been successfully re-assessed and systematically compared with the results from previous studies.
3. Pu-U property diagrams – phase fraction and chemical composition as functions of temperature, molar enthalpy and its derivative *dH/dT* – have been presented and can be used as guidelines to design experiments at specific alloy compositions: $Pu_{0.99}U_{0.01}$, $Pu_{0.40}U_{0.60}$, and $Pu_{0.22}U_{0.78}$ to collect useful information for further validating the thermodynamic database.
4. The Pu-Ga and U-Ga thermodynamic properties and phase diagrams have been reviewed.
5. The thermodynamic data for the three binaries have been put together to study the thermodynamic properties and the phase diagram of the ternary Pu-U-Ga alloy system. Once again, property diagrams have been proposed to validate the thermodynamic predictions (obtained so far without any data on the ternary system), and to study the influence of the η and ζ intermediate phases on aging.

VII Acknowledgments

This work was performed under the auspices of the U.S Department of Energy by Lawrence Livermore National Laboratory under contract DE-AC52-07NA27344. Work at LLNL was funded by the Laboratory Directed Research and Development Program under project tracking code 12-SI-008. This work was done as part of the international agreement on cooperation between DOE-NNSA and CEA-DAM in fundamental science supporting stockpile stewardship. A.P. gratefully acknowledges the financial support from the CEA-Centre de Valduc and the Post-doctoral program at LLNL.

The authors would like to thank Masaki Kurata - *JAEA, Tokai, Japan* - for fruitful discussions and also for providing data on the Pu-U system.

VIII References

Introduction

[I.1] Kaufman L, Bernstein H. Computer Calculation of Phase Diagrams with Special Reference to Refractory Metals, Academic Press, New Y ork; 1970.

[I.2] Saunders N, Miodownik AP. in: R.W. Cahn (Ed.) CALPHAD, Calculation of Phase Diagrams, A Comprehensive Guide, Pergamon Materials Series, vol. 1, Pergamon Press, Oxford; 1998.

[I.3] Lukas HL, Fries SG, Sundman B. Computational Thermodynamics: The Calphad Method, Cambridge University Press; 2007.

[I.4] Smith JF. Introduction to Phase Diagrams, in: Zhao J-C (Ed.). Methods for Phase Diagram Determination, Elsevier; 2007.

The Pu-U system

[II.1] F. H. Ellinger, R. O. Elliott, and E. M. Cramer, "The plutonium-uranium system", J. of Nucl. Mater. **3**, 233-243 (1959).

[II.2] M. B. Waldron, in: "The Metal Plutonium", A. S. Coffinberry, W. N. Miner (eds.), University of Chicago Press, Chicago (1961).

[II.3] A. A. Bochvar, S. T. Konobeevsky, V. I. Kutaitsev, T. S. Menshikova, N. T. Chebotarev: Proc. U.N. Conf. Peaceful Uses At. Energy, 2nd, Geneva, Vol. 6, IAEA, Vienna, Austria 184-193 (1958).

[II.4] R. O. Elliot and A. C. Larson, in: "The Metal Plutonium", A. S. Coffinberry, W. N. Miner (eds.), University of Chicago Press, Chicago (1961).

[II.5] D. E. Peterson and E. M. Foltyn, Bull. Alloy Phase Diagrams 10, 160-164 (1989).

[II.6] D. Calais, M. Dupuy, M. Mouchnino, A. Y. Portnoff, A. Van Craeynest, Plutonium 1965, A. E. Kay and M. B. Waldron, Ed., Chapman and Hall, London, 358-391 (1967).

[II.7] AEC Research and Development REPORT, Mound Laboratory report, MLM-1402 (1966).

[II.8] AEC Research and Development REPORT, Mound Laboratory report, MLM-1445 (1967).

[II.9] S. Rosen, M. V. Nevitt, and J. J. Barker, "The U-Pu-C ternary phase diagram below 50 atomic percent carbon", J. Nucl. Mater. **9**, 128-136 (1963).

[II.10] J. I. Bramman, R. M. Sharpe, and R. Dixon, "Fission-product inclusions in irradiated uranium-plutonium carbide", J. of Nucl. Mater. **38**, 226-229 (1971).

[II.11] F. L. Oettings, M. H. Rand, and R. J. Ackermann, The Chemical Thermodynamics of Actinide Elements and Compound – Part I (IAEA, Vienna, 1976).

[II.12] Toru Ogawa, "Alloying behaviour among U, Np, Pu and Am predicted with the Brewer valence bond model", J. of Alloys and Compounds **194**, 1-7 (1993).

[II.13] M. C. Petri, A. G. Hins, J. E. Sanecki, and M. A. Dayananda, "Uranium-plutonium interdiffusion at 750 ^{o}C", J. of Nucl. Mater. **211**, 1-10 (1994).

[II.14] Yoshihiro Okamoto, Atsushi Maeda, Yasufumi Suzuki and Toshihiko Ohmichi, "Investigation of the Pu-U phase diagram", J. of Alloys and Compounds **213/214**, 372-374 (1994).

[II.15] T. Ogawa, M. Akabori, F. Kobayashi, and R. G. Haire, "Thermochemical modeling of actinide alloys related to advanced fuel cycles", J. of Nucl. Mater. **247**, 215-221 (1997).

[II.16] E. Fisher, "Thermodynamic modeling of the C-Pu-U system", CALPHAD **33**, 487-494 (2009).

[II.17] L. Leibowitz, E. Veleckis, R. A. Blomquist, and A. D. Pelton, "Solidus and liquidus temperatures in the Uranium-Plutonium-Zirconium system", J. of Nucl. Mater. **154**, 145-153 (1988).

[II.18] L. Leibowitz, and R. A. Blomquist, and A. D. Pelton, "Thermodynamic modeling of the phase equilibria of the plutonium-uranium system", J. of Nucl. Mater. **184**, 59-64 (1991).

[II.19] Arthur D. Pelton, "Thermodynamic modeling and phase equilibrium calculations in nuclear materials", Pure & Appl. Chem. **69** (11), 2245-2252 (1997).

[II.20] M. Kurata, "Thermodynamic assessment of the Pu-U, Pu-Zr, and Pu-U-Zr systems", CALPHAD **23** (3-4), 305-337 (1999).

[II.21] M. Kurata, "Thermodynamic database on U-Pu-Zr-Np-Am-Fe alloy system I – Re-evaluation of U-Pu-Zr alloy system", Mater. Sci. and Eng. **9**, 012022-1 to 8 (2010).

[II.22] M. Kurata, in "Comprehensive Nuclear Materials", Vol. 2: "Material Properties/Oxide Fuels for Light Water Reactors and Fast Neutron Reactors", "Phase Diagrams of Actinides Alloys", 139-195 (2012).

[II.23] P. E. A. Turchi and A. I. Landa, *Thermodynamic Database, Lower Length Scale – Part I: Thermodynamic assessment of the Ternary Alloy System Mo-Pu-U*, LLNL-TR-553775 (2012). And: A. Landa, P. Söderlind, P. E. A. Turchi, L. Vitos, and A. Ruban, *Density-functional study of Zr-based actinide alloys: 2. U-Pu-Zr system*, J. of Nucl. Mater. **393**, 141-145 (2009).

[II.24] P. Chiotti, V. V. Akhachinskiy, I. Ansara, and M. H. Rand, *The Chemical Thermodynamics of Actinide Elements and Compounds, part 5 – The Actinide Binary Alloys*, IAEA, Vienna (1981).

[II.25] M. Kurata, and Y. Okamoto, presented at 1997 fall meeting of the Japan Atomic Energy Society, Sep. 26-28, 1007, Okinawa.

[II.26] A. T. Dinsdale, "SGTE data for pure elements", CALPHAD **15**, 317-425 (1991).

[II.27] P. E. A. Turchi, A. I. Landa, and P. A. Söderlind, "Thermodynamic assessment of the Am-Pu system with input from *ab initio*", J. of Nucl. Mater. **418**, 165-173 (2011).

[II.28] A. C. Lawson, J. A. Goldstone, B. Cort, R. J. Martinez, F. A. Vigil, T. G. Zocco, J. W. Richardson Jr, and M. H. Mueller, "Structure of ζ-Phase Plutonium-Uranium", Acta Cryst. **B52**, 32-37 (1996).

[II.29] Ladislav Havela, Anna Adamska, Rachel Eloirdi, Eric Colineau, Jean-Christophe Griveau, Thomas Gouder b, Frank Huber, Daniel Bouexière, and Alexander B. Shick, "Bulk properties and photoelectron spectroscopy of the ζ-U–Pu phase", J. of Nucl. Mater. **414**, 458-463 (2011).

[II.30] T. R .G. Kutty, K. Ravi, Santu Kaity, S. K. Swarnkar, and Arun Kumar, "Effect of temperature on hardness of binary U-15%Pu alloy and T91 cladding", J. of Nucl. Mater. **429**, 341-345 (2012).

[II.31] Santu Kaity, Joydipta Banerjee, K. Ravi, R. Keswani, T.R.G. Kutty, Arun Kumar, and G.J. Prasad, "Characterization and property evaluation of U–15 wt%Pu alloy for fast reactor", J. of Nucl. Mater. **433**, 206-214 (2013).

The Pu-Ga system

[III.1] P. E. A. Turchi, L. Kaufman, Z. –K. Liu, and S. Zhou, "Thermodynamics and Kinetics of phase transformations in plutonium alloys – Part I, UCRL-TR-206658 (2004).

[III.2] P. E. A. Turchi, L. Kaufman, S. Zhou, and Z. –K. Liu, "Thermostatics and kinetics of transformations in Pu-based alloys", J. Alloys Compds **444-445**, 28-35 (209).

[III.3] B. Ravat, B. Oudot, A. Perron, F. Lalire, and F. Delaunay, "Phase transformations in PuGa 1 at.% alloy: Study of whole reversion process following martensitic transformation", J. Alloys Compds **580**, 298-309 (2013).

[III.4] A. Perron, B. Ravat, B. Oudot, F. Lalire, K. Mouturat, and F. Delaunay, "Phase transformation in Pu-Ga alloy: Synergy between simulations and experiments to elucidate direct and indirect reversion competition", Acta Mat. **61**, 7109-7120 (2013).

The U-Ga system

[IV.1] J. Wang, X. J. Liu and C. P. Wang, "Thermodynamic calculation of phase equilibria of the U-Ga and U-W systems", J. of Nucl. Mater. **380**, 105-110 (2008).

[IV.2] K. H. J. Bushow, "Phase relationships and magnetic properties of uranium-gallium compounds", J. Less-Common Met. **31**, 165-168 (1973).

[IV.3] E. S. Makarov and V. A. Levdik, Kristallograftya **1**, 644 (1956).

[IV.4] D. Dayan, G. Kimmel and M. P. Dariel, "Shear-like transformation in beta-stabilized U-1.5 at-percent Ga alloy - structure of the intermetallic compound U_3Ga_5",J. of Nucl. Mater. **135**, 40-45 (1985).

[IV.5] P. Gardie, G. Bordier, J. J. Poupeau and J. Le Ny, "Thermodynamic activity measurements of U-Fe and U-Ga alloys by mass spectrometry", J. of Nucl. Mater. **189**, 85-96 (1992).

[IV.6] H. Okamoto, Desk Handbook-Phase Diagrams for Binary Alloys, ASM International (2000).

[IV.7] I. Johnson and H. M. Feder, Proceedings of the Symposium on Thermodynamics of Nuclear Materials, Vienna, vol. **319**, IAEA, Vienna (1962).

[IV.8] V. A. Lebedev, V. N. Seregin, A. M. Poyarkov, I. F. Nichkov and S. P. Raspopin, Russ. J. Phys. Chem. **47**, 402-XXX (1973).

[IV.9] C. B. Alcock, J. B. Cornish and P. Grieveson, Proceedings of the Symposium on Thermodynamics of Nuclear Materials, Vienna, vol. **211**, IAEA, Vienna (1966).

[IV.10] P. Chiotti, V. V. Akhachinskij, I. Ansara and M. H. Rand, The Chemical Thermodynamics of Actinide Elements and Compounds, Part 5, The actinide Binary Alloys, vol. **120**, IAEA, Vienna (1981).

[IV.11] B. Prabhakara Reddy, R. Babu, K. Nagarajan and P. R. Vasudeva Rao, "Enthalpies of formation of UGa_2 and UGa_3 by calorimetry", J. Alloy. Compd. **217–273**, 395-399 (1998).

[IV.12] A. T. Dinsdale, "SGTE data for pure elements", CALPHAD **15**, 317-425 (1991).

IX Appendix A: CALPHAD modeling

In the CALPHAD (CALculation of PHAse Diagrams) approach [A.1-4], the Gibbs energy of individual phases is modeled, and the model parameters are collected in a thermodynamic database. It is the modeling of the Gibbs energy of individual phases and the coupling of phase diagram and thermo-chemistry that make the CALPHAD a powerful technique in computational thermodynamic of multi-component materials. Models for the Gibbs energy are based on the crystal structures of the phases. For pure elements and stoichiometric compounds, the most commonly used model is the one suggested by the Scientific Group Thermodata Europe (SGTE) [A.5] and has the following form (for simplicity, the pressure dependence and the magnetic contribution are not shown here),

$$G_m - H_m^{SER} = a + bT + cTln(T) + \sum d_i T^i \quad (1)$$

The left-hand side is defined as the Gibbs energy relative to a standard element reference state (SER), where H_m^{SER} is the enthalpy of the element in its stable state at 298.15 K and 1 bar of pressure. Coefficients, a, b, c and d_i are the model parameters. The SGTE data for all the pure elements of the periodic table have been compiled by Dinsdale [A.5]. For multi-component solution phases, the Gibbs energy has the following general expression:

$$G = G^0 + G_{mix}^{ideal} + G_{mix}^{xs} \quad (2)$$

where G^0 is the contribution from the mechanical mixing of the pure components, G_{mix}^{ideal} is the ideal mixing contribution, and G_{mix}^{xs} is the excess Gibbs energy of mixing due to non-ideal interactions. Sublattice models have been widely used to describe solution phases [A.2-3]. For example, for a simple phase with two sublattices in a A-B binary system where the two components enter both sublattices, the sublattice model is written as $(A,B)_p(A,B)_q$, where subscripts p and q denote the number of sites of each sublattice. More specifically, the three terms presented above are written as,

$$G^0 = y_A^I y_A^{II} G_{A:A}^0 + y_A^I y_B^{II} G_{A:B}^0 + y_B^I y_A^{II} G_{B:A}^0 + y_B^I y_B^{II} G_{B:B}^0 \quad (3)$$

$$G_{mix}^{ideal} = pRT(y_A^I lny_A^I + y_B^I lny_B^I) + qRT(y_A^{II} lny_A^{II} + y_B^{II} lny_B^{II}) \quad (4)$$

$$G_{mix}^{xs} = y_A^I y_B^I \left(y_A^{II} \sum_{k=0} L_{A,B:A}^k (y_A^I - y_B^I)^k + y_B^{II} \sum_{k=0} L_{A,B:B}^k (y_A^I - y_B^I)^k\right) + y_A^{II} y_B^{II} \left(y_A^I \sum_{k=0} L_{A:A,B}^k (y_A^{II} - y_B^{II})^k + y_B^I \sum_{k=0} L_{B:A,B}^k (y_A^{II} - y_B^{II})^k\right) \quad (5)$$

where y^I and y^{II} are the site fractions of A and B in the first and second sublattices, respectively. $G^0_{I:J}$ is the Gibbs energy of the compound I_pJ_q, expressed by Eq. 1. $L^k_{A,B:*}$ ($L^k_{*:A,B}$) is the k^{th} order interaction parameter between component A and B in the first (second) sublattice. In this notation, a colon separates components occupying different sublattices, and a coma separates interacting components in the same sublattice. These equations can be generalized for phases with multi-components and multi-sublattices, and they reduce to a random substitutional model when there is only one sublattice. For a multi-component solution in a particular phase Φ described with a single sublattice model, the three contributions to the total Gibbs energy reduce to:

$$^{\Phi}G^0 = \sum_I c_I \, {}^{\Phi}G^0_I \tag{6}$$

$$^{\Phi}G^{ideal}_{mix} = RT \sum_I c_I ln c_I \tag{7}$$

$$^{\Phi}G^{xs}_{mix} = \sum_I \sum_{J>I} c_I c_J \sum_k {}^{\Phi}L^k_{I,J} \left(c_I - c_J\right)^k \tag{8}$$

where the molar Gibbs energy of mixing is expressed by a Redlich-Kister expansion [A.6]. In these expressions, c_I is the composition of the alloy in species I, and the $L^k_{I,J}$ is the k^{th}-order binary interaction parameter between species I and J usually expressed as a first-order polynomial in temperature:

$$L^k_{I,J} = a^k_{I,J} + b^k_{I,J} T \tag{9}$$

Note that in both sets of expressions the excess Gibbs energy due to non-ideal contributions is expressed within the Muggianu approximation [A.7].

[A.1] Kaufman L, Bernstein H. Computer Calculation of Phase Diagrams with Special Reference to Refractory Metals, Academic Press, New Y ork; 1970.

[A.2] Saunders N, Miodownik AP. in: R.W. Cahn (Ed.) CALPHAD, Calculation of Phase Diagrams, A Comprehensive Guide, Pergamon Materials Series, vol. 1, Pergamon Press, Oxford; 1998.

[A.3] Lukas HL, Fries SG, Sundman B. Computational Thermodynamics: The Calphad Method, Cambridge University Press; 2007.

[A.4] Smith JF. Introduction to Phase Diagrams, in: Zhao J-C (Ed.). Methods for Phase Diagram Determination, Elsevier; 2007.

[A.5] A. T. Dinsdale, "SGTE data for pure elements", CALPHAD **15**, 317-425 (1991).

[A.6] O. Redlich and A. Kister, “Algebraic Representation of the Thermodynamic Properties and the Classification of Solutions”, Ind. Eng. Chem. **40**, 345-348 (1948).

[A.7] Y. M. Muggianu, M. Gambino, and J. P. Bros, “Enthalpies de Formation des Alliages Liquides Bismuth-Etain-Gallium a 723 K. Choix d’une Représentation analytique des Grandeurs d’Excès Intégrales et Partielles de Mélange”, J. Chem. Phys. **22**, 83-88 (1975).

X Appendix B: .POP file

```
$ POP file for assessment of Pu-U system
$ Based on MK data and modified by AP for Ellinger and Calais data
$ Enter some constants used later.
ENTER_SYMBOL CONSTANT DX1=0.01,DX2=0.02,DX5=0.05,DX10=0.1,P0=101325
ENTER_SYMBOL CONSTANT DH=500,DT1=1,DT2=2,DT5=5,DT10=10,DT20=20,DT50=50
$
CREATE_NEW_EQUILIBRIUM 1 1
CHANGE_STATUS PHASE BCC_A2,LIQUID=FIX 1
SET-CONDITION P=P0 X(BCC_A2,U)-X(LIQUID,U)=0
EXPERIMENT T=883:DT10 X(BCC_A2,Pu)=0.88:DX5 X(LIQUID,U)=0.12:DX5
SET_START_VALUE T=883 Y(BCC_A2,Pu)=0.88 Y(LIQUID,U)=0.12
LABEL ACON
COMMENT Ellinger congruent
$
CREATE_NEW_EQUILIBRIUM 2 1
CHANGE_STATUS PHASE BCC_A2 ETA TETRAGONAL_U=FIX 1
SET-CONDITION P=P0
EXPERIMENT T=978:DT2 X(BCC_A2,Pu)=0.30:DX5
EXPERIMENT X(ETA,Pu)=0.295:DX5 X(TETRAGONAL_U,U)=0.8:DX5
SET_START_VALUE T=978 Y(BCC_A2,Pu)=0.30 Y(ETA,Pu)=0.295 Y(TETRAGONAL_U,U)=0.8
LABEL AINV
COMMENT Ellinger peritectoid
$
CREATE_NEW_EQUILIBRIUM 3 1
CHANGE_STATUS PHASE ZETA ETA TETRAGONAL_U=FIX 1
SET-CONDITION P=P0
EXPERIMENT T=863:DT5 X(ZETA,Pu)=0.28:DX5 X(TETRAGONAL_U,U)=0.82:DX5
EXPERIMENT X(ETA,Pu)=0.325:DX5
SET_START_VALUE T=863 Y(ZETA,Pu)=0.28 Y(ETA,Pu)=0.325 Y(TETRAGONAL_U,U)=0.82
LABEL AINV
COMMENT Ellinger peritectoid
$
CREATE_NEW_EQUILIBRIUM 4 1
CHANGE_STATUS PHASE ZETA TETRAGONAL_U ORTHORHOMBIC_U=FIX 1
SET-CONDITION P=P0
EXPERIMENT T=833:DT5 X(ZETA,Pu)=0.26:DX5 X(ORTHORHOMBIC_U,U)=0.85:DX5
EXPERIMENT X(TETRAGONAL_U,U)=0.83:DX5
SET_START_VALUE T=833 Y(ZETA,Pu)=0.26 Y(TETRAGONAL_U,U)=0.83 Y(ORTHORHOMBIC_U,U)=0.85
LABEL AINV
COMMENT Ellinger eutectoid
$
CREATE_NEW_EQUILIBRIUM 5 1
CHANGE_STATUS PHASE TETRAGONAL_PU BCC_A2 ETA=FIX 1
SET-CONDITION P=P0
EXPERIMENT T=728:DT2 X(TETRAGONAL_PU,Pu)=0.987:DX2
EXPERIMENT X(BCC_A2,Pu)=0.975:DX2 X(ETA,U)=0.045:DX2
SET_START_VALUE T=728 Y(TETRAGONAL_PU,Pu)=0.987 Y(BCC_A2,Pu)=0.975 Y(ETA,U)=0.045
LABEL AINV
COMMENT Ellinger eutectoid
$
CREATE_NEW_EQUILIBRIUM 6 1
CHANGE_STATUS PHASE TETRAGONAL_PU FCC_A1 ETA=FIX 1
SET-CONDITION P=P0
EXPERIMENT T=715:DT5 X(TETRAGONAL_PU,Pu)=0.988:DX5 X(ETA,U)=0.04:DX5
S_A_C X(FCC_A1,U)=0.003:DX5
SET_START_VALUE T=715 Y(FCC_A1,U)=0.003 Y(TETRAGONAL_PU,Pu)=0.988 Y(ETA,U)=0.04
LABEL AINV
COMMENT Ellinger eutectoid
```

```
$
CREATE_NEW_EQUILIBRIUM 7 1
CHANGE_STATUS PHASE GAMMA_PU FCC_A1 ETA=FIX 1
SET-CONDITION P=P0
EXPERIMENT T=593:DT5 X(ETA,U)=0.02:DX5
S_A_C X(GAMMA_PU,Pu)=0.999:DX5 X(FCC_A1,Pu)=0.999:DX5
SET_START_VALUE T=593 Y(GAMMA_PU,Pu)=0.997 Y(FCC_A1,Pu)=0.998 Y(ETA,U)=0.02
LABEL AINV
COMMENT Ellinger peritectoid
$
CREATE_NEW_EQUILIBRIUM 8 1
CHANGE_STATUS PHASE GAMMA_PU BETA_PU ETA=FIX 1
SET-CONDITION P=P0
EXPERIMENT T=553:DT5 X(GAMMA_PU,Pu)=0.992:DX5
EXPERIMENT X(BETA_PU,Pu)=0.98:DX5 X(ETA,U)=0.029:DX5
SET_START_VALUE T=553 Y(GAMMA_PU,Pu)=0.992 Y(BETA_PU,Pu)=0.98 Y(ETA,U)=0.029
LABEL AINV
COMMENT Ellinger peritectoid
$
CREATE_NEW_EQUILIBRIUM 9 1
CHANGE_STATUS PHASE BETA_PU ETA ZETA=FIX 1
SET-CONDITION P=P0
EXPERIMENT T=551:DT5 X(BETA_PU,Pu)=0.98:DX5 X(ETA,Pu)=0.97:DX5
S_A_C X(ZETA,U)=0.26:DX5
SET_START_VALUE T=551 Y(BETA_PU,Pu)=0.98 Y(ETA,Pu)=0.97 Y(ZETA,U)=0.26
LABEL AINV
COMMENT Ellinger eutectoid
$
CREATE_NEW_EQUILIBRIUM 10 1
CHANGE_STATUS PHASE ALPHA_PU BETA_PU ZETA=FIX 1
SET-CONDITION P=P0
EXPERIMENT T=398:DT5 X(ZETA,U)=0.3:DX10
S_A_C X(ALPHA_PU,PU)=1:DX5 X(BETA_PU,U)=.001:DX5
SET_START_VALUE T=398 Y(ZETA,U)=0.3 Y(ALPHA_PU,PU)=1 X(BETA_PU,U)=.001
LABEL AINV
COMMENT Ellinger eutectoid
$
CREATE_NEW_EQUILIBRIUM 11 1
CHANGE_STATUS PHASE BCC_A2 ETA=FIX 1
SET-CONDITION P=P0 T=978
EXPERIMENT X(BCC_A2,Pu)=0.30:DX5
S_A_C X(ETA,Pu)=0.295:DX5
SET_START_VALUE Y(BCC_A2,Pu)=0.30 Y(ETA,Pu)=0.295
LABEL ASS
COMMENT Ellinger
$
CREATE_NEW_EQUILIBRIUM 12 1
CHANGE_STATUS PHASE BCC_A2 TETRAGONAL_U=FIX 1
SET-CONDITION P=P0 T=978
EXPERIMENT X(BCC_A2,Pu)=0.30:DX5
S_A_C X(TETRAGONAL_U,U)=0.8:DX5
SET_START_VALUE Y(BCC_A2,Pu)=0.30 Y(TETRAGONAL_U,U)=0.8
LABEL ASS
COMMENT Ellinger
$
CREATE_NEW_EQUILIBRIUM 13 1
CHANGE_STATUS PHASE ETA TETRAGONAL_U=FIX 1
SET-CONDITION P=P0 T=978
EXPERIMENT X(ETA,Pu)=0.295:DX5 X(TETRAGONAL_U,U)=0.8:DX5
SET_START_VALUE Y(ETA,Pu)=0.295 Y(TETRAGONAL_U,U)=0.8
LABEL ASS
COMMENT Ellinger
```

```
$
CREATE_NEW_EQUILIBRIUM 14 1
CHANGE_STATUS PHASE ETA TETRAGONAL_U=FIX 1
SET-CONDITION P=P0 T=863
EXPERIMENT X(TETRAGONAL_U,U)=0.82:DX5
S_A_C X(ETA,Pu)=0.325:DX5
SET_START_VALUE Y(ETA,Pu)=0.325 Y(TETRAGONAL_U,U)=0.82
LABEL ASS
COMMENT Ellinger
$
CREATE_NEW_EQUILIBRIUM 15 1
CHANGE_STATUS PHASE ETA ZETA=FIX 1
SET-CONDITION P=P0 T=863
EXPERIMENT X(ZETA,Pu)=0.28:DX5
S_A_C X(ETA,Pu)=0.325:DX5
SET_START_VALUE Y(ETA,Pu)=0.325 Y(ZETA,Pu)=0.28
LABEL ASS
COMMENT Ellinger
$
CREATE_NEW_EQUILIBRIUM 16 1
CHANGE_STATUS PHASE ZETA TETRAGONAL_U=FIX 1
SET-CONDITION P=P0 T=863
EXPERIMENT X(ZETA,Pu)=0.28:DX5 X(TETRAGONAL_U,U)=0.82:DX5
SET_START_VALUE Y(ZETA,Pu)=0.28 Y(TETRAGONAL_U,U)=0.82
LABEL ASS
COMMENT Ellinger
$
CREATE_NEW_EQUILIBRIUM 17 1
CHANGE_STATUS PHASE TETRAGONAL_U ORTHORHOMBIC_U=FIX 1
SET-CONDITION T=833 P=P0
EXPERIMENT X(TETRAGONAL_U,U)=0.83:DX5 X(ORTHORHOMBIC_U,U)=0.85:DX5
SET_START_VALUE Y(TETRAGONAL_U,U)=0.83 Y(ORTHORHOMBIC_U,U)=0.85
LABEL ASS
COMMENT Ellinger
$
CREATE_NEW_EQUILIBRIUM 18 1
CHANGE_STATUS PHASE TETRAGONAL_U ZETA=FIX 1
SET-CONDITION T=833 P=P0
EXPERIMENT X(TETRAGONAL_U,U)=0.83:DX5 X(ZETA,Pu)=0.26:DX5
SET_START_VALUE Y(TETRAGONAL_U,U)=0.83 Y(ZETA,Pu)=0.26
LABEL ASS
COMMENT Ellinger
$
CREATE_NEW_EQUILIBRIUM 19 1
CHANGE_STATUS PHASE ZETA ORTHORHOMBIC_U=FIX 1
SET-CONDITION P=P0 T=833
EXPERIMENT X(ZETA,Pu)=0.26:DX5 X(ORTHORHOMBIC_U,U)=0.85:DX5
SET_START_VALUE Y(ZETA,Pu)=0.26 Y(ORTHORHOMBIC_U,U)=0.85
LABEL ASS
COMMENT Ellinger
$
CREATE_NEW_EQUILIBRIUM 20 1
CHANGE_STATUS PHASE TETRAGONAL_PU BCC_A2=FIX 1
SET-CONDITION P=P0 T=728
EXPERIMENT X(TETRAGONAL_PU,Pu)=0.987:DX2 X(BCC_A2,Pu)=0.975:DX2
SET_START_VALUE Y(TETRAGONAL_PU,Pu)=0.987 Y(BCC_A2,Pu)=0.975
LABEL ASS
COMMENT Ellinger
$
CREATE_NEW_EQUILIBRIUM 21 1
CHANGE_STATUS PHASE TETRAGONAL_PU ETA=FIX 1
SET-CONDITION P=P0 T=728
```

```
EXPERIMENT X(TETRAGONAL_PU,Pu)=0.987:DX2 X(ETA,U)=0.045:DX2
SET_START_VALUE Y(TETRAGONAL_PU,Pu)=0.987 Y(ETA,U)=0.045
LABEL ASS
COMMENT Ellinger
$
CREATE_NEW_EQUILIBRIUM 22 1
CHANGE_STATUS PHASE BCC_A2 ETA=FIX 1
SET-CONDITION P=P0 T=728
EXPERIMENT X(BCC_A2,Pu)=0.975:DX2 X(ETA,U)=0.045:DX2
SET_START_VALUE Y(BCC_A2,Pu)=0.975 Y(ETA,U)=0.045
LABEL ASS
COMMENT Ellinger
$
CREATE_NEW_EQUILIBRIUM 23 1
CHANGE_STATUS PHASE TETRAGONAL_PU ETA=FIX 1
SET-CONDITION P=P0 T=715
EXPERIMENT X(TETRAGONAL_PU,Pu)=0.988:DX5 X(ETA,U)=0.04:DX5
SET_START_VALUE Y(TETRAGONAL_PU,Pu)=0.988 Y(ETA,U)=0.04
LABEL ASS
COMMENT Ellinger
$
CREATE_NEW_EQUILIBRIUM 24 1
CHANGE_STATUS PHASE FCC_A1 TETRAGONAL_PU=FIX 1
SET-CONDITION P=P0,T=715
EXPERIMENT X(TETRAGONAL_PU,Pu)=0.988:DX5
S_A_C X(FCC_A1,U)=0.003:DX5
SET_START_VALUE Y(TETRAGONAL_PU,Pu)=0.988 Y(FCC_A1,U)=0.003
LABEL ASS
COMMENT Ellinger
$
CREATE_NEW_EQUILIBRIUM 25 1
CHANGE_STATUS PHASE FCC_A1 ETA=FIX 1
SET-CONDITION P=P0,T=715
EXPERIMENT X(ETA,Pu)=0.96:DX10
S_A_C X(FCC_A1,U)=0.003:DX5
SET_START_VALUE Y(ETA,Pu)=0.96 Y(FCC_A1,U)=0.003
LABEL ASS
COMMENT Ellinger
$
CREATE_NEW_EQUILIBRIUM 26 1
CHANGE_STATUS PHASE FCC_A1 ETA=FIX 1
SET-CONDITION P=P0 T=593
EXPERIMENT X(ETA,Pu)=0.98:DX5
S_A_C X(FCC_A1,U)=0.002:DX5
SET_START_VALUE Y(FCC_A1,U)=0.002 Y(ETA,Pu)=0.98
LABEL ASS
COMMENT Ellinger
$
CREATE_NEW_EQUILIBRIUM 27 1
CHANGE_STATUS PHASE GAMMA_PU FCC_A1=FIX 1
SET-CONDITION P=P0,T=593
EXPERIMENT X(FCC_A1,U)=0.002:DX5 X(GAMMA_PU,Pu)=0.997:DX5
SET_START_VALUE Y(GAMMA_PU,Pu)=0.997 Y(FCC_A1,U)=0.002
LABEL ASS
COMMENT Ellinger
$
CREATE_NEW_EQUILIBRIUM 28 1
CHANGE_STATUS PHASE GAMMA_PU ETA=FIX 1
SET-CONDITION P=P0,T=593
EXPERIMENT X(ETA,U)=0.02:DX5
S_A_C X(GAMMA_PU,Pu)=0.997:DX5
SET_START_VALUE Y(GAMMA_PU,Pu)=0.997 Y(ETA,U)=0.02
```

```
LABEL ASS
COMMENT Ellinger
$
CREATE_NEW_EQUILIBRIUM 29 1
CHANGE_STATUS PHASE GAMMA_PU ETA=FIX 1
SET-CONDITION P=P0 T=553
EXPERIMENT X(GAMMA_PU,Pu)=0.992:DX5 X(ETA,U)=0.029:DX5
SET_START_VALUE Y(GAMMA_PU,Pu)=0.992 Y(ETA,U)=0.029
LABEL ASS
COMMENT Ellinger
$
CREATE_NEW_EQUILIBRIUM 30 1
CHANGE_STATUS PHASE BETA_PU ETA=FIX 1
SET-CONDITION P=P0 T=553
EXPERIMENT X(BETA_PU,Pu)=0.98:DX5 X(ETA,U)=0.029:DX5
SET_START_VALUE Y(BETA_PU,Pu)=0.98 Y(ETA,U)=0.029
LABEL ASS
COMMENT Ellinger
$
CREATE_NEW_EQUILIBRIUM 31 1
CHANGE_STATUS PHASE BETA_PU GAMMA_PU=FIX 1
SET-CONDITION P=P0 T=553
EXPERIMENT X(BETA_PU,Pu)=0.98:DX5 X(GAMMA_PU,Pu)=0.992:DX5
SET_START_VALUE Y(BETA_PU,Pu)=0.98 Y(GAMMA_PU,Pu)=0.992
LABEL ASS
COMMENT Ellinger
$
CREATE_NEW_EQUILIBRIUM 32 1
CHANGE_STATUS PHASE BETA_PU ETA=FIX 1
SET-CONDITION P=P0 T=551
EXPERIMENT X(BETA_PU,Pu)=0.98:DX5 X(ETA,U)=0.03:DX5
SET_START_VALUE Y(BETA_PU,Pu)=0.98 Y(ETA,U)=0.03
LABEL ASS
COMMENT Ellinger
$
CREATE_NEW_EQUILIBRIUM 33 1
CHANGE_STATUS PHASE BETA_PU ZETA=FIX 1
SET-CONDITION P=P0 T=551
EXPERIMENT X(BETA_PU,Pu)=0.98:DX5
S_A_C X(ZETA,U)=0.26:DX10
SET_START_VALUE Y(BETA_PU,Pu)=0.98 Y(ZETA,U)=0.26
LABEL ASS
COMMENT Ellinger
$
CREATE_NEW_EQUILIBRIUM 34 1
CHANGE_STATUS PHASE ETA ZETA=FIX 1
SET-CONDITION P=P0 T=551
EXPERIMENT X(ETA,U)=0.03:DX5
S_A_C X(ZETA,U)=0.26:DX10
SET_START_VALUE Y(ETA,U)=0.03 Y(ZETA,U)=0.26
LABEL ASS
COMMENT Ellinger
$
CREATE_NEW_EQUILIBRIUM 35 1
CHANGE_STATUS PHASE ALPHA_PU ZETA=FIX 1
SET-CONDITION P=P0 T=398
EXPERIMENT X(ZETA,U)=0.3:DX10
S_A_C X(ALPHA_PU,PU)=1:DX5
SET_START_VALUE Y(ZETA,U)=0.3 Y(ALPHA_PU,PU)=1
LABEL ASS
COMMENT Ellinger
$
```

```
CREATE_NEW_EQUILIBRIUM 36 1
CHANGE_STATUS PHASE BETA_PU ZETA=FIX 1
SET-CONDITION P=P0 T=398
EXPERIMENT X(ZETA,U)=0.3:DX10
S_A_C X(BETA_PU,U)=.001:DX5
SET_START_VALUE Y(ZETA,U)=0.3 Y(BETA_PU,U)=.001
LABEL ASS
COMMENT Ellinger
$
CREATE_NEW_EQUILIBRIUM 37 1
CHANGE_STATUS PHASE ZETA ORTHORHOMBIC_U=FIX 1
SET-CONDITION P=P0 T=683
EXPERIMENT X(ZETA,Pu)=0.314:DX5 X(ORTHORHOMBIC_U,U)=0.889:DX5
SET_START_VALUE Y(ZETA,Pu)=0.314 Y(ORTHORHOMBIC_U,U)=0.889
LABEL ASS
COMMENT Sheldon
$
TABLE_HEAD 40
CREATE_NEW_EQUILIBRIUM @@ 1
CHANGE_STATUS PHASE TETRAGONAL_U BCC=FIX 1
SET_CONDITION T=@3 P=P0
EXPERIMENT X(BCC,U)=@1:DX5
S_A_C X(TETRAGONAL_U,Pu)=@2:DX5
SET_START_VALUE Y(TETRAGONAL_U,Pu)=@2 Y(BCC,U)=@1
TABLE_VALUES
$ mole fraction U in BCC   Pu in tet      T/K
$  0.95                    0.04          1033
$  0.90                    0.08          998
$  0.886                   0.10          1012
$  0.798                   0.12          991
$  0.778                   0.16          980
  0.95                    0.04          1033
  0.90                    0.08          1013
  0.86                    0.10          1003
  0.80                    0.13          993
  0.75                    0.15          988
TABLE_END
LABEL ASS
COMMENT Ellinger Okamoto
$
TABLE_HEAD 45
CREATE_NEW_EQUILIBRIUM @@ 1
CHANGE_STATUS PHASE TETRAGONAL_U BCC=FIX 1
SET_CONDITION T=@3 P=P0
EXPERIMENT X(TETRAGONAL_U,Pu)=@2:DX5
S_A_C X(BCC,U)=@1:DX5
SET_START_VALUE Y(TETRAGONAL_U,Pu)=@2 Y(BCC,U)=@1
TABLE_VALUES
$ mole fraction U in BCC   Pu in tet      T/K
  0.91                    0.05          1033
  0.85                    0.10          1010
  0.76                    0.18          982
TABLE_END
LABEL ASS
COMMENT MOUND REPORT
$
TABLE_HEAD 50
CREATE_NEW_EQUILIBRIUM @@ 1
CHANGE_STATUS PHASE TETRAGONAL_U BCC=FIX 1
SET_CONDITION T=@3 P=P0
EXPERIMENT X(BCC,U)=@1:DX5
S_A_C X(TETRAGONAL_U,Pu)=@2:DX5
```

```
SET_START_VALUE Y(TETRAGONAL_U,Pu)=@2 Y(BCC,U)=@1
TABLE_VALUES
$ mole fraction U in BCC   Pu in tet       T/K
  0.95                0.04          1047
  0.90                0.08          1037
  0.82                0.18          1015
TABLE_END
LABEL ASS
COMMENT (Ellinger) Okamoto
$
CREATE_NEW_EQUILIBRIUM 53 1
CHANGE_STATUS PHASE TETRAGONAL_U ORTHORHOMBIC_U=FIX 1
SET-CONDITION P=P0 T=866
EXPERIMENT X(ORTHORHOMBIC_U,U)=0.886:DX5
S_A_C X(TETRAGONAL_U,U)=0.87:DX5
SET_START_VALUE Y(TETRAGONAL_U,U)=0.87 Y(ORTHORHOMBIC_U,U)=0.886
LABEL ASS
COMMENT Okamoto
$
CREATE_NEW_EQUILIBRIUM 54 1
CHANGE_STATUS PHASE TETRAGONAL_U ORTHORHOMBIC_U=FIX 1
SET-CONDITION P=P0 T=846
EXPERIMENT X(ORTHORHOMBIC_U,U)=0.9:DX5
S_A_C X(TETRAGONAL_U,U)=0.88:DX5
SET_START_VALUE Y(TETRAGONAL_U,U)=0.88 Y(ORTHORHOMBIC_U,U)=0.9
LABEL ASS
COMMENT MOUND REPORT
$
CREATE_NEW_EQUILIBRIUM 55 1
CHANGE_STATUS PHASE TETRAGONAL_U ORTHORHOMBIC_U=FIX 1
SET-CONDITION P=P0 T=875
EXPERIMENT X(TETRAGONAL_U,U)=0.9:DX5
S_A_C X(ORTHORHOMBIC_U,U)=0.92:DX5
SET_START_VALUE Y(TETRAGONAL_U,U)=0.9 Y(ORTHORHOMBIC_U,U)=0.92
LABEL ASS
COMMENT MOUND REPORT
$
TABLE_HEAD 60
CREATE_NEW_EQUILIBRIUM @@ 1
CHANGE_STATUS PHASE LIQUID BCC_A2=FIX 1
SET_CONDITION T=@3 P=P0
EXPERIMENT X(LIQUID,U)=@1:DX5
S_A_C X(BCC_A2,Pu)=@2:DX5
SET_START_VALUE Y(LIQUID,U)=@1 Y(BCC_A2,Pu)=@2
TABLE_VALUES
$ mole frac. U in liqid    Pu in BCC    T/K
  0.886               0.07          1338
  0.798               0.15          1279
  0.778               0.17          1263
  0.697               0.24          1204
  0.605               0.32          1130
  0.416               0.50          1014
  0.220               0.77          901
$  0.106                0.894         892
TABLE_END
LABEL ALS
COMMENT Okamoto liquidus
$
TABLE_HEAD 70
CREATE_NEW_EQUILIBRIUM @@ 1
CHANGE_STATUS PHASE LIQUID BCC_A2=FIX 1
SET_CONDITION T=@3 P=P0
```

```
EXPERIMENT X(BCC_A2,Pu)=@2:DX5
S_A_C X(LIQUID,U)=@1:DX5
SET_START_VALUE Y(LIQUID,U)=@1 Y(BCC,Pu)=@2
TABLE_VALUES
$ mole frac. U in liqid    Pu in BCC    T/K
  0.82                0.114        1307
  0.65                0.202        1213
  0.63                0.222        1209
  0.57                0.303        1131
  0.42                0.395        1065
  0.37                0.584        963
  0.19                0.804        895
TABLE_END
LABEL ALS
COMMENT Okamoto solidus
$
CREATE_NEW_EQUILIBRIUM 80 1
CHANGE_STATUS PHASE LIQUID BCC_A2=FIX 1
SET_CONDITION T=1254 P=P0
EXPERIMENT X(LIQUID,U)=0.74:DX5
S_A_C X(BCC_A2,Pu)=0.19:DX5
SET_START_VALUE Y(LIQUID,U)=0.74 Y(BCC_A2,Pu)=0.19
LABEL ALS
COMMENT Nakajima
$
CREATE_NEW_EQUILIBRIUM 81 1
CHANGE_STATUS PHASE LIQUID BCC_A2=FIX 1
SET_CONDITION T=1181 P=P0
EXPERIMENT X(BCC_A2,U)=0.74:DX5
S_A_C X(LIQUID,Pu)=0.33:DX5
SET_START_VALUE Y(BCC_A2,U)=0.74 Y(LIQUID,Pu)=0.33
LABEL ALS
COMMENT Nakajima
$
TABLE_HEAD 85
CREATE_NEW_EQUILIBRIUM @@ 1
CHANGE_STATUS PHASE LIQUID BCC_A2=FIX 1
SET_CONDITION T=@3 P=P0
EXPERIMENT X(LIQUID,U)=@1:DX5
S_A_C X(BCC_A2,Pu)=@2:DX5
SET_START_VALUE Y(LIQUID,U)=@1 Y(BCC_A2,Pu)=@2
TABLE_VALUES
$ mole frac. U in liqid    Pu in BCC    T/K
  0.95                0.03         1378
  0.90                0.05         1353
  0.80                0.10         1298
  0.70                0.17         1238
  0.65                0.21         1198
  0.60                0.25         1168
  0.55                0.29         1128
  0.50                0.33         1098
  0.45                0.38         1058
  0.425               0.40         1043
  0.375               0.46         1008
  0.35                0.50         993
  0.30                0.56         958
  0.25                0.64         928
  0.20                0.74         898
$  0.15               0.85         903
$  0.10               0.89         893
$  0.05               0.94         903
TABLE_END
```

```
LABEL ALS
COMMENT Ellinger liquidus
$
TABLE_HEAD 103
CREATE_NEW_EQUILIBRIUM @@ 1
CHANGE_STATUS PHASE LIQUID BCC_A2=FIX 1
SET_CONDITION T=@3 P=P0
EXPERIMENT X(BCC_A2,Pu)=@2:DX5
S_A_C X(LIQUID,U)=@1:DX5
SET_START_VALUE Y(LIQUID,U)=@1 Y(BCC,Pu)=@2
TABLE_VALUES
$ mole frac. U in liqid    Pu in BCC    T/K
  0.83                0.10         1313
  0.725               0.15         1248
  0.68                0.20         1223
  0.60                0.25         1168
  0.39                0.45         1033
  0.36                0.50         998
$  0.23                0.75         888
  0.15                0.80         888
$  0.15                0.85         883
$  0.10                0.91         883
  0.06                0.95         888
TABLE_END
LABEL ALS
COMMENT Ellinger solidus
$
TABLE_HEAD 113
CREATE_NEW_EQUILIBRIUM @@ 1
CHANGE_STATUS PHASE LIQUID BCC_A2=FIX 1
SET_CONDITION T=@3 P=P0
EXPERIMENT X(LIQUID,U)=@1:DX5
S_A_C X(BCC_A2,Pu)=@2:DX5
SET_START_VALUE Y(LIQUID,U)=@1 Y(BCC_A2,Pu)=@2
TABLE_VALUES
$ mole frac. U in liqid    Pu in BCC    T/K
  0.75                0.16         1256
  0.70                0.20         1226
  0.65                0.24         1190
  0.60                0.29         1165
  0.50                0.38         1103
  0.40                0.47         1046
  0.30                0.59         973
  0.20                0.73         926
  0.15                0.85         893
  0.10                0.90         893
  0.05                0.94         907
TABLE_END
LABEL ALS
COMMENT MOUND-REPORT liquidus
$
TABLE_HEAD 124
CREATE_NEW_EQUILIBRIUM @@ 1
CHANGE_STATUS PHASE LIQUID BCC_A2=FIX 1
SET_CONDITION T=@3 P=P0
EXPERIMENT X(BCC_A2,Pu)=@2:DX5
S_A_C X(LIQUID,U)=@1:DX5
SET_START_VALUE Y(LIQUID,U)=@1 Y(BCC,Pu)=@2
TABLE_VALUES
$ mole frac. U in liqid    Pu in BCC    T/K
  0.76                0.18         1244
  0.73                0.21         1208
```

```
  0.67              0.25        1190
  0.60              0.30        1147
  0.54              0.35        1112
  0.48              0.40        1068
  0.39              0.50        1023
  0.33              0.60        973
  0.26              0.70        931
$  0.18              0.80         892
$  0.15              0.85         887
$  0.11              0.90         890
  0.04              0.95        896
TABLE_END
LABEL ALS
COMMENT MOUND-REPORT solidus
$
TABLE_HEAD 140
CREATE_NEW_EQUILIBRIUM @@ 1
CHANGE_STATUS PHASE LIQUID=FIX 1
SET-CONDITION T=@3 P=P0 X(LIQUID,U)=@1
SET_REFERENCE_STATE Pu LIQUID,,,,
EXPERIMENT ACR(Pu)=@2:DX5
TABLE_VALUES
$mole-frac. U     activity Pu   T/K
 .248          .64         2073
 .506          .33         2073
 .804          .081         2073
 .248          .64         1873
 .506          .33         1873
 .804          .081         1873
 .248          .64         1673
 .506          .33         1673
 .804          .081         1673
 .248          .64         1473
 .506          .33         1473
 .804          .081         1473
TABLE_END
LABEL AACT
COMMENT Nakajima
$
TABLE_HEAD 152
CREATE_NEW_EQUILIBRIUM @@ 1
CHANGE_STATUS PHASE LIQUID=FIX 1
SET-CONDITION T=@3 P=P0 X(LIQUID,U)=@1
SET_REFERENCE_STATE Pu LIQUID,,,,
EXPERIMENT ACR(Pu)=@2:DX5
TABLE_VALUES
$mole-frac. U     activity Pu   T/K
 .248          .634         2073
 .506          .330         2073
 .804          .081         2073
 .248          .598         1973
 .506          .325         1973
 .804          .091         1973
 .248          .560         1873
 .506          .319         1873
 .804          .104         1873
 .248          .521         1773
 .506          .313         1773
 .804          .120         1773
 .248          .481         1673
 .506          .306         1673
 .248          .439         1573
```

```
 .506          .298        1573
 .248          .396        1473
 .506          .290        1473
TABLE_END
LABEL AACT
COMMENT Nakajima
$
$ activity in the Liq phase from [Okamoto]
TABLE_HEAD 170
CREATE_NEW_EQUILIBRIUM @@ 1
CHANGE_STATUS PHASE LIQUID=FIX 1
SET-CONDITION T=@3 P=P0 X(LIQUID,U)=@1
SET_REFERENCE_STATE Pu LIQUID,,,,
EXPERIMENT ACR(Pu)=@2:DX5
TABLE_VALUES
$mole-frac. U     activity Pu   T/K
 .200          .68         1473
 .420          .35         1473
 .500          .32         1473
 .800          .15         1473
TABLE_END
LABEL AACT
COMMENT Okamoto Activity
$
TABLE_HEAD 180
CREATE_NEW_EQUILIBRIUM @@ 1
CHANGE_STATUS PHASE ETA BCC_A2=FIX 1
SET_CONDITION T=@3 P=P0
EXPERIMENT X(BCC_A2,Pu)=@2:DX5
S_A_C X(ETA,U)=@1:DX5
SET_START_VALUE  Y(ETA,U)=@1 Y(BCC_A2,Pu)=@2
TABLE_VALUES
$ mole fraction U in ETA   Pu in BCC    T/K
 0.705                0.300       975
 0.65                 0.395       968
 0.55                 0.420       955
 0.50                 0.584       929
 0.25                 0.804       833
 0.15                 0.894       767
 0.045                0.975       728
TABLE_END
LABEL ASS
COMMENT Okamoto BCC-ETA
$
TABLE_HEAD 190
CREATE_NEW_EQUILIBRIUM @@ 1
CHANGE_STATUS PHASE ETA BCC_A2=FIX 1
SET_CONDITION T=@3 P=P0
EXPERIMENT X(ETA,U)=@1:DX5
S_A_C X(BCC_A2,Pu)=@2:DX5
SET_START_VALUE Y(ETA,U)=@1 Y(BCC,Pu)=@2
TABLE_VALUES
$ mole fraction U in ETA   Pu in BCC    T/K
 0.045                0.975       728
 0.106                0.93        738
 0.196                0.83        789
 0.416                0.70        901
 0.605                0.40        957
 0.705                0.30        975
 0.697                0.35        964
TABLE_END
LABEL ASS
```

```
COMMENT Okamoto BCC-ETA
$
TABLE_HEAD 200
CREATE_NEW_EQUILIBRIUM @@ 1
CHANGE_STATUS PHASE ETA BCC_A2=FIX 1
SET_CONDITION T=@3 P=P0
EXPERIMENT X(BCC_A2,Pu)=@2:DX5
S_A_C X(ETA,U)=@1:DX5
SET_START_VALUE  Y(ETA,U)=@1 Y(BCC_A2,Pu)=@2
TABLE_VALUES
$ mole fraction U in ETA   Pu in BCC    T/K
 0.64                0.40       973
 0.60                0.45       963
 0.575               0.50       958
 0.52                0.55       943
 0.48                0.60       928
 0.43                0.65       913
 0.39                0.70       898
 0.33                0.75       873
 0.27                0.80       848
 0.21                0.85       823
TABLE_END
LABEL ASS
COMMENT Ellinger BCC-ETA
$
TABLE_HEAD 210
CREATE_NEW_EQUILIBRIUM @@ 1
CHANGE_STATUS PHASE ETA BCC_A2=FIX 1
SET_CONDITION T=@3 P=P0
EXPERIMENT X(ETA,U)=@1:DX5
S_A_C X(BCC_A2,Pu)=@2:DX5
SET_START_VALUE Y(ETA,U)=@1 Y(BCC,Pu)=@2
TABLE_VALUES
$ mole fraction U in ETA   Pu in BCC    T/K
 0.65                0.40       973
 0.60                0.45       963
 0.55                0.53       948
 0.50                0.58       933
 0.45                0.625      923
 0.40                0.69       898
 0.35                0.725      883
 0.25                0.81       838
 0.20                0.86       813
 0.15                0.89       798
 0.10                0.925      773
TABLE_END
LABEL ASS
COMMENT Ellinger BCC-ETA
$
TABLE_HEAD 221
CREATE_NEW_EQUILIBRIUM @@ 1
CHANGE_STATUS PHASE ETA BCC_A2=FIX 1
SET_CONDITION T=@3 P=P0
EXPERIMENT X(BCC_A2,Pu)=@2:DX5
S_A_C X(ETA,U)=@1:DX5
SET_START_VALUE  Y(ETA,U)=@1 Y(BCC_A2,Pu)=@2
TABLE_VALUES
$ mole fraction U in ETA   Pu in BCC    T/K
 0.62                0.40       975
 0.53                0.50       963
 0.45                0.60       923
 0.36                0.70       900
```

```
 0.27                0.80      858
 0.23                0.85      834
 0.19                0.90      804
 0.17                0.92      788
TABLE_END
LABEL ASS
COMMENT MOUND REPORT BCC-ETA
$
TABLE_HEAD 230
CREATE_NEW_EQUILIBRIUM @@ 1
CHANGE_STATUS PHASE ETA BCC_A2=FIX 1
SET_CONDITION T=@3 P=P0
EXPERIMENT X(ETA,U)=@1:DX5
S_A_C X(BCC_A2,Pu)=@2:DX5
SET_START_VALUE Y(ETA,U)=@1 Y(BCC,Pu)=@2
TABLE_VALUES
$ mole fraction U in ETA   Pu in BCC    T/K
 0.60                0.42      968
 0.50                0.54      926
 0.40                0.66      896
 0.30                0.78      855
 0.20                0.89      807
 0.15                0.95      786
 0.10                0.97      751
 0.08                0.98      738
TABLE_END
LABEL ASS
COMMENT MOUND REPORT BCC-ETA
$
TABLE_HEAD 240
CREATE_NEW_EQUILIBRIUM @@ 1
CHANGE_STATUS PHASE ZETA ETA=FIX 1
SET_CONDITION T=@3 P=P0
EXPERIMENT X(ZETA,U)=@1:DX5
S_A_C X(ETA,Pu)=@2:DX5
SET_START_VALUE Y(ZETA,U)=@1 Y(ETA,Pu)=@2
TABLE_VALUES
$ mole fraction U in ZETA   Pu in ETA       T/K
 0.20                0.97          551
 0.28                0.89          620
 0.416               0.80          695
 0.605               0.45          813
 0.697               0.30          854
TABLE_END
LABEL ASS
COMMENT Okamoto ZETA-ETA
$
TABLE_HEAD 250
CREATE_NEW_EQUILIBRIUM @@ 1
CHANGE_STATUS PHASE ZETA ETA=FIX 1
SET_CONDITION T=@3 P=P0
EXPERIMENT X(ETA,Pu)=@2:DX5
S_A_C X(ZETA,U)=@1:DX5
SET_START_VALUE Y(ZETA,U)=@1 Y(ETA,Pu)=@2
TABLE_VALUES
$ mole fraction U in ZETA   Pu in ETA       T/K
 0.53                0.584         753
 0.65                0.395         825
TABLE_END
LABEL ASS
COMMENT Okamoto ZETA-ETA
$
```

```
TABLE_HEAD 255
CREATE_NEW_EQUILIBRIUM @@ 1
CHANGE_STATUS PHASE ZETA ETA=FIX 1
SET_CONDITION T=@3 P=P0
EXPERIMENT X(ZETA,U)=@1:DX5
S_A_C X(ETA,Pu)=@2:DX5
SET_START_VALUE Y(ZETA,U)=@1 Y(ETA,Pu)=@2
TABLE_VALUES
$ mole fraction U in ZETA   Pu in ETA       T/K
 0.65                0.40          848
 0.60                0.475          823
 0.55                0.53          798
 0.50                0.60          773
 0.45                0.67          738
TABLE_END
LABEL ASS
COMMENT Ellinger ZETA-ETA
$
TABLE_HEAD 260
CREATE_NEW_EQUILIBRIUM @@ 1
CHANGE_STATUS PHASE ZETA ETA=FIX 1
SET_CONDITION T=@3 P=P0
EXPERIMENT X(ETA,Pu)=@2:DX5
S_A_C X(ZETA,U)=@1:DX5
SET_START_VALUE Y(ZETA,U)=@1 Y(ETA,Pu)=@2
TABLE_VALUES
$ mole fraction U in ZETA   Pu in ETA       T/K
 0.67                0.35          847
 0.64                0.40          830
 0.56                0.50          800
 0.48                0.60          770
 0.40                0.70          718
 0.32                0.80          673
 0.28                0.85          632
 0.24                0.90          590
 0.22                0.92          570
 0.20                0.95          551
TABLE_END
LABEL ASS
COMMENT MOUND REPORT ZETA-ETA
$
TABLE_HEAD 270
CREATE_NEW_EQUILIBRIUM @@ 1
CHANGE_STATUS PHASE ZETA ETA=FIX 1
SET_CONDITION T=@3 P=P0
EXPERIMENT X(ZETA,U)=@1:DX5
S_A_C X(ETA,Pu)=@2:DX5
SET_START_VALUE Y(ZETA,U)=@1 Y(ETA,Pu)=@2
TABLE_VALUES
$ mole fraction U in ZETA   Pu in ETA       T/K
 0.65                0.37          823
 0.60                0.43          808
 0.50                0.55          763
 0.40                0.67          703
 0.30                0.79          646
 0.20                0.93          560
TABLE_END
LABEL ASS
COMMENT MOUND REPORT ZETA-ETA
$
TABLE_HEAD 280
CREATE_NEW_EQUILIBRIUM @@ 1
```

```
CHANGE_STATUS PHASE ORTHORHOMBIC_U ZETA=FIX 1
SET_CONDITION T=@3 P=P0
EXPERIMENT X(ORTHORHOMBIC_U,Pu)=@2:DX5 X(ZETA,U)=@1:DX5
SET_START_VALUE Y(ORTHORHOMBIC_U,Pu)=@2 Y(ZETA,U)=@1
TABLE_VALUES
$ mole fraction U in ZETA   Pu in ORT       T/K
$  0.6                     0.08            400
$  0.62                    0.09            500
  0.686                    0.111           683
  0.698                    0.120           715
  0.707                    0.133           753
  0.718                    0.141           783
  0.732                    0.153           819
TABLE_END
LABEL ASS
COMMENT Calais
$
CREATE_NEW_EQUILIBRIUM 300 1
CHANGE_STATUS PHASE TETRAGONAL_U ORTHORHOMBIC_U=FIX 1
SET-CONDITION P=P0 T=858
EXPERIMENT X(ORTHORHOMBIC_U,U)=0.9:DX5
S_A_C X(TETRAGONAL_U,PU)=0.12:DX5
SET_START_VALUE Y(ORTHORHOMBIC_U,U)=0.9 Y(TETRAGONAL_U,PU)=0.12
LABEL ASS
COMMENT Ellinger
$
CREATE_NEW_EQUILIBRIUM 301 1
CHANGE_STATUS PHASE TETRAGONAL_U ORTHORHOMBIC_U=FIX 1
SET-CONDITION P=P0 T=893
EXPERIMENT X(ORTHORHOMBIC_U,U)=0.95:DX5
S_A_C X(TETRAGONAL_U,PU)=0.06:DX5
SET_START_VALUE Y(ORTHORHOMBIC_U,U)=0.95 Y(TETRAGONAL_U,PU)=0.06
LABEL ASS
COMMENT Ellinger
$
$ Do not forget the following line!
SAVE_WORKSPACES
$
$ References
$ Ellinger: F.H. Ellinger et al., J. Nucl. Mater. 3 (1959) 233-243.
$ Okamoto: H. Okamoto, J. Ph. Equil. 17 (1996) 372.
$ Mound Report: AEC Research and Development Report, MLM-1402 (1966).
$ Mound Report: AEC Research and Development Report, MLM-1445 (1967).
$ Nakajima: private communication
$ Okamoto: M. Kurata and Y. Okamoto, presented at 1997 fall meeting of the Japan Atomic Energy Society, Sep. 26-
28, 1997, Okinawa, Japan.
$ Calais: D. Calais et al., Plutonium 1965, Chapman and Hall, London, 358-391 (1967).
```

XI Appendix C: .TDB Thermodynamic database

```
$ Database file written 2013-12-12
$ From database: Pu-U-Ga database assembled by Aurelien Perron and Patrice Turchi

 ELEMENT /-   ELECTRON_GAS              0.0000E+00  0.0000E+00  0.0000E+00!
 ELEMENT VA   VACUUM                    0.0000E+00  0.0000E+00  0.0000E+00!
 ELEMENT GA   ORTHORHOMBIC_GA           6.9723E+01  5.5731E+03  4.0828E+01!
 ELEMENT PU   SIMPLE_MONOCLINIC         2.4406E+02  0.0000E+00  0.0000E+00!
 ELEMENT U    ORTHORHOMBIC(A20)         2.3803E+02  0.0000E+00  0.0000E+00!

 FUNCTION GHSERGA   298.14 -21312.331+585.263691*T-108.2287832*T*LN(T)
    +.227155636*T**2-1.18575257E-04*T**3+439954*T**(-1);
     302.9146 Y
    -7055.643+132.73019*T-26.0692906*T*LN(T)+1.506E-04*T**2
    -4.0173E-08*T**3-118332*T**(-1)+1.645E+23*T**(-9);
     3000 N !

 FUNCTION GHSERPU   298.14 -7396.309+80.301382*T-18.1258*T*LN(T)-.02241*T**2;
     400 Y
    -16605.962+236.786603*T-42.4187*T*LN(T)-.00134493*T**2
    +2.63443E-07*T**3+579325*T**(-1);
     944 Y
    -14462.156+232.961553*T-42.248*T*LN(T);
     3000 N !

 FUNCTION GHSERUU   298.14 -8407.734+130.955151*T-26.9182*T*LN(T)
    +.00125156*T**2-4.42605E-06*T**3+38568*T**(-1);
     955 Y
    -22521.8+292.121093*T-48.66*T*LN(T);
     3000 N !

 FUNCTION UN_ASS 298.15 +0; 300 N !

 TYPE_DEFINITION % SEQ *!
 DEFINE_SYSTEM_DEFAULT ELEMENT 2 !
 DEFAULT_COMMAND DEF_SYS_ELEMENT VA /- !

 PHASE LIQUID:L %  1  1.0  !
   CONSTITUENT LIQUID:L :GA,PU,U :  !
  PARAMETER G(LIQUID,GA;0)             298.14 +GHSERGA#+5491.298
    -18.073995*T-7.017E-17*T**7;
     302.9146 Y
    -1389.188+114.049043*T-26.0692906*T*LN(T)+1.506E-04*T**2
    -4.0173E-08*T**3-118332*T**(-1);
     3000 N REF1 !
  PARAMETER G(LIQUID,PU;0)             298.14 +6608.1-12.5133*T+GHSERPU#;
     3000 N REF1 !
  PARAMETER G(LIQUID,U;0)              298.14 +12355.5-10.3239*T+GHSERUU#;
     3000 N REF1 !
  PARAMETER G(LIQUID,GA,PU;0)          298.14  -121696+18.762*T;
     3000  N REF4 !
  PARAMETER G(LIQUID,GA,PU;1)          298.14    -31927-5.288*T;
     3000  N REF4 !
  PARAMETER G(LIQUID,GA,PU;2)          298.14    +12711-7.134*T;
     3000  N REF4 !
  PARAMETER G(LIQUID,GA,U;0)           298.14    -37988+6.292*T;
     3000 N REF5 !
  PARAMETER G(LIQUID,GA,U;1)           298.14   -43307+16.045*T;
```

```
    3000 N REF5 !
  PARAMETER G(LIQUID,GA,U;2)            298.14    -11520+5.048*T;
    3000 N REF5 !
  PARAMETER G(LIQUID,GA,U;3)            298.14   -20434+12.021*T;
    3000 N REF5 !
  PARAMETER G(LIQUID,PU,U;0)            298.14     +13839-19.6*T;
    3000 N REF3 !
  PARAMETER G(LIQUID,PU,U;1)            298.14            -7093;
    3000 N REF3 !

PHASE ALPHA_PU  %  1  1.0  !
  CONSTITUENT ALPHA_PU  :GA,PU :  !
  PARAMETER G(ALPHA_PU,GA;0)            298.14  +2000+GHSERGA#;
    3000 N REF4 !
  PARAMETER G(ALPHA_PU,PU;0)            298.14       +GHSERPU#;
    3000 N REF1 !
  PARAMETER G(ALPHA_PU,GA,PU;1)         298.14           66500;
    3000  N REF4 !

TYPE_DEFINITION & GES A_P_D BCC_A2 MAGNETIC  -1.0    4.00000E-01 !
PHASE BCC_A2  %&  2 1   3 !
  CONSTITUENT BCC_A2  :GA,PU,U : VA :  !
  PARAMETER G(BCC_A2,GA:VA;0)           298.14 +GHSERGA#+4500-11.7*T;
    3000 N REF1 !
  PARAMETER G(BCC_A2,PU:VA;0)           298.14 -1358.984+116.603882*T
    -27.094*T*LN(T)-.009105*T**2+2.061667E-06*T**3+20863*T**(-1);
    745 Y
    -2890.817+156.878957*T-33.72*T*LN(T);
    956 Y
    +29313.619-132.788248*T+6.921*T*LN(T)-.02023305*T**2+1.426922E-06*T**3
    -4469245*T**(-1);
    2071 Y
    -938.428-5.539698*T+GHSERPU#;
    3000 N REF1 !
  PARAMETER G(BCC_A2,U:VA;0)            298.14 -752.767+131.5381*T
    -27.5152*T*LN(T)-.00835595*T**2+9.67907E-07*T**3+204611*T**(-1);
    1049 Y
    -4698.365+202.685635*T-38.2836*T*LN(T);
    3000 N REF1 !
  PARAMETER G(BCC_A2,GA,PU:VA;0)        298.14    -126805+18.8*T;
    3000 N REF4 !
  PARAMETER G(BCC_A2,GA,PU:VA;1)        298.14    -10489-26.68*T;
    3000 N REF4 !
  PARAMETER G(BCC_A2,GA,PU:VA;2)        298.14       -10000+10*T;
    3000 N REF4 !
  PARAMETER L(BCC_A2,GA,U:VA;0)         298.14    -19097+0.204*T;
    3000 N REF5 !
  PARAMETER G(BCC_A2,PU,U:VA;0)         298.14  -4.808E+03+0.2*T;
    3000 N REF3 !
  PARAMETER G(BCC_A2,PU,U:VA;1)         298.14        -1.389E+03;
    3000 N REF3 !

PHASE BETA_PU  %  1  1.0  !
  CONSTITUENT BETA_PU  :PU,U :  !
  PARAMETER G(BETA_PU,PU;0)             298.14 -4873.654+123.249151*T
    -27.416*T*LN(T)-.00653*T**2;
    679.50 Y
    +2435.094+43.566585*T-15.7351*T*LN(T)-.0154772*T**2+1.524942E-06*T**3
    -864940*T**(-1);
    1464 Y
    +503.094-4.739938*T+GHSERPU#;
    3000 N REF1 !
```

```
 PARAMETER G(BETA_PU,U;0)              298.14 +2000+GHSERUU#; 3000 N REF2 !
 PARAMETER G(BETA_PU,PU,U;0)           298.14 -4343; 3000 N REF3 !

PHASE ETA  %  1  1.0  !
  CONSTITUENT ETA  :PU,U :  !
 PARAMETER G(ETA,PU;0)                 298.14 +103.397327-3920.781
  +127.586536*T-28.4781*T*LN(T)-.0054035*T**2;
   990 Y
  +103.397327+3528.208+41.52572*T-15.7351*T*LN(T)-.0154772*T**2
  +1.524942E-06*T**3-864940*T**(-1);
   1464 Y
  +103.397327+1596.208-6.780803*T+GHSERPU#;
   3000 N REF2 !
 PARAMETER G(ETA,U;0)                  298.14 +229.212144-5156.136
  +106.976316*T-22.841*T*LN(T)-.01084475*T**2+2.7889E-08*T**3
  +81944*T**(-1);
   941.50 Y
  +229.212144-14327.309+244.16802*T-42.9278*T*LN(T);
   3000 N REF2 !
 PARAMETER G(ETA,PU,U;0)               298.14 -12970+8.3*T; 3000 N REF3 !
 PARAMETER G(ETA,PU,U;1)               298.14 +2690-3.5*T; 3000 N REF3 !

PHASE ETA_GAPU  %  1  1.0  !
  CONSTITUENT ETA_GAPU  :GA,PU :  !
 PARAMETER G(ETA_GAPU,GA;0)            298.14  +4000+.01*T+GHSERGA#;
   3000  N REF4 !
 PARAMETER G(ETA_GAPU,PU;0)            298.14  +50+.1*T
  -3920.781+127.586536*T-28.4781*T*LN(T)-.0054035*T**2;
   990 Y
  +50+.1*T+3528.208+41.52572*T-15.7351*T*LN(T)-.0154772*T**2
  +1.524942E-06*T**3-864940*T**(-1);
   1464 Y
  +50+.1*T+1596.208-6.780803*T+GHSERPU#;
   3000  N REF4 !
 PARAMETER G(ETA_GAPU,GA,PU;0)         298.14  -183945+31.388*T;
   3000  N REF4 !
 PARAMETER G(ETA_GAPU,GA,PU;1)         298.14       -68327-10*T;
   3000  N REF4 !
 PARAMETER G(ETA_GAPU,GA,PU;2)         298.14      -2516.3+.1*T;
   3000  N REF4 !

TYPE_DEFINITION ' GES A_P_D FCC_A1 MAGNETIC  -3.0    2.80000E-01 !
PHASE FCC_A1  %'  2 1   1 !
  CONSTITUENT FCC_A1  :GA,PU,U : VA :  !
 PARAMETER G(FCC_A1,GA:VA;0)           298.14 +GHSERGA#+3800-10.2*T;
   3000 N REF1 !
 PARAMETER G(FCC_A1,PU:VA;0)           298.14 -3920.781+127.586536*T
  -28.4781*T*LN(T)-.0054035*T**2;
   990 Y
  +3528.208+41.52572*T-15.7351*T*LN(T)-.0154772*T**2+1.524942E-06*T**3
  -864940*T**(-1);
   1464 Y
  +1596.208-6.780803*T+GHSERPU#;
   3000 N REF1 !
 PARAMETER G(FCC_A1,U:VA;0)            298.14   +GHSERUU#+2000;
   3000 N REF2 !
 PARAMETER G(FCC_A1,GA,PU:VA;0)        298.14  -182428+58.42*T;
   3000 N REF4 !
 PARAMETER G(FCC_A1,GA,PU:VA;1)        298.14  +19215-79.062*T;
   3000 N REF4 !
 PARAMETER G(FCC_A1,PU,U:VA;0)         298.14           +3136;
   3000 N REF3 !
```

```
 PHASE GAMMA_PU  %  1  1.0  !
   CONSTITUENT GAMMA_PU  :GA,PU,U :  !
  PARAMETER G(GAMMA_PU,GA;0)            298.14  +2500+GHSERGA#;
    3000 N REF4 !
  PARAMETER G(GAMMA_PU,PU;0)            298.14  -16766.303+419.402655*T
   -77.5802*T*LN(T)+.0816415*T**2-2.8103833E-05*T**3+574825*T**(-1);
    487.90 Y
   -2942.77+88.325069*T-22.0233*T*LN(T)-.0114795*T**2;
    593.90 Y
   -9336.967+160.314641*T-32.3405*T*LN(T)-.0070383*T**2+6.92887E-07*T**3
   +630600*T**(-1);
    1179 Y
   +2026.406-6.829936*T+GHSERPU#;
    3000 N REF1 !
  PARAMETER G(GAMMA_PU,U;0)             298.14  +2000+GHSERUU#;
    3000 N REF2 !
$  PARAMETER G(GAMMA_PU,GA,PU;0)         298.14          +12*T;
$    3000 N REF4 !
$  PARAMETER G(GAMMA_PU,GA,PU;1)         298.14   +321000-580*T;
$    3000 N REF4 !
   PARAMETER G(GAMMA_PU,PU,U;0)          298.14          +4090;
    3000 N REF3 !

 PHASE ORTHORHOMBIC_GA  %  1  1.0  !
   CONSTITUENT ORTHORHOMBIC_GA  :GA,U :  !
  PARAMETER G(ORTHORHOMBIC_GA,GA;0)      298.14 +GHSERGA#; 3000 N REF1 !
  PARAMETER G(ORTHORHOMBIC_GA,U;0)       298.14 +GHSERUU#; 3000 N REF5 !
  PARAMETER G(ORTHORHOMBIC_GA,GA,U;0)    298.14     +2000; 3000 N REF5 !

 PHASE ORTHORHOMBIC_U  %  1  1.0  !
   CONSTITUENT ORTHORHOMBIC_U  :GA,PU,U :  !
  PARAMETER G(ORTHORHOMBIC_U,GA;0)       298.14 +GHSERGA#; 3000 N REF5 !
  PARAMETER G(ORTHORHOMBIC_U,PU;0)       298.14 +2026.01916+GHSERPU#;
    3000 N REF2 !
  PARAMETER G(ORTHORHOMBIC_U,U;0)        298.14 +GHSERUU#; 3000 N REF1 !
  PARAMETER G(ORTHORHOMBIC_U,GA,U;0)     298.14         -7000; 3000 N REF5 !
  PARAMETER G(ORTHORHOMBIC_U,PU,U;0)     298.14  -12689+3.9*T; 3000 N REF3 !
  PARAMETER G(ORTHORHOMBIC_U,PU,U;1)     298.14  +9712-11.8*T; 3000 N REF3 !

 PHASE TETRAGONAL_PU  %  1  1.0  !
   CONSTITUENT TETRAGONAL_PU  :GA,PU,U :  !
  PARAMETER G(TETRAGONAL_PU,GA;0)        298.14 +GHSERGA#+3500-10*T;
    3000 N  REF1 !
  PARAMETER G(TETRAGONAL_PU,PU;0)        298.14 -496.178+54.586547*T
   -16.43*T*LN(T)-.024006*T**2+5.166667E-06*T**3-158470*T**(-1);
    736 Y
   -6122.307+173.35008*T-35.56*T*LN(T);
    757 Y
   +3982.078+63.890352*T-19.756*T*LN(T)-.00937295*T**2+6.59882E-07*T**3
   -1112565*T**(-1);
    2157 Y
   -738.383-4.905143*T+GHSERPU#;
    3000 N REF1 !
  PARAMETER G(TETRAGONAL_PU,U;0)         298.14 +2000+GHSERUU#; 3000 N REF2 !
  PARAMETER G(TETRAGONAL_PU,PU,U;0)      298.14 +2411; 3000 N REF3 !

 PHASE TETRAGONAL_U  %  1  1.0  !
   CONSTITUENT TETRAGONAL_U  :GA,PU,U :  !
  PARAMETER G(TETRAGONAL_U,GA;0)         298.14 +3500-10*T+GHSERGA#;
    3000 N REF5 !
  PARAMETER G(TETRAGONAL_U,PU;0)         298.14 +227.531893-3920.781
```

```
   +127.586536*T-28.4781*T*LN(T)-.0054035*T**2;
    990 Y
   +227.531893+3528.208+41.52572*T-15.7351*T*LN(T)-.0154772*T**2
   +1.524942E-06*T**3-864940*T**(-1);
    1464 Y
   +227.531893+1596.208-6.780803*T+GHSERPU#;
    3000 N REF2 !

  PARAMETER G(TETRAGONAL_U,U;0)         298.14 -5156.136+106.976316*T
   -22.841*T*LN(T)-.01084475*T**2+2.7889E-08*T**3+81944*T**(-1);
    941.50 Y
   -14327.309+244.16802*T-42.9278*T*LN(T);
    3000 N REF1 !
  PARAMETER G(TETRAGONAL_U,GA,U;0)      298.14         -8500; 3000 N REF5 !
  PARAMETER G(TETRAGONAL_U,PU,U;0)      298.14  -12577+8.9*T; 3000 N REF3 !

PHASE ZETA  %  1  1.0  !
  CONSTITUENT ZETA  :PU,U :  !
  PARAMETER G(ZETA,PU;0)              298.14 +500-1358.984+116.603882*T
   -27.094*T*LN(T)-.009105*T**2+2.061667E-06*T**3+20863*T**(-1);
    745 Y
   +500-2890.817+156.878957*T-33.72*T*LN(T);
    956 Y
   +500+29313.619-132.788248*T+6.921*T*LN(T)-.02023305*T**2
   +1.426922E-06*T**3-4469245*T**(-1);
    2071 Y
   +500-938.428-5.539698*T+GHSERPU#;
    3000 N REF2 !
  PARAMETER G(ZETA,U;0)               298.14 +332.097517-752.767
   +131.5381*T-27.5152*T*LN(T)-.00835595*T**2+9.67907E-07*T**3
   +204611*T**(-1);
    1049 Y
   +332.097517-4698.365+202.685635*T-38.2836*T*LN(T);
    3000 N REF2 !
  PARAMETER G(ZETA,PU,U;0)            298.14 -87904+99.2*T; 3000 N REF3 !
  PARAMETER G(ZETA,PU,U;1)            298.14 -23547+54.6*T; 3000 N REF3 !
  PARAMETER G(ZETA,PU,U;2)            298.14 +33907-19.9*T; 3000 N REF3 !

PHASE AGA3PU  %  2 3   1 !
  CONSTITUENT AGA3PU  :GA : PU :  !
  PARAMETER G(AGA3PU,GA:PU;0)  298.14  -238852.78+44.987767*T
                              +3*GHSERGA#+GHSERPU#;
                              3000 N REF4 !

PHASE BGA3PU  %  2 3   1 !
  CONSTITUENT BGA3PU  :GA : PU :  !
  PARAMETER G(BGA3PU,GA:PU;0)  298.14  -238856.45+44.993926*T
                              +3*GHSERGA#+GHSERPU#;
                              3000 N REF4 !

PHASE CGA3PU  %  2 3   1 !
  CONSTITUENT CGA3PU  :GA : PU :  !
  PARAMETER G(CGA3PU,GA:PU;0)  298.14  -194728+8.101*T
                              +3*GHSERGA#+GHSERPU#;
                              3000 N REF4 !

PHASE AGAPU  %  2 1   1 !
  CONSTITUENT AGAPU  :GA : PU :  !
  PARAMETER G(AGAPU,GA:PU;0)  298.14  -102978+10.073*T
                             +GHSERGA#+GHSERPU#;
                             3000 N REF4 !
```

```
PHASE BGAPU  %  2 1   1 !
  CONSTITUENT BGAPU  :GA : PU :  !
 PARAMETER G(BGAPU,GA:PU;0)  298.14  -100577+7.22*T
                          +GHSERGA#+GHSERPU#;
                          3000 N REF4 !

PHASE AGAPU3  %  2 1   3 !
  CONSTITUENT AGAPU3  :GA : PU :  !
 PARAMETER G(AGAPU3,GA:PU;0)  298.14  -155100+43.37*T
                          +GHSERGA#+3*GHSERPU#;
                          3000 N REF4 !

PHASE BGAPU3  %  2 1   3 !
  CONSTITUENT BGAPU3  :GA : PU :  !
 PARAMETER G(BGAPU3,GA:PU;0)  298.14  -155735+44.37*T
                          +GHSERGA#+3*GHSERPU#;
                          3000 N REF4 !

PHASE GA11PU3  %  2 .787   .213 !
  CONSTITUENT GA11PU3  :GA : PU :  !
 PARAMETER G(GA11PU3,GA:PU;0)  298.14  -57000+16.1*T
                           +.787*GHSERGA#+.213*GHSERPU#;
                           3000 N REF4 !

PHASE GA15PU2  %  2 .882   .118 !
  CONSTITUENT GA15PU2  :GA : PU :  !
 PARAMETER G(GA15PU2,GA:PU;0)  298.14  -38000+22*T
                           +.882*GHSERGA#+.118*GHSERPU#;
                           3000 N REF4 !

PHASE GA2PU  %  2 2   1 !
  CONSTITUENT GA2PU  :GA : PU :  !
 PARAMETER G(GA2PU,GA:PU;0)  298.14  -165980+8*T
                          +2*GHSERGA#+GHSERPU#;
                          3000 N REF4 !

PHASE GA3PU2  %  2 3   2 !
  CONSTITUENT GA3PU2  :GA : PU :  !
 PARAMETER G(GA3PU2,GA:PU;0)  298.14  -271300+20*T
                          +3*GHSERGA#+2*GHSERPU#;
                          3000 N REF4 !

PHASE GA3PU5  %  2 3   5 !
  CONSTITUENT GA3PU5  :GA : PU :  !
 PARAMETER G(GA3PU5,GA:PU;0)  298.14  -387150+76*T
                          +3*GHSERGA#+5*GHSERPU#;
                          3000 N REF4 !

PHASE GA4PU  %  2 .8   .2 !
  CONSTITUENT GA4PU  :GA : PU :  !
 PARAMETER G(GA4PU,GA:PU;0)  298.14  -53820+14.9*T
                          +.8*GHSERGA#+.2*GHSERPU#;
                          3000 N REF4 !

PHASE GA6PU  %  2 .857   .143 !
  CONSTITUENT GA6PU  :GA : PU :  !
 PARAMETER G(GA6PU,GA:PU;0)  298.14  -41000+12.4*T
                          +.857*GHSERGA#+.143*GHSERPU#;
                          3000 N REF4 !

PHASE GA7PU2  %  2 .778   .222 !
  CONSTITUENT GA7PU2  :GA : PU :  !
```

```
 PARAMETER G(GA7PU2,GA:PU;0)  298.14  -59000+17.8*T
                              +.778*GHSERGA#+.222*GHSERPU#;
                              3000 N REF4 !

PHASE GA3U2  %  2 .6   .4 !
  CONSTITUENT GA3U2  :GA : U :  !
 PARAMETER G(GA3U2,GA:U;0)  298.14  -33747+1.007*T
                            +0.600*GHSERGA#+0.400*GHSERUU#;
                            3000 N REF5 !

PHASE GA2U  %  2 .667   .333 !
  CONSTITUENT GA2U  :GA : U :  !
 PARAMETER G(GA2U,GA:U;0)  298.14  -35903+1.082*T
                           +0.667*GHSERGA#+0.333*GHSERUU#;
                           3000 N REF5 !

PHASE GA3U  %  2 .75   .25 !
  CONSTITUENT GA3U  :GA : U :  !
 PARAMETER G(GA3U,GA:U;0)  298.14  -33644+0.561*T
                           +0.750*GHSERGA#+0.250*GHSERUU#;
                           3000 N REF5 !

LIST_OF_REFERENCES
NUMBER  SOURCE
 REF1     'Alan Dinsdale, SGTE Data for Pure Elements, Calphad
       Vol  15 (1991) p317-425'
 REF2     'Masaki Kurata, Calphad
       Vol  23 (1999) p305-37'
 REF3     'Aurelien Perron, Patrice Turchi, Alexander Landa (2013)'
 REF4     'Patrice Turchi et al. for Pu-Ga (2004)'
 REF5     'J. Wang, X.J. Liu and C.P. Wang, JNM
       Vol 380 (2008) p105-110'
 !
```